ULB

FACULTE DES SCIENCES
Laboratoire de Physiologie Végétale
Laboratoire de Thermodynamique Electrochimique

MECHANISM OF ION TRANSPORT IN PLANT CELLS : A BIOPHYSICAL APPROACH.

Dr. Fabrice HOMBLE

Thèse présentée pour
l'obtention du grade
d'Agrégé de l'Enseignement Supérieur

Année académique 1989/90

Etude biophysique du mécanisme de transport ionique chez les cellules végétales.

Les cellules végétales sont caractérisées par une paroi cellulaire qui a des propriétés d'echangeur ionique. Le cytoplasme est limité par deux membranes : le plasmalemme et le tonoplaste.

La polarisation électrique des membranes végétales résulte d'un transport actif de proton et d'une diffusion passive. Différents modèles théoriques ont été proposés pour expliquer l'origine du potentiel de repos du plasmalemme.

Les techniques qui permettent l'étude des propriétés électriques des membranes des cellules végétales sont décrites.

Le mécanisme du transport passif est analysé en détail tant au niveau cellulaire qu'au niveau moléculaire.

FOREWORD

Plants are the primary synthetizers of organic compounds and accumulators of inorganic nutrients and therefore they play an important role in the biogeochemical cycles.

Plant nutrition is a process involving an exchange of matter and energy between plant cells and their environment. Any particle which move in or out a plant cell must cross at least two barriers: the cell wall and the plasmalemma. Inside the cell, each organelle is surrounded by at least one membrane which control the exchange of matter between the compartment and the surrounding cytoplasm.

In many lower plants, the population of cells forming the plant body is predominantly of a single type. The exchange between the plant and its environment are simpler than that which occur in higher plants were various tissues have acquired a specific physiological function. This partly explains the reason why certain algal cells and fungal hyphae have been widely used as model for the study of transport process. However, we can now recognize that the general mechanism of ion transport of those plant cell models is ubiquitous throughout the plant kingdom.

My research was carried out at the Université Libre de Bruxelles (Laboratoire de Physiologie Végétale and Laboratoire de Thermodynamique Electrochimique) and at the University of Toronto (Department of Botany and Medical Research Council Group in Periodontal Physiology) and I would like to thanks all the members of those laboratories for their support and encouragement during my work.

1 ION TRANSPORT IN PLANT CELLS: THE CURRENT POSITION

The exchange of matter between the plant cell and its environment must take place across the plasmalemma. Since that membrane provides an inherent permeability barrier to most solutes, the transport systems and receptors embedded in it must play a major role in controlling cellular responses to environmental stimulus. The molecular mechanisms by which plasma membrane proteins carry out transport are only now beginning to be understood, along with the control systems which regulate the transporters. Nevertheless, recent striking advances in molecular biological and electrophysiological methodology now enable many molecular questions to be addressed.

It is useful at the outset to recognize two distinct classes of transport phenomena in membranes:

a) passive transport, due to the diffusion of ions down their electrochemical gradient, and

b) active transport which is energy-dependent and occurs against their electrochemical gradient.

A chemiosmotic hypothesis for transport across plant cell membranes, in which a primary H^+-pump provides energy in the form of an electrochemical protons gradient that drives active transport of other ions and of organic molecules via proton cotransport systems (secondary transports), has gained wide acceptance (Poole 1978, Reinhold and Kaplan 1984). Primary transports are directly linked to a chemical reaction. Secondary transports are not connected with any chemical reaction but often linked to an ionic gradient. The energy requires for primary active proton pumping may be provided by adenosine triphosphate, pyrophosphate or redox reactions. The best evidence for the existence of such cotransport is for sugars and neutral amino acids because the depolarization of the membrane produced by the external addition of neutral molecules can be interpreted unambiguously as the result of transport via a cotransport system (Slayman and Slayman 1974, Etherton and Rubinstein 1978).

It has been difficult to demonstrate the existence of proton cotransport systems in the plasmalemma of higher plants because there are problems inherent in interpreting the electrical responses to external addition of ions. Thus, while voltage-clamping experiments in giant Chara cells suggest a stoechiometry of 2:1 for the Cl^-/H^+ symport (Sanders 1980b), the corresponding measurements in higher plant cells are difficult due to the problems of placing an electrode in the cytoplasm, and because of the current pathway provided by plasmodesmata.

Three main types of ion translocating ATPases have been described, P-, F- and V-type (Pederson and Carafoli 1987). The P-type carry out active transport of cations usually across the plasma membrane. They are sensitive to vanadate. The F-ATPases are found on the inner membranes of mitochondria and chloroplasts. They are reversible, i.e., they can function both in ATP-driven proton pumping and in ATP synthesis. F-type ATPases are vanadate-insesitive and can be dissociated into an integral membrane proton channel complex (F_o) and a water soluble catalytic complex (F_1). V-type ATPases are found in the tonoplast. They have enzymatic properties similar to F-ATPases. However, V-ATPases have a unique subunit composition and have a neutral rather than an alkaline pH optimum (Bowman et al. 1988).

Ion transport across the plasmalemma of most plant cells is dominated by a proton-extruding ATPase (H^+-pump) which generates a large negative membrane potential difference: between -100 and -250 mV. The resulting electrochemical potential gradient for protons drives influx of a wide variety of organic solutes and inorganic ions via symport and, in the case of Na^+, efflux via antiport. Finally, ionic channels provide dissipative pathways through the membrane for many ion species (Hedrich and Schroeder 1989). Because the H^+-ATPase keeps the membrane potential difference more negative than the equilibrium potential for all inorganic ions, the direction of net flux through channels is inward for cations and outward for anions.

Electrophysiological studies and kinetic measurements have led to the general agreement that the H^+-pump translocates a single proton in its reaction cycle (Lucas 1982, Brauer et al. 1989). The primary structure of a higher plant H^+-ATPase has recently been derived from a full-length cDNA clone of Arabidopsis (Harper et al. 1989). The enzyme is 36% homologous with the fungal plasma membrane H^+-ATPase, and also shows significant homology with other members of the P-class of ion-motive ATPases, such as the Na^+,K^+-ATPase of animal cell plasma membranes and the Ca^{2+}-ATPase of sarcoplasmic reticulum. The molecular mechanism of the plant H^+-ATPase remains poorly characterized. However, it has been suggested that all P-type ATPases have similar structure-function relations because they have several sequence analogy.

Redox systems that transfert electrons from cytoplasmic donors to electron acceptors in the apoplast also occur in the plasmalemma. They may also be involved in creating an electrochemical potential difference across the membrane (Bienfait and Lüttge (1988). The nature of the electron donor(s) is not known. However, several evidences suggest that NAD(P)H would be the donor.

The presence of pyrophosphate-driven proton pumping (PPase) was found in the tonoplast of various plants (Rea andd Poole 1985, Chanson et al. 1985, Wang et al. 1986, Takeshige and Hager 1988).

2 THE CHARALES

2.1 Systematics and evolution

The Charales pose for systematist and taxonomist considerable problems because they have many features in common with both green algae and bryophytes. For this reason, many have regarded them as representing not only a distinct class, but even a distinct division: the Charophyta.

Many features of reproduction and cell biology are evolutionarily conservative and thus may be less susceptible to evolution than are characters of external morphology. The conservative characters of greatest significance include certain biochemical features, the organization of the cell-division process, and the fine structure of the flagellar apparatus and cytoskeleton in motile reproductive cells.

The Characeae are separated from other algal lineages because, like land plants, advanced charophytes possess phragmoplast microtubules which appears during the final stages of cell division. Moreover, like bryophytes, pteridophytes and certain gymnosperms the reproductive cells of charophytes are flagellated. Their sexual reproduction is always oogamous and the reproductive organs have acquired a degree of complexicity unmatched elsewhere in the green algae. For instance, the reproductive cells are enclosed by a specialized sheath of sterile cells. Finally, the only substantial evidence for the occurrence of phytochrome (a light-activated protein plant pigment involved in development) in "green algae" comes from members of the charophycean line (Taylor and Bonner 1967). For those reasons, it is becoming widely accepted that members of the Charophyceae represent the closest extant green-algal relatives of bryophytes.

2.2 Distribution

The members of the family Characeae are widely distributed in waters which afford the sandy or muddy substratum in which the anchoring rhizoids can root. Some species are confined to fresh water (Chara corallina), others to brackish (Nitellopsis obtusa) or salt (Chara baltica) waters.

2.3 Vegetative structure

The plants are erect and grow to a height ranging from some centimeters up to several meters. They are green in color and formed of cylindrical internodes which are composed of a single cell and of multicellular nodes. In some Chara species the elongate internodes are corticated. The whorled arrangement of the laterals which arise from node cells gives the plants an equisetum-like habit (Figure 1). Visible encrustations of $CaCO_3$ occur in the cell wall and has long been associated with the dissolved inorganic carbon assimilation (Smith 1985). The large size of Characean cells (about 1 mm in diameter and up to several centimeters in length) and the ability of internodal cells to survive isolation from the plant make them a convenient material for electrical studies of plant cell membranes like the plasmalemma and the tonoplast.

3 THE CELL WALL

3.1 The ion exchanger

The absorption of ions by plant cells is a two-step process: ions must first pass through the cell wall from the external bathing solution to the plasmalemma where they are then transported across the membrane. It is thought that the plasmalemma does not directly perceive the ionic milieu that bathes the cell, for it is argued that the negatively charged cell wall modifies the local ionic composition at the surface of the plasmalemma (Haynes 1980, Sentenac and Grignon 1981). Cations concentrations are enhanced in the cell wall phase, and anions are excluded, by the negatively charged sites which are regarded as localised primarily in the polyuronate fraction of the cell wall.

In order to model the ion behaviour in the cell wall the classical Donnan homogeneous two-phase theory have been applied by Dainty and Hope (1959) working on Chara corallina. Dainty and Hope (1961) also developped a formal equivalent the Donnan model based on Gouy-Chapman theory, which they applied to the cell wall of Chara corallina.

The cell wall selectively binds cations of different species. For instance, in isolated algal cell walls Tyree (1972) found the selectivity sequence to be: $Ca^{2+} > K^{+} > Rb^{+} > Na^{+}$ in Chara corallina; and Van Cutsem and Gillet (1982) observed $Cu^{2+} >> Zn^{2+} > Ca^{2+}$ in Nitella flexilis.

3.2 Uronic acid

The average uronic acid determination for Chara corallina, 1210 ± 133 µeq/gDW (Richter 1986), was higher than the 852 µeq/gDW estimate calculated from the data of Dainty et al. (1960) obtained using the decarboxylation essay. But both of these estimates agreed well with the highest CEC's measured by cation absorption uptake. Dainty et al. (1960) measured the CEC to be 727 µeq/gDW in the presence of 5-20 meq/l Na^{+} and Ca^{2+} at unspecified pH; while the highest CEC measured by Homblé et al. (1989) was 1393 ± 58µeq/gDW by incubating acid -washed Chara cell walls for 4 days in the presence of 10 meq/l $CaCl_2$ at pH 6.5.

3.3 Amino acids

Additional ion-exchange sites could be provided by the side chains of ionisable amino acid in the protein fraction of the cell wall. Gillet and Lefebvre (1978, 1981) found that cationic transport numbers in isolated Nitella flexilis cell walls (calculated from diffusion potentials) increased when the pH of the bathing solutions was raised from 5.8 to 8.5, or when the walls were treated with difluoronitrobenzene (DNFB). These results reflect a reduction in positive fixed charges in the wall caused by the dissociation of protonated amino groups in the first case or the reaction of DNFB with protein amino groups in the second case. Such results suggest that the basic amino acids (histidine, lysine and arginine) are contributing to the anion exchange capacity of cell walls. The acidic amino acids (aspartic acid, glutamic acid, cysteine and tyrosine) can, on the other hand, add, in principle, to the cation exchange capacity of cell walls; but in most studies they have been ignored on the assumption that the uronic acids are the dominating exchange species.

TABLE 1 : Amino acid composition of Nitella opaca cell walls expressed in µmol/g DW wall material.

Asp	85
Thr	21
Ser	32
Glu	29
Pro	64
Gly	74
Ala	58
Cys	51
Val	24
Ile	18
Leu	23
Tyr	9
Phe	14
Lys	65
His	7
Arg	22

The Characean alga Nitella opaca has a wall protein content of 6.5 to 10% (w/w; Thompson and Preston 1967). Amino acid analyses in the literature for Nitella opaca cell wall proteins are listed in table 1. Assuming all side chains are free, the anion and cation exchange capacities of the cell wall proteins can be estimated. Taking, for convenience, the wall pH to be 7 and assuming that the pK's of the side chains are not affected by any interaction between charged groups along the peptides, the anionic and cationic exchange capacities for Nitella opaca wall proteins are 87 and 114 μeq/gDW, respectively. Gillet and Lefebvre (1981) give an estimate for the anionic exchange capacity for the Nitella flexillis wall based on diffusion potential measurements. Their estimate of 45 meq/l is equivalent to 119 μeq/gDW assuming a wall dry matter density of 1.8 g/ml and a water content of 79% (v/v) (Tyree 1972) is in good agreement with the theoretical value calculated from the amino acid composition of the Nitella opaca wall protein. Thus, this result suggests that the basic amino acids can account for the anionic exchange capacity of the cell wall.

According to Schweiger (1962, 1964) the mechanism of binding of divalent cations to polyuronate (Figure 2) involves intermolecular chelation and intramolecular chelation and requires additional coordinations with hydroxyl groups beyond the electrostatic COO-Ca bonds. In his review on ion binding on polyuronates Kohn (1975) discussed Schweiger's two proposals. Kohn argues against the intramolecular chelation for two reasons: a) because a model of the pectin molecule reveals that the shortest possible distance between dissociated carboxyl groups (0.55-0.58 nm) is too large to form a chelate bond; and b) because the activity of calcium ions in a digalacturonate solution is close to that of a monogalacturonate solution which did not differ much from the calcium activity in an equimolar $CaCl_2$ solution. Moreover, only when the degree of polymerisation exceeds 30 does the calcium activity reach the minimum, in support of the "egg-box" model of Grant et al. (1973) shown in Figure 2c. The formation of polyuronate aggregates cross-linked by Ca^{2+} ions is thought to explain gel formation in the presence of divalents. The requirement, then, that divalents must form intermolecular bonds, indicates that conformational changes must occur in the cell wall as calcium bind to the exchange sites.

Experimental and theoretical investigations of the ion-exchange properties of plant cell walls have always assumed that negative charges are homogeneously distributed in the cell wall (Dainty and Hope, 1959; 1961; Demarty et al., 1978; Morvan et al., 1979; Sentenac and Grignon, 1981).

The banding pattern of $CaCO_3$ along the length of the internode is a result of alternating zones of acid and alkaline pH in the cell wall (Spear et al., 1969). Scanning the cell surface with a miniature pH electrode indicates that the alkaline bands are about pH 9.5 and adjacent acid bands are as low as pH 5.5 (Lucas and Smith, 1973). The zoning is associated with spatial variation of the electrical potential along the cell surface (Walker and Smith, 1977; Ogata, 1983; Ogata et al., 1983; Ogata et al., 1987; Toko et al., 1988). Regions of high electrical potential correspond to acidic zones and those of low electrical potential to alkaline zones. It has now been shown that the establishment of these zones arises from light-activated electrogenic active transport in the plasmalemma (Lucas, 1983). Calcium carbonate precipitates in the alkaline zone when the concentrations of calcium and carbonate reach their solubility point.

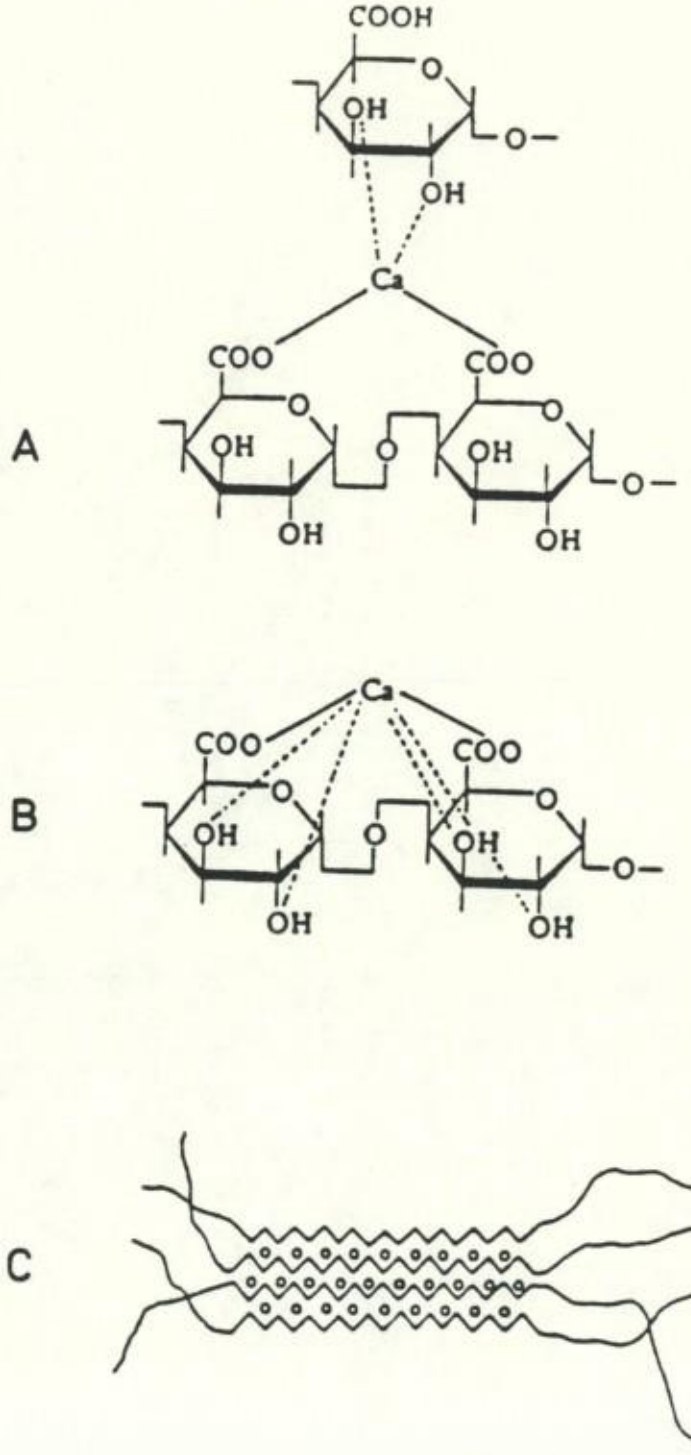

Figure 2: Models of calcium binding to polyuronates. A) Schweiger's intermolecular and B) intromolecular chelation models; C) the "eggbox" model.

Calcium ions bridge carboxylic groups of different pectic chains to stabilize the structure of the cell wall (Somers, 1973; Wuytack and Gillet, 1978; Morvan et al., 1979; Sentenac and Grignon, 1981; Demarty et al., 1984; Hombié et al., 1989). Cell wall proteins are also stabilized by calcium ions (Hombié et al. 1990). Moreover, the Fourier transform infra-red investigation of Chara cell walls shows that the distribution of polymers and proteins in the cell wall is homogeneous in the acid band but not in the alkaline band (Hombié et al. 1990).

4 ION TRANSPORT AND MEMBRANE POTENTIAL DIFFERENCE

4.1 The Nernst-Planck approach

Ion transfert across cell membranes results from simultaneous active transport and passive diffusion. It is basically the operation of the ion pumps which produces the electrochemical potential differences for ions across the membrane. These quantities in turn become the driving forces for the passive ionic fluxes whose values determine the resting membrane potential (E^M). The same arguments as developed in animal cells have been used for many years in plant cells in order to relate the resting membrane potenial with the ionic compositions inside and outside the cell. Accordingly, it was suggested that ion pumps do not transfert net electrical current across the membrane and therefore the total diffusive or passive ion transport across the membrane should correspond to a total zero electric current, thus

$$Z_i J_i^A = Z_i J_i^P = 0$$

where J is the flux of species i and superscripts A and P refer to the active and passive transport, respectively.

The Goldman-Hodgkin-Katz equation

$$E^M = E^G = \frac{RT}{F} \ln \frac{P_K \cdot C_K^I \cdot P_{Na} \cdot C_{Na}^I \cdot P_{Cl} \cdot C_{Cl^-}^{II}}{P_K \cdot C_K^{II} \cdot P_{Na} \cdot C_{Na}^{II} \cdot P_{Cl} \cdot C_{Cl^-}^I} \quad 1$$

becomes valid with the conditions state above, applied to the major univalent cations and anions. Its derivation relies moreover on the assumption of a constant electric field in the membrane interior. In equation [1], the P_i's are the permeability coefficients and C_i^I and C_i^{II} are respectively the external and internal concentrations. We deduce immediately from equation [1] that the value of E^G can only vary within extreme values set by the equilibrium potential of the ions that exhibit the highest permeabilty P_i. In connection with the determination of E^M, it must be stressed that the internal activity of any diffusible ion which does not participate to any active transport is determined by the equality of its equilibrium potential difference with E_M. The transport rate of such ion is given by its exchange transfer rate across the membrane.

For most plant cells placed in ordinary life conditions, we cannot accept any more today the validity of the Goldman-Hogkin-Katz equation for E_M. Many investigations made obvious that the model of neutral pumps and related passive diffusion are inadequate. Among numerous experimental facts that bear evidence as to the transfer by the pumps of a net charge across the membrane, the so-called electrogenic process, let us mention the phenomena of hyperpolarization where the resting potential, E^M, is displaced towards more negative value than E^G, the strong correlation between inhibition of pumps and membrane conductance and the important temperature effects on E^M and on the membrane conductivity. The recognition of an electrogenic transfert across plant membranes has led to several theoretical treatments with a view to correct the Goldman-Hodgkin-Katz equation. These treatments generally admit that one type of ionic pump is prevailingly responsible for the overall electrogenic effect in each type of membrane system. In non-marine plants like in Characean cells, the strong external and/or

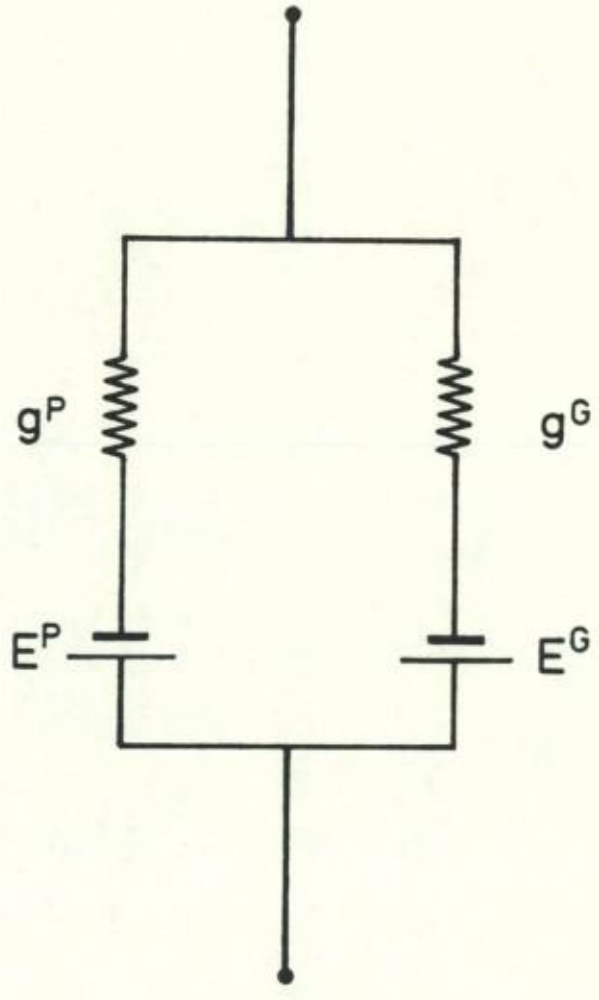

Figure 3: Electrical equivalent circuit for a membrane containing electrogenic ion pump.

internal pH dependence of both membrane potential difference and conductance have led to assess the role of an electrogenic proton pump. A perfect selective proton transfert mechanism is easily conceivable and its role appears particularly suggestive in relation to the paradigmatic frame of reference of the chemiosmotic theories.

The cell is represented by a single compartment of finite volume II in contact across a living membrane with an external medium I of fixed composition and pH and of unlimited dimension.

Working on Nitella clavata, Kitasato (1968) put forward the hypothesis that a large passive influx of protons had to be correlated to an electrogenic efflux of protons. Therefore, he introduced C_H^I and C_H^{II}, respectively, in the numerator and denominator of equation [1], both terms being affected by a permeability factor P_H of high value. He assumes further that the electrogenic pump works as current source and he described the membtrane potential by the equation

$$E^M = E^G - \frac{F J_{H^+}^A}{g^M} = E^{H^+} - \frac{F J_{H^+}^A}{g^M} \qquad [2]$$

where g^M is the chord conductance of the membrane and E^{H^+} the equilibrium potential of H^+. A theoretical justification of this expression cannot be readily found unless one refers to the equation given by Rapoport (1976):

$$E^M = \frac{\sum lowerig_i^M}{\sum} lowerig_i^M \qquad [3]$$

which is only valid in the case of a linear relationship between the passive flux and the membrane potential.

It is found experimentally that E^M tends towards E^{H^+}, when the pump is inhibited and not towards E^{H^+}, as given by equation [2]. This remark has led Spanswick (1972) to reject the hypothesis of a large passive H^+ influx and to propose an alternative explanation in terms of an electric analog for the membrane (Figure 3). In this circuit the conductances of the passive channels have been lumped together as g^D and are in series with the diffusion potential, E^D (equal to E^G). The pump is in parallel with the passive channels and has a conductance, g^P, and an electromotive force, E^P. According to the electrical equivalent circuit of Figure 3 the membrane potential difference may be written in terms of the potentials and conductances as:

$$E^M = \frac{E^P g^P + E^D g^D}{g^P + g^D} \qquad [4]$$

The value of E^P has been obtained from Rapoport's (1976) thermodynamic treatment under the condition of the proton pump at equilibrium

$$E^P = \frac{\Delta\mu^P}{\nu_{H^+} \cdot F} - RT \ln \frac{(H^+)^I}{(H^+)^{II}} \qquad [5]$$

a condition which does not seem to be realized in the case of Characean cells. This equation could obviously account for the observed dependence of the membrane potential difference on the external pH if g^P is much greater than g^D.

The hypothesis that the electrogenic pump contributes the major part of the membrane conductance received support from experiments which show a correlation between the decrease of membrane conductance and the membrane depolarization (Spanswick 1972, 1974, Keifer and Spanswick 1978). This hypotesis did not achieve a universal acceptance. For instance, in both intact and perfused tonoplast-free cells of Chara it was shown that there is a poor correlation between the membrane depolarization and the decrease in membrane conductance (Fujii et al 1979, Tazawa and Shimmen 1980, Homblé 1987). This suggests that the pump conductance is not coupled directly to the electrogenic active transport. Moreover, from their measurements on perfused tonoplast-free cells Fujii et al. (1979) infer that the pump conductance is much smaller than the passive conductance.

In my opinion the Spanswick's model lacks physical consistency: if the proton pump is at equilibrium and has the largest conductance ($g^P >> g^D$) no net proton flux will be expected at steady state. This is obviously not the case (Fujii et al. 1979, Kawamura et al. 1980, Shimmen and Tazawa 1980b, Tazawa and Shimmen 1982).

It has been suggested that in Characeae cells the cytoplasmic pH is controlled by the proton pump: the so called biophysical pH-stat (Smith and Raven 1979). According to Spanswick's model an increase in pH difference across the plasmalemma can be achieve only at the expense of a membrane hyperpolarization. This is what happens in Chara over an external pH range 5 to 7, resulting in an almost constant cytoplasmic pH (Smith 1984a, 1984b). At alkaline pH an active influx of HCO_3^- might be involved in cytoplasmic pH regulation. In charophytes, HCO_3^- influx is spatially separate from OH^- efflux, resulting in zones of low and high pH along the cell surface (Lucas and Smith 1973, Lucas 1976).

Assuming that in Chara corallina the cytoplasmic pH can be only controlled by a biophysical pH-stat mechanism a less restrictive modellistic approach has been developed (Homblé 1984, Jenard et al. 1986, Homblé et al. 1988, Homblé 1989). It assumes that there are essentially three types of transferable chemical species across the membranes:

a) Species which are neither actively transported by themselves, nor involved in chemical reactions (at equilibrium) with others which would be themselves actively transfered. The condition of stationaruty and the finiteness of the cell volume impose the equilibrium distribution of these species.

b) Species which are acively transfered and not involved in chemical equilibrium and not involved in chemical equilibrium with other transferable species. Their overall flux is zero by mutual compensation of active and passive transferts For instance, the calculation takes into account an anion (Cl^-), two monovalent cations (K^+, Na^+) and two divalent cations (Ca^{2+}, Mg^{2+}).

The two classes so far defined are called unreactive species.

c) Species involved in at least one chemical equilibrium with other transferable species. They are called reactive species and their flux balance must take into account the chemical reactions in the lateral phases. Only two types of reactions were considered: the water dissociation and the first dissociation of the carbonic acid. The three flux balances of the five chemical species which are interconnected by the conditions for equilibria are as follow:

$$J^{A}_{H^+} + J^{P}_{H^+} + J^{P}_{H_2O} + J^{A}_{H_2CO_3} + J^{P}_{H_2CO_3} = 0$$

$$J^{A}_{OH^-} + J^{P}_{OH^-} + J^{P}_{H_2O} = 0$$

$$J^{A}_{H_2CO_3} + J^{P}_{H_2CO_3} + J^{A}_{HCO_3^-} + J^{P}_{HCO_3^-} = 0$$

Assuming the continuity of the electrical potential, the continuity of the electrical displacement, and the electroneutrality inside the membrane, the integration of the Nernst–Planck equation leads to

$$C_i^{II} = \left(C_i^{I} - \frac{J_i^P RT}{z_i P_i F (\psi_s^{II} - \psi_s^{I})} \left\{ \exp\left(\frac{z_i F \psi_s^{II}}{RT} \right) - \exp\left(\frac{z_i F \psi_s^{I}}{RT} \right) \right\} \right) \exp\left(- \frac{z_i F E^M}{RT} \right)$$

which reduces to the equilibrium condition when $J^P=0$. The factor J_i^A/P_i represents a parameter which emphasizes the fact that the efficiency of a particular active ion flux in generating composition and potential difference is not accounted for by its magnitude only but also by the ability of the species to flow back passively through the membrane. In equation [6] P_i, C_i and z_i are respectively the permeability coefficient, concentration and number of charge (with sign) of the ionic species, ψ_s the potential at the membrane surface and E^M the membrane potential difference. According to this model, consistent values of E^M and of internal concentrations are generated if values of $(J^A/P)_{Cl}$ and $(J^A/P)_{HCO_3^-}$ are both positive (inward flow) and are, at least, of one order of magnitude larger than values of all other $(J^A/P)_i$. The existence of an inward electrogenic active transport of anions appears thus of prime importance for the generation of both resting membrane potential and overall internal ionic concentration. This model, which accounts for a biophysical regulation of the cytoplasmic pH, supports experimental investigations showing that in experimental conditions which are close to natural living conditions the inward pumping of HCO_3^- is electrogenic (Walker and Smith 1977, Keifer and Spanswick 1978). According to Lucas (1975) the maximum HCO_3^- influx is 60 pmol cm^{-2} S^{-1}. Therefore, the maximum conductance of the HCO_3^- pump is 100 μS cm^{-2}. This value is close to the observed membrane conductance at pH 6 to 10 (Richards and Hope 1974, Keifer and Spanswick 1978, Bisson and Walker 1982, Bisson 1986). The concentration of HCO_3^- in solution at pH 6 is 5 μM when in equilibrium with air. The rate of HCO_3^- fixation in Chara corallina is dependent on its concentrantion in the extracellular solution. This relationship is well fitted using the Michaelis–Menten equation with K_m = 0.6 mM and V_{max} = 70 pmol cm^{-2} s^{-1} (Lucas 1975). Thus, at a concentration of 5 μM the fixation of HCO_3^- will be about 0.58 pmol cm^{-2} s^{-1}. This is equivalent to a conductance of about 2.9 μS cm^{-2} which is two orders of magnitude smaller than the measured membrane conductance. Alkaline solutions should

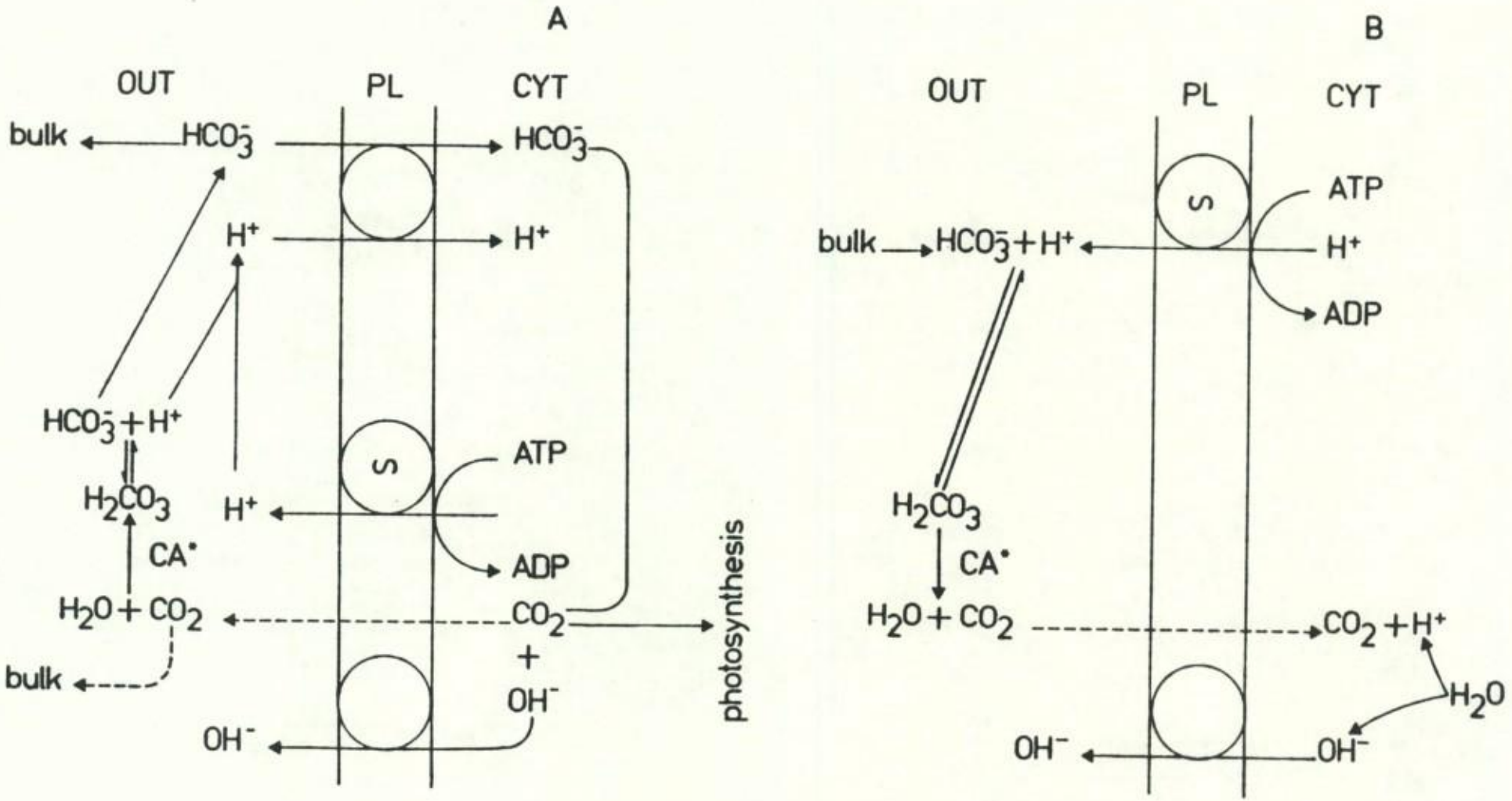

Figure 4: Mechanism of inorganic carbon acquisition

contain significant amounts of HCO_3^- to saturate the operation of the HCO_3^- uptake mechanism and to account for the measured values of membrane conductance.

4.2 The chemiosmotic conceptual approach.

A lot of work have been done to explain membrane transports on the base of the chemiosmotic theory. For instance, in Chara plasma membrane these transports include:

a) an H^+-ATPase which is electrogenic. The transport of one proton requires the hydrolysis of two ATP and magnesium as cofactor.

b) a $2H^+/Cl^-$-symport which is electrogenic. Using perfused tonoplast-free cell of Chara corallina Sanders (1980a) found that the active Cl^- influx is a secondary active transport of 1 Cl^- with 2 H^+. This Cl^- influx is controlled by both cytoplasmic pH and cytoplasmic Cl^- concentration (Sanders 1980b, Sanders and Hansen 1981).

c) an electrogenic urea uptake whose pH-dependence is consistent with its being an H^+ symport (Wilson et al. 1988).

d) an H^+/HCO_3^- (electrogenic?) -symport which provides a carbon-acquisition mechanism at alkaline pH. It has been suggested that carbon-acquisition could involved an external carbonic anhydrase. Both views are consistent with experimental findings and in any case an H^+-uniport will be expected.

e) uniports of K^+ and NH_4^+ (Walker et al. 1979)

f) a Na^+/H^+-antiport which would keep cytoplasmic Na^+ low (Clint and MacRobbie 1987).

g) in Chara which show sprouting of new shoots and rhizoids at their nodes the electrochemical gradient of Na^+ can be used to cotransport K^+ and urea (Smith and Walker 1989).

There are three possible mechanism for HCO_3^- uptake by charophyte cells: HCO_3^- uniport, H^+-HCO_3^- symport and CO2 uptake. All three mechanisms generate OH^- and electric currents. The latter two mechanisms must be linked to the primary active H^+ transport. The HCO_3^- uniport mechanism can be ruled out because it has been shown that localized pH banding and electric currents exists when Chara cells are in alkaline solutions which contain no HCO_3^- or CO_2 (Lucas 1976, 1982). However, whether or not HCO_3^-, per se, is carried across the plasmalemma remains controversial. The alternative to HCO_3^- transport is the extracellular production of CO_2 from the exogenous HCO_3^- in the unstirred layer of solution surrounding the plasmalemma (Ferrier 1980, Walker et al. 1980). The work of Price et al. (1985) suggests that carbonic anhydrase has an important role in dissolved inorganic carbon assimilation by Chara. The conclusion is based on the carbonic anhydrase inhibitor, ethoxyzolamide, which inhibits photosynthesis at pH 9.3, but not at pH 5.5. The location of the carbonic anhydrase is unknown, but it could be extracellular, as it is in Chalmydomonas reinhardtii (Kimpel 1983). If Chara possesses a H^+-HCO_3^- symport mechanism that is driven by a proton ATPase then the carbonic anhydrase must recapture the CO_2 that has leaked out from the cytoplasm (Figure 4a). Alternatively, if the H^+-HCO_3^- cotransport system does not exist, then this enzyme functions to dehydrate the carbonic acid (Figure 4b).

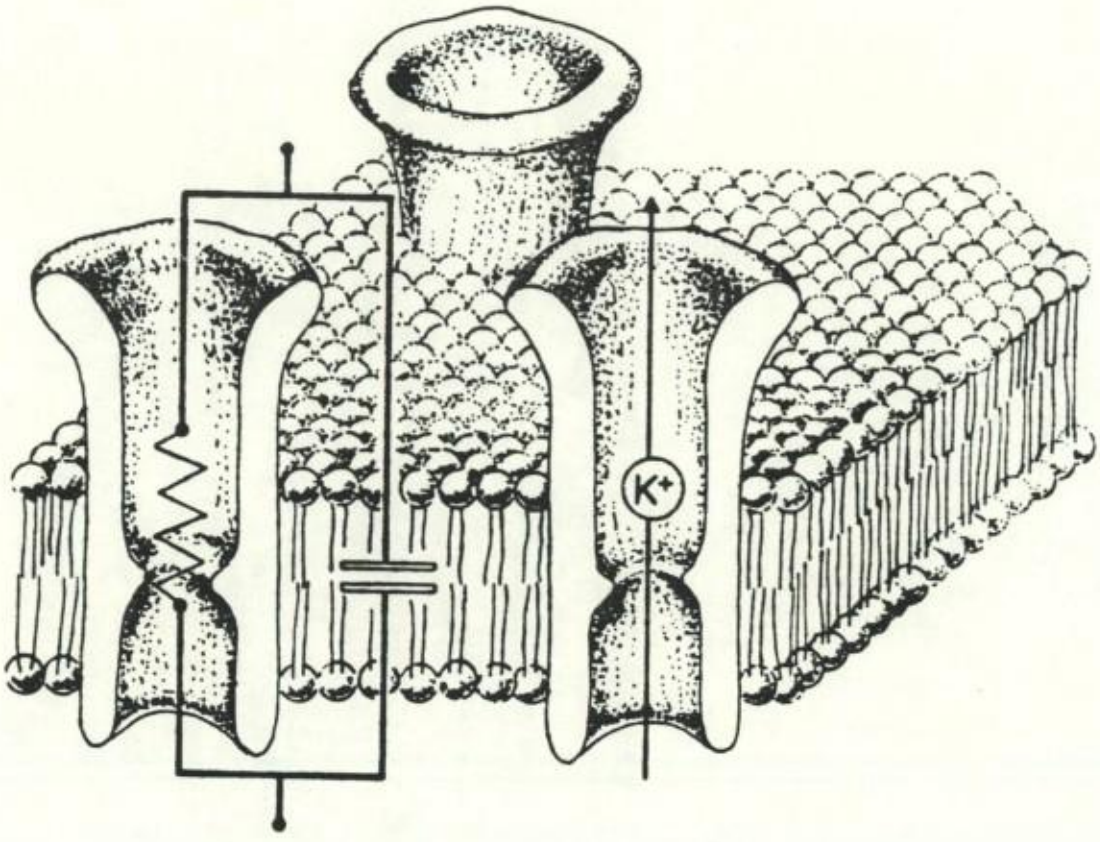

Figure 5: Electrical equivalent circuit of a membrane.

5 ELECTRICAL PROPERTIES OF PLANT CELL MEMBRANES

5.1 Introduction

The use of electricity in plant physiology is natural from the biophysical point of view, since many substances transported in the plant are charged, and since electrical signals have properties suitable for both transfer and transduction of informations. Moreover, it is now well established that most cells use the flow of electric current to perform some of their natural functions.

It is a common practice to analyze the properties of a membrane in terms of an electrical equivalent circuit consisting of a resistor in parallel with a capacitor (Figure 5). It is now generally accepted that the unit membrane can be described by the "Lipid-Protein Mosaic" model proposed by Singer and Nicolson (1972). According to this model the structure of the unit membrane consists of a fluid lipid bilayer, to the surface of which may be attached functional proteins (the extrinsic proteins) and which may contain intrinsic proteins embedded in the bilayer. Some of the intrinsic proteins can span the membrane; others are exposed only on one of its surfaces. A protein will penetrate the lipid bilayer to different depths, depending upon the relative number and location of its hydrophobic and hydrophilic groups.

The presence of transmembrane proteins helps account for some specific biophysical and biochemical properties of the membrane. For instance, active and passive transports of specific ions are some of the electrical functions attributable to these proteins. These transport functions are responsible for the conductance properties of the membrane.

An active transport is the transfer of a particle against its electrochemical gradient, and it requires energy which is usually provided by the cellular metabolism, whereas a passive transport occurs when a particle moves down its electrochemical gradient. More recently, these two kinds of transport have been distinguished on the basis of their rate of ion transport. For instance, the rate of passive transport of potassium ions through a single K^+-channel of Chara corallina is $5\ 10^7$ ions/s at -5 mV (Homblé et al. 1987) whereas the rate of active transport through the sodium-potassium pump is $5\ 10^2$ Na^+/s (Jorgensen 1975).

The fact that biological membranes behave as capacitors implies that a steady state membrane potential difference is associated with a charge separation. The lipid bilayer of membranes separates both internal and external electrolyte solutions by a thin insulating layer, which impedes the movement of ions from one side of the membrane to the other. Such interface between two conducting solutions forms a significant electrical capacitor.

It is interesting to point out that some authors put an electromotive force in series with the resistor of the electrical equivalent circuit of the membrane to emphasize that the net driving force on an ion, i, is the difference between the membrane potential (E^M) and the equilibrium potential of that ion (E^i) and not simply the membrane potential, as suggested by Ohm's law. For instance, for the case of potassium ions the steady state current-voltage law is given by:

$$I_K = g_K\left(E^M - E^K\right), \qquad [7]$$

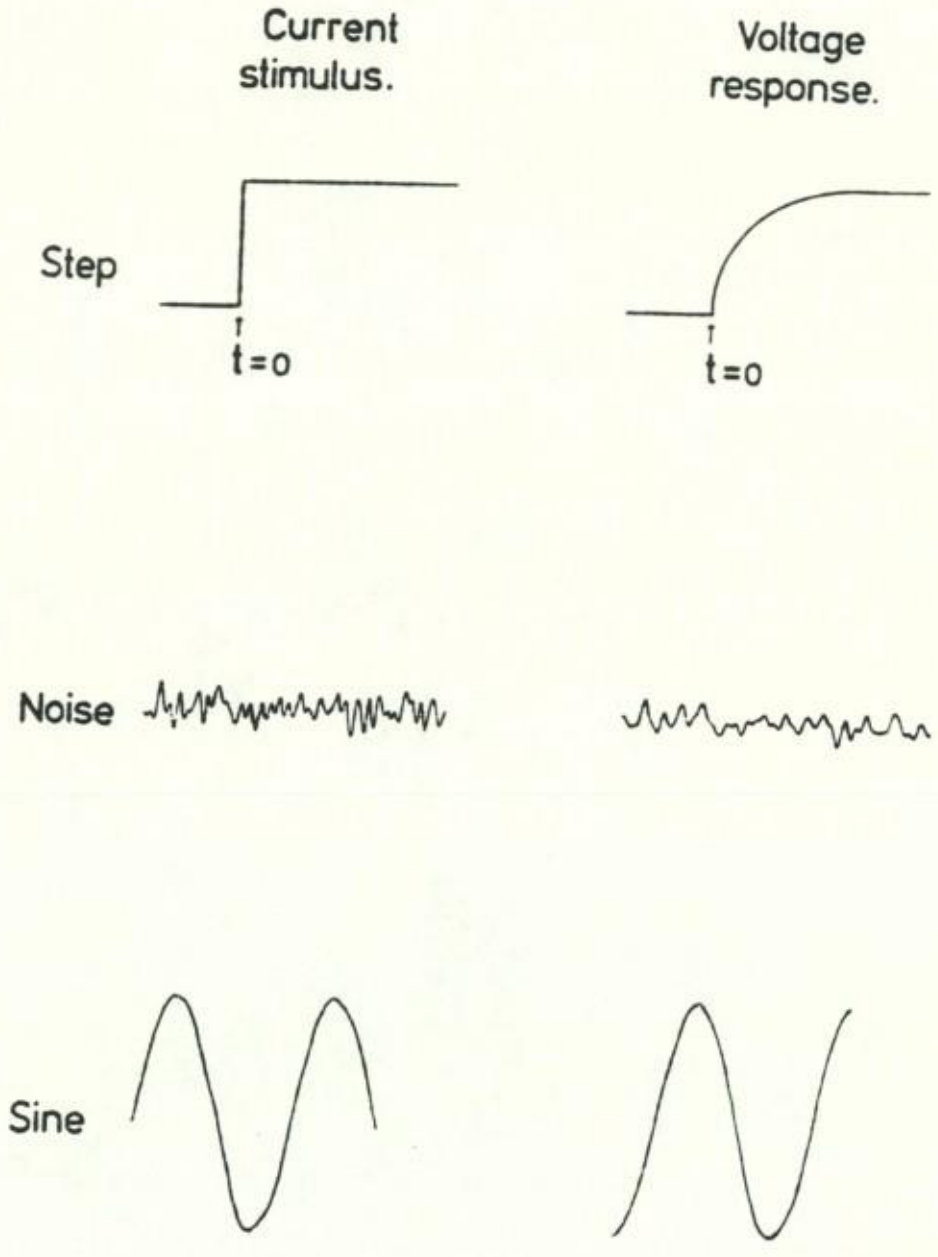

Figure 6: Electrical signals used for the impedance spectroscopy.

where I_K is the specific potassium current and g_K is the specific potassium conductance.

The general approach used for impedance spectroscopy experiments on plant cells is to apply an electrical stimulus (a known voltage or current) to the membrane and to observe the response (the resulting current or voltage respectively). Three different types of electrical method are used in impedance spectroscopy (Figure 6):

a) the transient method: a step function of current may be applied at t=0 to the membrane, and the resulting time-varying voltage measured. The electrical signals are usually mathematically transformed into the frequency domain using the Laplace transform in order to calculate the frequency dependent impedance. For this reason we have called this method the Laplace transform analysis (Homblé and Jenard 1986; 1987);

b) the white noise analysis: in this case the stimulus is an electrical current composed of random (white) noise, and the resulting voltage is measured. One generally Fourier-transforms the electrical signals to pass into the frequency domain (Marmarelis and Marmarelis 1978; Ross et al. 1985);

c) the sinusoidal analysis: this is the most common method used for impedance spectroscopy measurements. The impedance is measured directly in the frequency domain by applying a single-frequency sinusoidal current to the membrane and measuring the phase shift and amplitude of the resulting voltage signal at that frequency (Kishimoto 1974; Coster and Smith 1977; Vorobiev and Musaev 1979).

5.2 The Laplace and Fourier transform

The transform theory is developed in many textbook on mathematics (Boas 1966), and we will here only mention definitions and transform properties which are related to our purpose.

The bilateral Laplace transform (X(s)) of a function x(t) is defined by the following equalities:

$$X(s) = L\{x(t)\} = \int_{-\infty}^{+\infty} x(t)\exp(-st)dt \qquad [8]$$

where the symbol L is a linear operator which satisfies the important property of superposition:

$$L(uV + vW) = L(uV) + L(vW) = uL(V) + vL(W) \qquad [9]$$

where u is a constant and V and W are functions of t. When the linear operator L applies upon variables and functions which have a physical meaning, t and s have inverse dimensions. In the most frequent case, and especially when we are dealing with the study of an electrical signal, t has the dimension of a time and s has the dimension of a frequency.

The variable s is a complex number:

$$s = \sigma + j\omega \quad \text{where } j = \sqrt{-1}. \qquad [10]$$

When s is purely imaginary (s = j ω), the Laplace transform of x(t) reduces to the Fourier transform of x(t), that is:

$$X(j\omega) = \int_{-\infty}^{+\infty} x(t)\exp(-j\omega)dt. \qquad [11]$$

Transforms have their reciprocal counterpart (called inverse transforms) which permit the recovery of x(t) when X(s) is known. In general cases the inverse Laplace transform is given by:

$$x(t) = L^{-1}\{X(s)\} = \frac{1}{j2\pi}\int_{\sigma-j\omega}^{\sigma+j\omega} X(s)\exp(st)ds. \qquad [12]$$

The inverse Laplace transform is much more difficult to perform than the direct one, for reasons related essentially to the condition of convergence of the integral. Thus, if you are not a trained expert, you should refer to a published table of transform pairs (e.g., Abramowitz and Stegum 1970) when you will be confronted to such necessity.

Practically, the lowest time limit of the integral in equation [2] is kept at $-\infty$ in the Fourier transform and is set to zero in other cases. Therefore, a somewhat different form of the Laplace transform, often referred to as the unilateral Laplace transform or simply the Laplace transform, can be defined which plays an important role in analyzing linear systems. The (unilateral) Laplace transform L(s) of a signal x(t) is written:

$$L(s) = \int_{0}^{+\infty} x(t)\exp(-st)dt \qquad [13]$$

The main difference in the definition of the bilateral and unilateral Laplace transforms (equations [8] and [13], respectively) lies in the lower limit on the integral. The unilateral Laplace transform depends on the signal from t = 0 to t = $+\infty$, whereas the bilateral Laplace transform depends on the whole signal from t = $-\infty$ to t = $+\infty$. The unilateral Laplace transform must not be seen as a new kind of transform, but simply as a bilateral Laplace transform of a function whose value is set to zero for t < 0. Therefore, two signals which are identical for t > 0 but differ for t < 0 will have the same unilateral Laplace transform but a different bilateral Laplace transform. From the experimental point of view the Laplace transform (unilateral) is particularly relevant when a linear system is stimulated by a step function (Figure 6), because in this case both input and output signals and their derivatives will be equal to zero for t < 0 but not necessarily for t > 0.

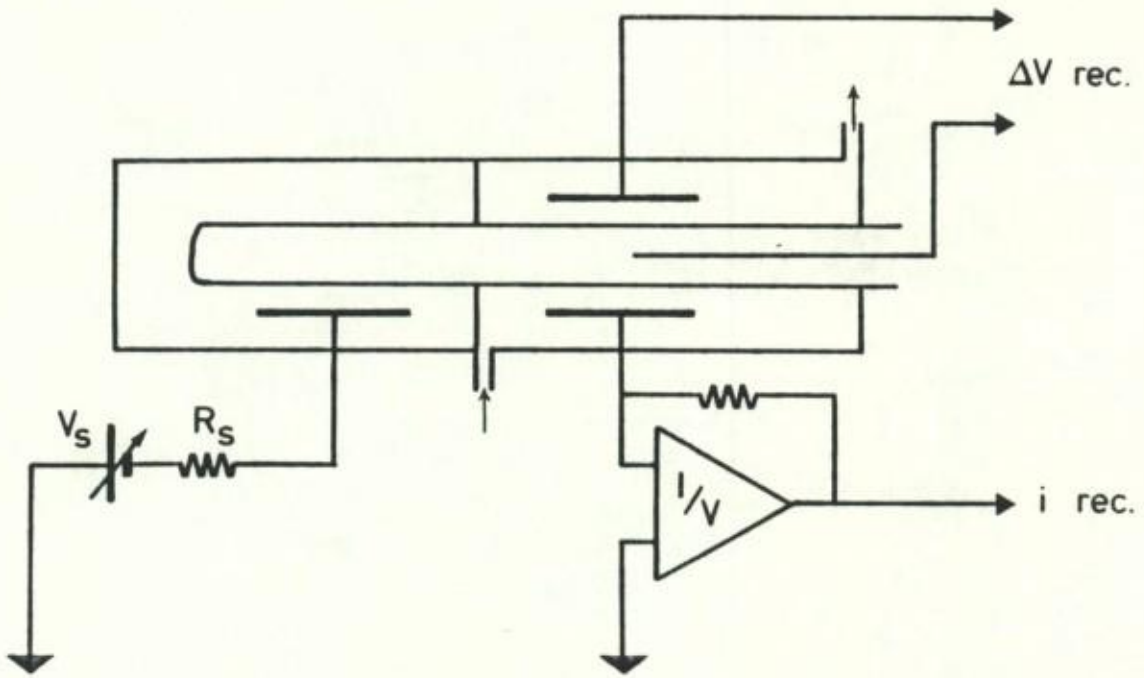

Figure 7: Schematic diagram of a simple current clamp device.

5.3 Measuring techniques

Impedance spectroscopy measurements require electronic devices for recording bioelectric signals and for the stimulation of plant cells. Any arbitrary time domain excitation can be used to measure the membrane impedance, provided that both applied excitation and recorded response are over a sufficiently long time to complete the Laplace transform over the desired frequency band. In order to study the electrical properties of plant cells, different kind of electrical stimulus may be used. When the stimulus is a voltage signal, the membrane current is the response. Conversely, one gets a membrane voltage response when a current stimulus is applied to the membrane.

5.4 Current clamp and voltage clamp techniques

Both time- and voltage-dependent ionic conductances and voltage-independent ionic conductances are found in biological membranes. Two experimental methods have been developed in order to determine the relationship between the voltage applied across the membrane and the current flowing through it: these are the constant current or current clamp and the constant voltage or voltage clamp techniques. In the case of the current clamp, one applies a constant current step to the membrane and records the resulting membrane potential changes. In the case of the voltage clamp, the magnitude of the membrane potential is imposed, and one monitors the resulting current which flows through the membrane. The current clamp method is of limited use when ionic conductances change at a threshold potential, because in this case unstable potentials arise which are not attainable by a constant current.

A current clamp system is easier to set up than a voltage clamp system. A constant current source is obtained with a power supply V_s in series with high value resistor R_o (Homblé et al. 1988). The series resistor must be much more larger than the membrane resistance in order to avoid any current change in response to a change in membrane conductance. This system is depicted in Figure 7.

A voltage clamp system involves the use of a negative feedback circuit. Different electronic circuits have been described in detail in the literature (Kishimoto 1961; Beilby and Coster 1979a; Homblé 1988). In Figure 8 a simple and general scheme of a voltage clamp set up is displayed. In this diagram, the properties of the electrometer which feels the membrane potential and the current to voltage converter (I/V) are both assumed to be ideal (no phase shift and potential perturbation). The membrane potential difference (E^M) is compared to a command potential (E) at the input of a large gain amplifier (G). The polarities are so arranged that the output voltage of G(ΔV) force the membrane potential to be equal to the command potential. The access resistance R_A arises from the electrodes, and R_o is the serial resistance which accounts for the solution conductivity. Assuming that the values of the circuit elements are at steady state, the operation of the voltage clamp circuit can be readily understood. The output voltage of the feedback amplifier G is equal to:

$$\Delta V = \left(E - E^{M}\right)G \qquad [14]$$

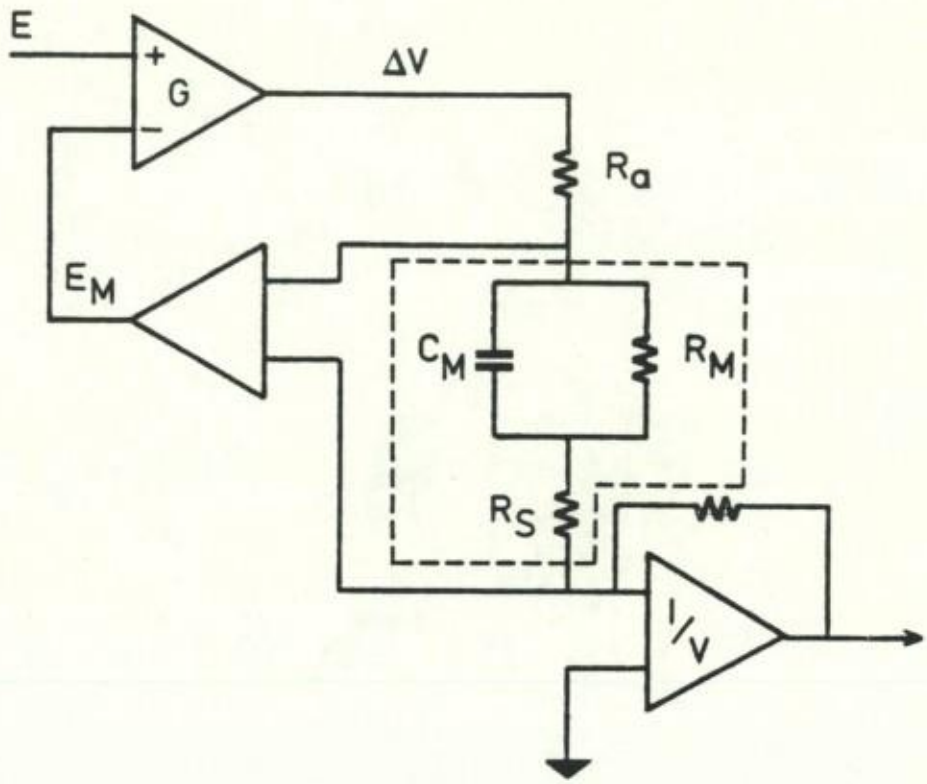

Figure 8: Schematic diagram of a voltage clamp device.

where G is the amplifier gain. Moreover, this output voltage is distributed between the voltage drop across the access resistance (R_A) and the voltage drop across the membrane , so that:

$$\Delta V = IR_A + E^M. \qquad [15]$$

Combining these two equations, we find:

$$E^M = \frac{EG}{(1+G)} - \frac{IR_A}{(1+G)}. \qquad [16]$$

Hence, we observed that a large gain for the feedback amplifier minimizes the effect of the access resistance and forces the membrane potential to be equal to the command potential. It is worth stressing the fact that E^M should be close to E. Because of the presence of R_S between the membrane and the voltage recording electrodes, E^M will differ from E by the voltage drop produced by the membrane current flowing across the series resistance R_o.

5.5 Instrumentation

Most biophysicists build at least part of their measuring equipment by themselves. Modern equipment is built with integrated circuits. Each integrated circuit may contain many transistors, along with capacitors and resistors, all fabricated on a single slab of highly purified silicon. We will briefly describe later the main electronic components which are now in common use in electrophysiological equipment. The brief account in this section can only be considered a survey. No attempt is made to derive the fundamental mathematical relations; a more complete treatment can be found in numerous textbooks (Graeme et al. 1971).

5.5.1 Operational amplifier

The term "operational amplifier" was originally introduced by workers in the analogue computer field to denote an amplifier circuit which performed various mathematical operations such as integration, differentiation, summation and multiplication.

It is not essential that the user of operational amplifiers be familiar with the intricacies of the internal circuit details, but he must understand the function of the external terminals provided by the manufacturer. In a first consideration of operational amplifiers it is convenient to assume that the amplifier has ideal characteristics: infinite gain, infinite input impedance, zero output impedance and infinite frequency bandpass.

Most operational amplifiers have two input terminals, only one of which produces an inversion of sign. The terminals are conventionally marked + and −, as in Figure 9. These designations do not mean that terminals are to be connected only to potentials of the indicated sign, but rather that the one marked − gives sign inversion and the other (marked +) does not. In those operational amplifiers which have only a single input, it is always the non inverting one which is omitted. In case the non inverting input is

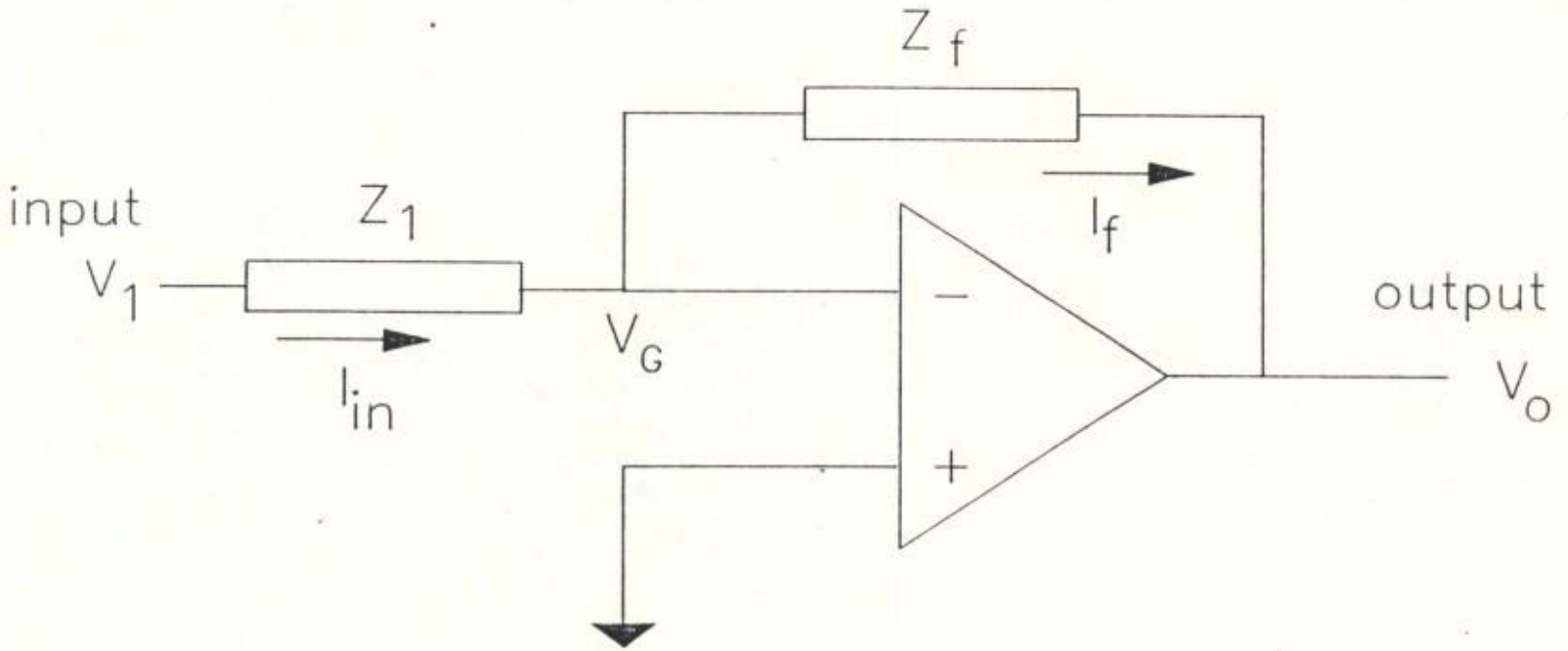

Figure 9: The operational amplifier.

not required in a particular application, it should be grounded to avoid instability.

The basic connections of an operational amplifier are shown in Figure 10.

Most circuits using operational amplifiers depend on negative feedback: a connection is made through a suitable impedance Z_f from the output to the inverting input. If the signal to be sensed by the amplifier is a voltage, then it must be applied through an impedance Z_1.

Since the input to the ideal amplifier draws negligible current (because of the infinite input impedance), the current flowing in Z_1, namely, $(V_1 - V_G)/Z_1$, must be equal to that in the feedback loop, given by $(V_G - V_0)/Z_f$. But the current in the feedback loop can come only from the output of the amplifier. Therefore, when an input signal is applied, the amplifier must adjust itself so that the feedback and input currents are precisely equal or:

$$I_i = I_f \qquad [17]$$

which leads to:

$$V_0 = \frac{V_G(Z_f + Z_i) - V_i Z_f}{Z_i}. \qquad [18]$$

This relation can be greatly simplified by taking into consideration the infinite gain of the ideal amplifier (often called its open-loop gain). This means that the potential V_G at the summing junction must be very small compared to V_0. Practically, V_G is so small (< 10 μV compared to ground) that the summing junction is commonly said to be at virtual ground. Hence, in equation [13] the term involving V_G can be neglected, giving:

$$V_0 = -V_i \frac{Z_f}{Z_i} \qquad [19]$$

which is the basic working equation of an operational amplifier.

If Z_f and Z_1 are purely resistive equation [18] shows that the output voltage will be the negative of the input multiplied by a constant. In case the value of Z_f is higher than Z_1, the ratio Z_f/Z_1 will be higher than 1, and the amplifier operates like a multiplicator; if Z_f is lower than Z_1 then the ratio Z_f/Z_1 will be lower than 1 and the amplifier operates as a divider.

Addition or substraction of several potentials may be accomplished by connecting different voltage sources to the summing junction through an appropriate resistor as shown in Figure 10.

The relation between the inputs currents and the feedback current is:

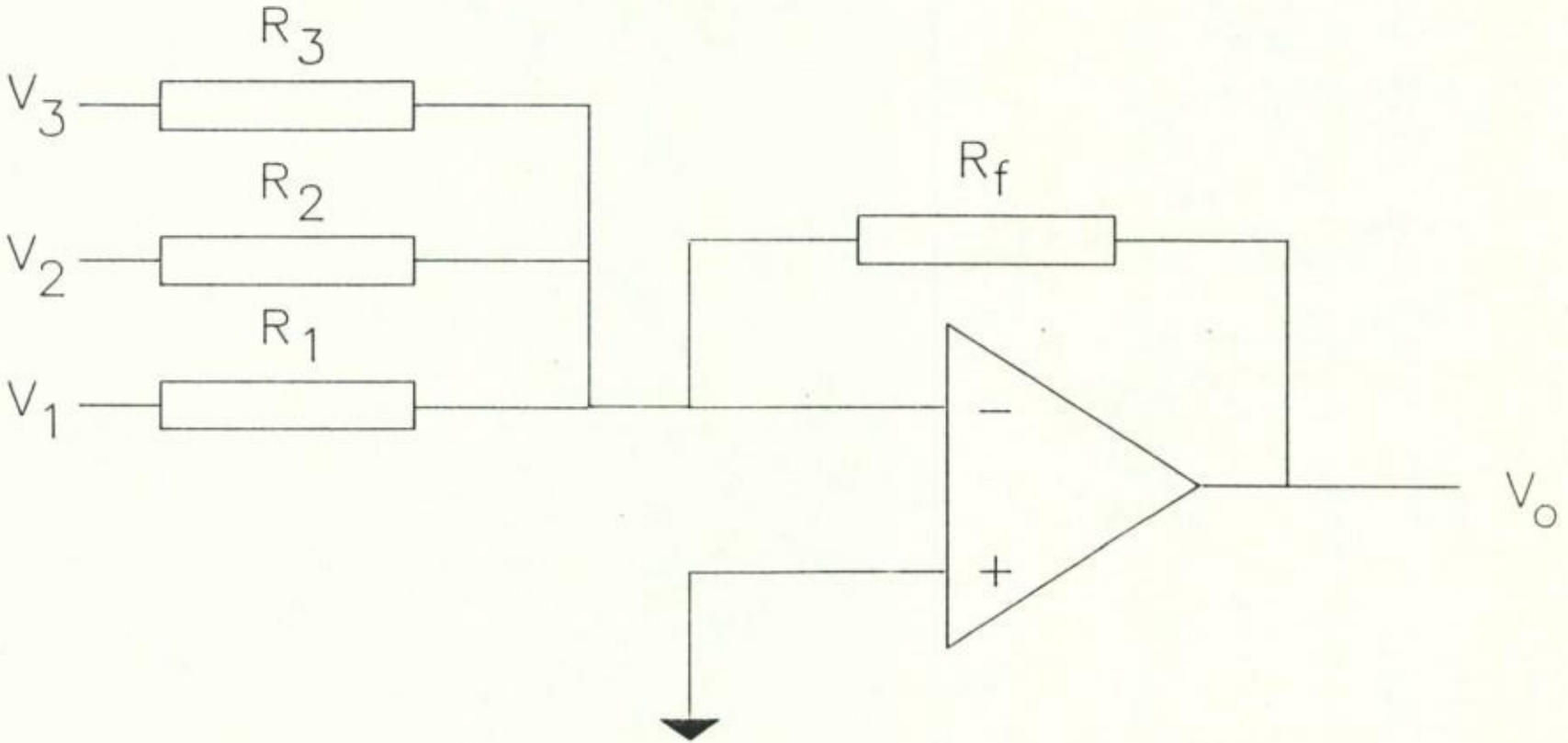

Figure 10: The summing amplifier.

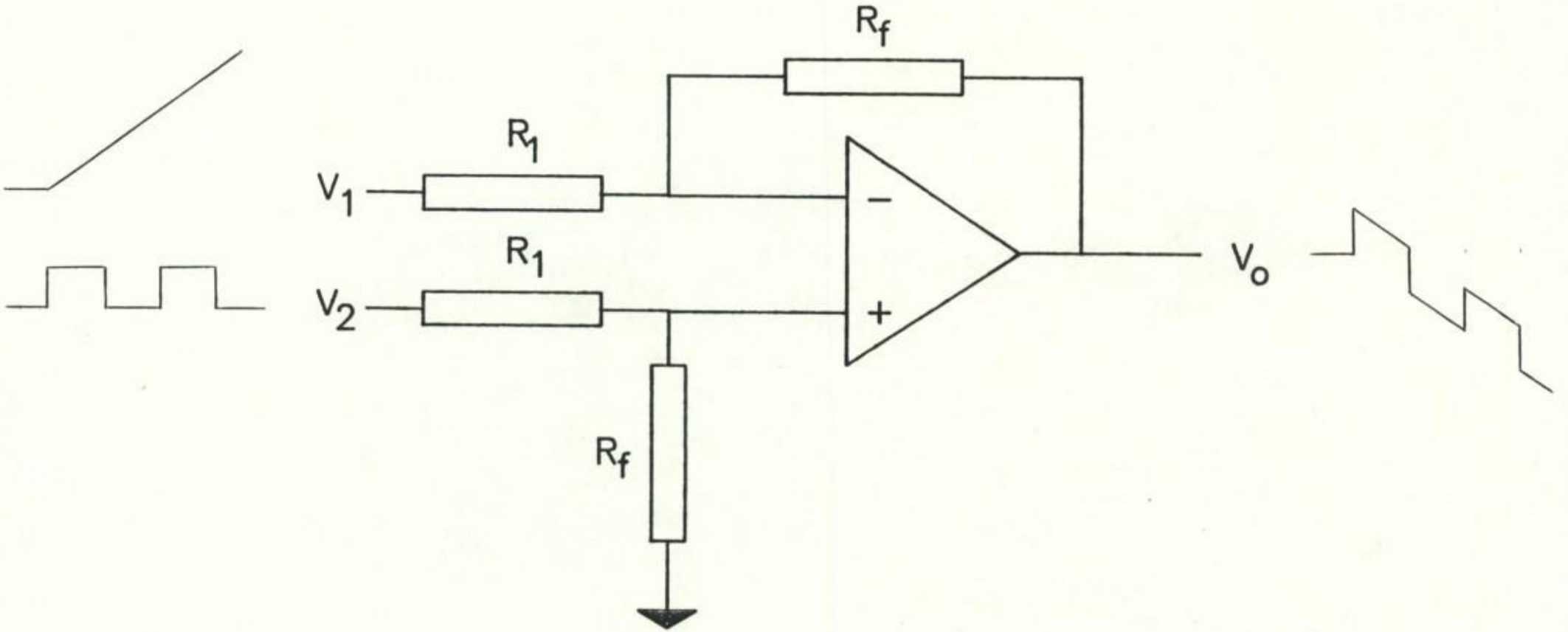

Figure 11: The differential amplifier.

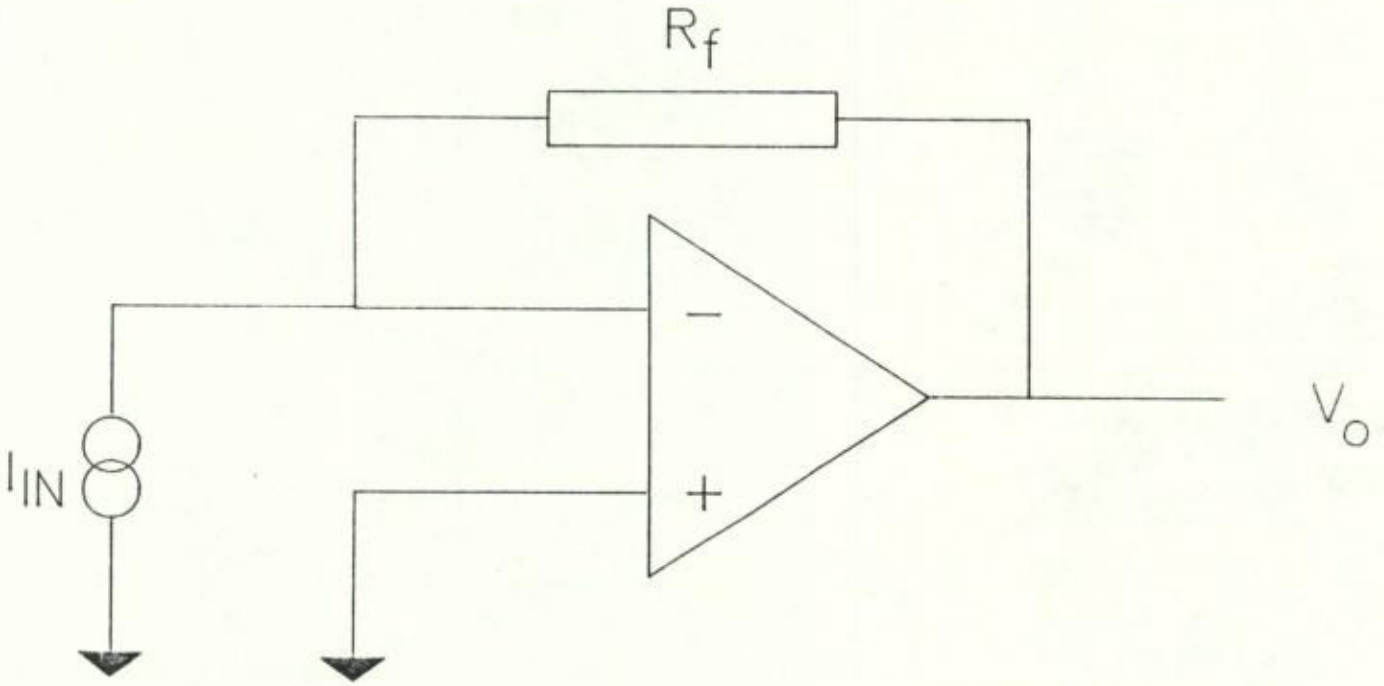

Figure 12: The current to voltage converter.

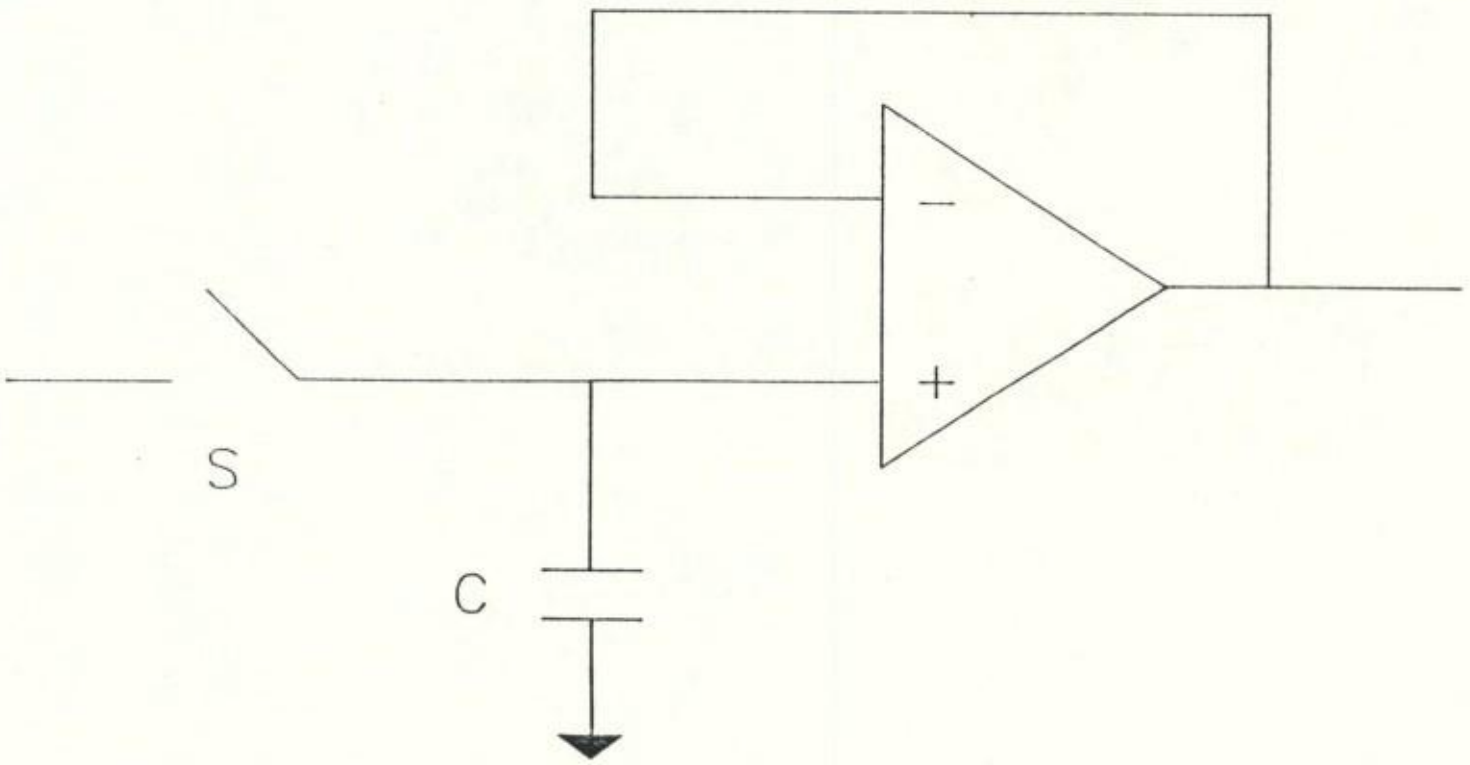

Figure 13: The sample-and-hold circuit.

$$-I_f = I_1 + I_2 + I_3 \qquad [20]$$

or, using Ohm's law:

$$-V_0 = \frac{R_f}{R_1}V_1 + \frac{R_f}{R_2}V_2 + \frac{R_f}{R_3}V_3 \qquad [21]$$

The differential amplifier (Figure 11) is widely used in instrumentation.

In this configuration it is the difference between the two input signals which is amplified. Following the same procedure as for equation [19] it can be shown that the equation governing this circuit is given by:

$$V_0 = -\frac{R_f}{R_1}(V_1 - V_2) \qquad [22]$$

where the suffix 1 and 2 refer to the negative and positive inputs respectively. The differential amplifier is advantageous because it discriminates against direct (zero frequency) current variations, drifts and noise.

Operational amplifiers are not only used to operate upon voltages. A current source may be connected to the inverting input of the amplifier (Figure 12).

Since the input impedance is infinite, no current flows into the operational amplifier, and the input current must be equal to the feedback current. Therefore, the output voltage will be equal to the product of the input current and the feedback resistor:

$$V_0 = -R_f I_i. \qquad [23]$$

5.5.2 Sample-and-hold

Although in practice one would generally use a ready-built sample-and-hold integrated circuit, it is useful to recall its basic operation. Figure 13 shows a very simple sample-and-hold circuit.

An incoming signal is fed into a capacitor when the (electronic) switch is closed. In this mode, the output of the amplifier will continuously follow the input signal. When the switch is opened and isolates the input signal from the capacitor, the output remains at the voltage last seen by the input capacitor.

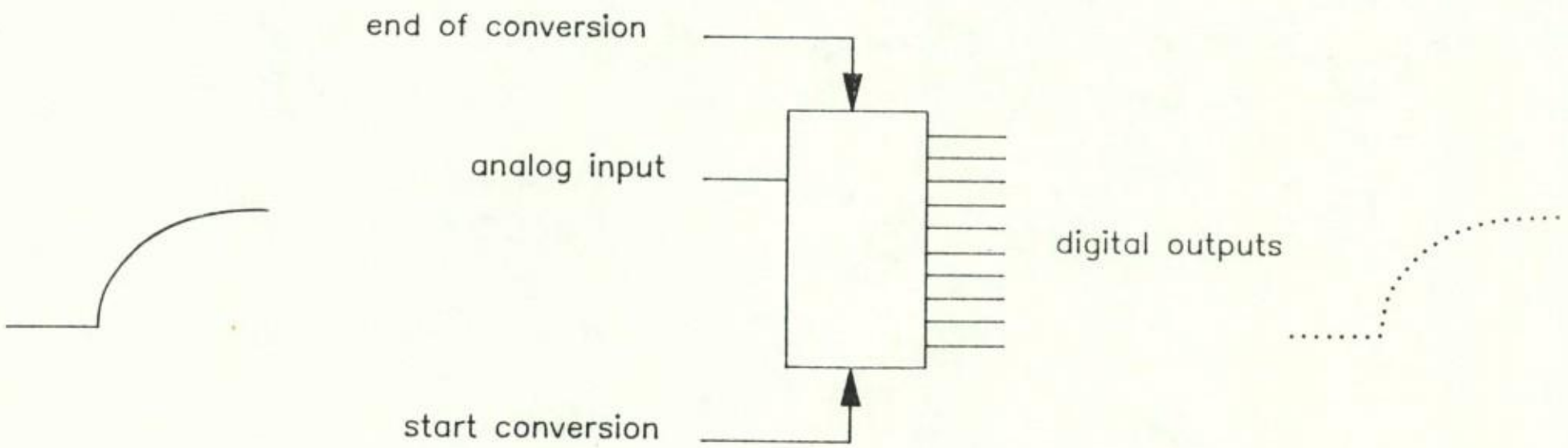

Figure 14: The analog to digital converter.

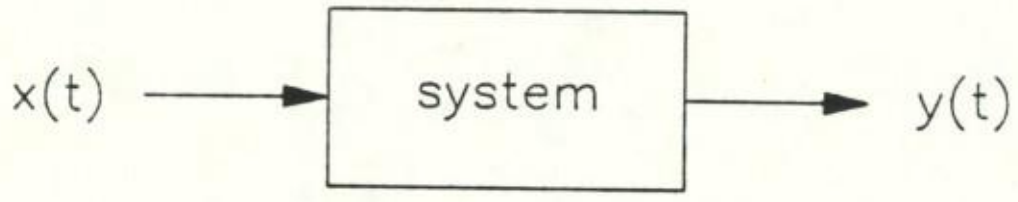

Figure 15: Basic diagram of a system.

5.5.3 Analog to digital converter

A typical analog to digital converter is illustrated in Figure 14. An analog to digital converter changes an analog or continuous voltage into a series of discrete digital values so that a computer can be presented with digital data in a format that it can handle. The conversion starts as soon as a pulse signal is sent to the appropriate input and lasts up to the time that an end of conversion signal is sensed by the analog to digital converter.

5.6 Data analysis technique

5.6.1 Theory

Electrical circuits built exclusively with passive elements such as resistors, capacitors and inductors belong to the class of linear systems. A linear system is one that possesses the property of superposition: if an input consists of the weighted sum of several signals, the output is simply the weighted sum (the superposition) of the responses of the system to each of those signals. Mathematically, this means that if $y_1(t)$ and $y_2(t)$ are the responses of a system to the continuous time functions $x_1(t)$ and $x_2(t)$ respectively then the system is linear if the response to:

$$ax_1(t)+bx_2(t) \text{ is } ay_1(t)+by_2(t) \qquad [24]$$

where a and b are any complex constant, and a system is defined as a "black box" that results in the transformation of signals. In plant physiology the black box might be a membrane, a cell, a tissue or even the whole plant. Such a system is usually represented pictorially, as in Figure 16, where x(t) is the input signal and y(t) is the output signal.

The behaviour of a linear system can be characterized by a linear constant-coefficient differential equation of the form:

$$y(t)+\sum_{i=1}^{n} A_i \frac{d^i y(t)}{dt^2} = B_0 x(t)+\sum_{k=1}^{n} B_k \frac{d^k x(t)}{dt^k} \qquad [25]$$

where t is the time, n is the order of the system and of its equation, A_i and B_k are constant coefficients depending of the circuit structure and of the magnitude of its elements, x(t) is the input signal imposed to the system and y(t) is the output signal. When x(t) is a known and derivable time function, the right hand side of equation [25] is a known time function, and the integration of this equation yields the output signal as solution.

In the case of plant cells, the system in consideration is an electric dipole which may be represented by a black box with two conducting wires coming out of it (Figure 15). There is a potential difference (V) between those wires, and they carry the same current (I), owing to the fact that there is no charge accumulation inside the black box.

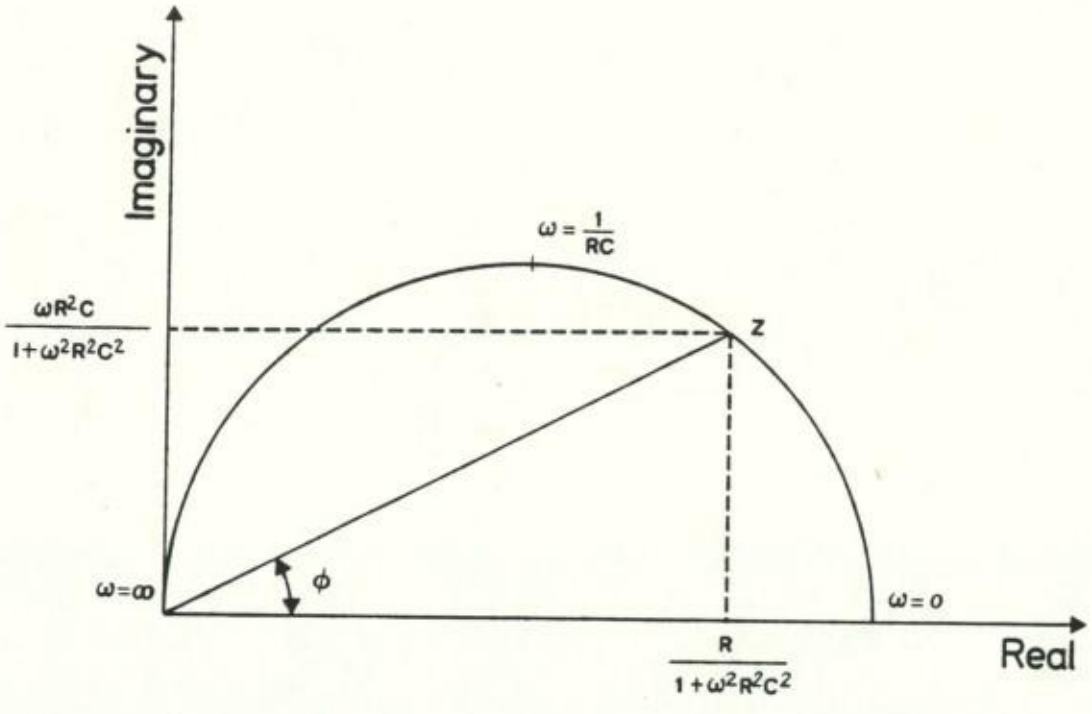

Figure 16: Impedance locus diagram for the parallel resistor-capacitor circuit

5.6.2 Complex impedance

Let us first consider the case where the steady state input voltage signal has the form:

$$V(t) = V_0 \cos(\omega t) = \Re\{V_0 \exp(j\omega t)\} = \Re\{V^*\} \qquad [26]$$

where V_0 is the amplitude of the signal and $\Re$ is the symbol for real numbers, indicating that we are dealing with the real part of the complex number enclosed in brackets only. This periodic signal has a single frequency component. Then the output current response (I) will have the form:

$$I(t) = I_0 \cos(\omega + \phi) = \Re\{I_0 \exp j(\omega t + \phi)\} = \Re\{I^*\} \qquad [27]$$

where I_0 is the amplitude and ϕ the phase of the current. Both amplitude and phase of the current response depend on ϕ and on the content of the black box. The quantity Z*, which is defined in the frequency domain by the relation:

$$Z^* = \frac{V^*}{I^*} \qquad [28]$$

is called the complex impedance of the system. The impedance is usually a complex quantity. For instance, the impedance of the electrical circuit in Figure 5 will be given by

$$Z(\omega) = \frac{R}{1 + \omega^2 R^2 C^2} - j\frac{R^2 \omega C}{1 + \omega^2 R^2 C^2} \qquad [29]$$

In the complex plane the real part is in the direction of the abscissa and the imaginary part is in the direction of the ordinate (Nyquist plot). The measurement of Z as a function of the frequency over a wide frequency range permits to draw the impedance locus diagram (Figure 16). Alternatively, the magnitude of the impedance vector and phase shift of the electrical signal can be plotted against frequency (Bode plot). In practice, the impedance locus diagram may differs from that shown in Figure 16 in three respects: a) the impedance tends to a finite real value as $\omega \to \infty$. This arises from the resistance in series with the membrane capacitance which is partly attribuable to the solution surrounding the membrane. b) the centre of the semicircle lies below the real-axis. This deviation from the ideal behaviour is still unexplained. c) in some cases, the impedance locus is not a simple semicircle. The deviations occur either because the membrane resistance change with time or because more than one membrane are in series between the measuring electrodes.

Changing the frequency of the input signal given by equation [29] and recording the corresponding current response will permit one to learn the complex impedance spectrum of the system. This procedure is time consuming because the experiment must be repeated for each frequency of interest.

It is possible to measure the frequency-dependent impedance of a biological membrane across a spectrum of frequencies simultaneously using the technique of Fourier analysis. The voltage power spectral density, $S_V(f)$, is equal to the current power spectral density, $S_I(f)$, multiplied by $|Z(f)|^2$, were (f) is the membrane impedance and f is the frequency. Fourier analysis of a time series consists in decomposing a function of time into a sum of sine and cosine waves of various frequencies and amplitudes. The relation between the parameters of the time domain to those of the frequency domain is given by Rayleigh's theorem:

$$\int_{-\infty}^{\infty} (\hat{}\, e(t) \,\hat{})^2 dt = \int_{-}^{\infty} \infty \left(\hat{}\, E(f)^2 \,\hat{}\right) df. \qquad [30]$$

This mean that the area uner the square modulus of a function, e(t), equals the area under the square modulus of its Fourier transform, E(f). For a signal which exists between t=0 and t=T, Rayleigh's theorem gives

$$\int_0^T e(t)^2 dt = \int_{-\infty}^{\infty} (\hat{}\, E(f) \,\hat{})^2 df. \qquad [31]$$

The average value of $e^2(t)$ is define as:

$$\langle e^2(t) \rangle = \frac{1}{T} \int_0^T e^2(t) dt. \qquad [32]$$

Thus, since |E(f)| is an even function of frequency, its integral may be expressed over all frequencies as twice the integral over the positive frequency. So, equation 32 can be written:

$$\langle e^2(t) \rangle = \frac{2}{T} \int_0^{\infty} \left(\hat{}\, E^2(f) \,\hat{}\right) df. \qquad [33]$$

The integrand on the right-hand side of Equation 33 is called the power spectral density. An ideal signal for this method is the white noise signal, which is a random signal having equal power spectral density at all frequency. The power spectral density associated with a record characteries the rapidity of fluctuations in the original record. For instance, if the measured current fluctuates at a very high rate, its Fourier decomposition would contain very many high frequency components so that its spectrum would have relatively large values for the high frequencies.

5.6.3 Operational impedance

Let us now consider the case where a transient signal formed from a whole set of frequencies is applied to the linear system. Equation [25] will describe the relation between the input and output signals. Applying the unilateral Laplace transform to both sides of equation [25] gives:

$$Y(s)\left\{1+\sum_{i=1}^{n}A_i s^i\right\}=X(s)\left\{\sum_{k=0}^{n}B_k s^k\right\} \qquad [34]$$

where $s = j\omega$, X(s) is the Laplace transform of the input signal (the voltage) and Y(s) is the Laplace transform of the output signal (the current). The quantity $Z_{op}(s)$, which is defined by:

$$Z_{op}=\frac{X(s)}{Y(s)} \qquad [35]$$

is called the operational impedance. It is worth noting that for a given circuit the expression of Z_{op} is identical to that of Z^*, where s is substituted for $j\omega$. Substituting equation [34] in [35] we obtain a general analytical expression for the operational impedance:

$$Z_{op}=\frac{\sum_{k=0}^{n}B_k s^k}{1+\sum_{i=1}^{n}A_i s^i}. \qquad [36]$$

As a relevant example we shall consider the operational impedance of the electrical equivalent circuit of figure 1. The differential equation relating the current (i) and the voltage (v) is:

$$i(t)=\frac{v(t)}{R}+C\frac{dv(t)}{dt}. \qquad [37]$$

Taking the Laplace transform of equation [37] we find:

$$I=\frac{V}{R}+CsV \qquad [38]$$

where I and V are the Laplace transform of the current and voltage respectively. Then from equation [35]:

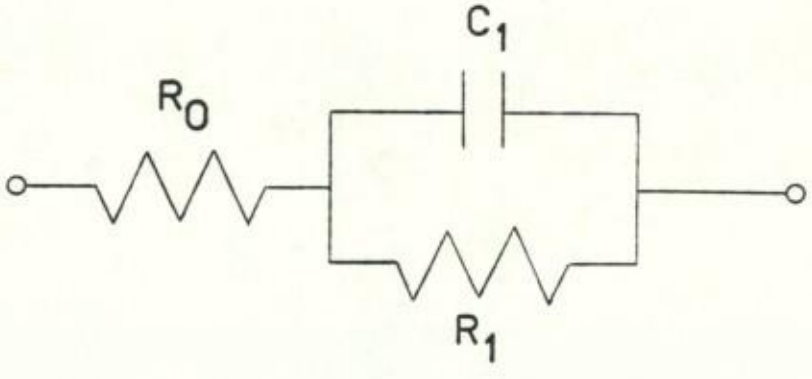

Figure 17: The simplest electrical equivalent circuit of a plant cell.

$$Z_{op} = \frac{R}{1 + RCs}. \qquad [39]$$

If a step of current is applied to this circuit, then i(t) = 0 for t<0 and i_{max} for t>0. The Laplace transform of i(t) is i_{max}/s. The Laplace transform of the voltage (V) is then given by equation [38], which, after rearrangement, is written:

$$V = \frac{i_{max} R}{1 + RCs}. \qquad [40]$$

We may consult a table of Laplace transform (ref) to find that the function of t, which has equation [40] as its Laplace transform, is:

$$v(t) = i_{max} R\left(1 - \exp -\left(\frac{t}{RC}\right)\right). \qquad [41]$$

In this simple example it is easy to verify that equation [41] is the solution of equation [37].

5.6.4 Computation

The problem is to find out the values of the elements of an electrical equivalent circuit which has the same operational impedance spectrum as that calculated from the experimental results. One major problem with such modeling arises from the inherent ambiguity of equivalent circuit fitting: an equivalent circuit involving three or more circuit elements can often be rearranged in various ways and still yield exactly the same operational impedance spectrum. Fortunately, an analysis of the structure of the system under investigation often suggests the equivalent circuit which is the most appropriate to describe the system. For instance, the simplest electrical circuit which may be used to describe a plant cell is shown in Figure 17. The choice of a resistor (R_1) in parallel with a capacitor (C_1) rests on considerations given in section 5.1. The series resistor (R_0) arises from the cell wall and from the solution which is between the measuring electrode and the membrane surface. The differential equation of this circuit is given by:

$$C_1 R_1 \frac{dv}{dt} + v = C_1 R_0 R_1 \frac{di}{dt} + (R_0 + R_1) i \qquad [42]$$

and its operational impedance is written as:

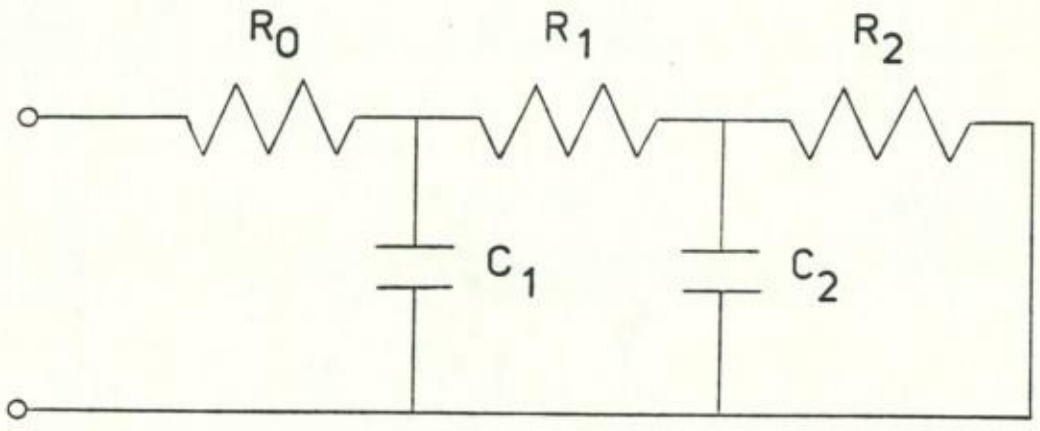

Figure 18: Electrical equivalent circuit used to fit the operational impedance spectrum of a two time-constant system.

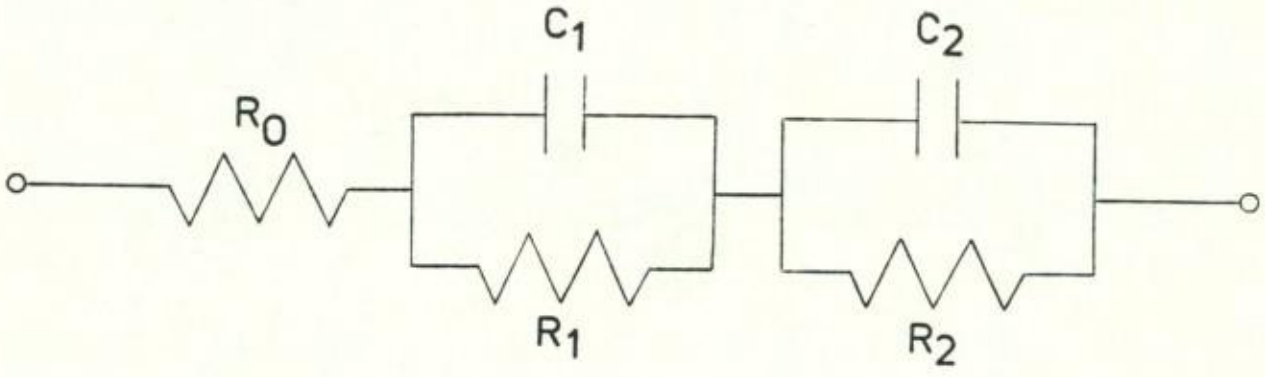

Figure 19: Electrical equivalent circuit of a plant cell consisting of a plasmalemma and tonoplast in series.

$$Z_{op} = R_0 + \frac{1}{\frac{1}{R_1} + sC_1}. \qquad [43]$$

Expanding equation [43] in power series of 1/s we get:

$$Z_{op} = R_0 + \frac{1}{sC_1} - \frac{1}{s^2 R_1 C_1^2} + \dots \qquad [44]$$

When Z_{op} is plotted versus 1/s, the intercept on the ordinate is R_0 and C_1 is equal to the reciprocal slope at the origin of the operational impedance spectrum. We can then calculate a new operational impedance spectrum (Z_{op}'):

$$Z'_{op} = \frac{Z_{op} - R_0}{1 - sC_1(Z_{op} - R_0)}. \qquad [45]$$

If the operational impedance spectrum of the system under investigation can be correctly fitted by the electrical equivalent circuit of Figure 17 then Z_{op}' is constant (independent of s) and is equal to R_1. If it is not the case, Z_{op}' will be a function of s, which means that the system contains at least one more resistor-capacitor loop. Assuming that R_1 is itself an impedance which has the same structure as that considered at the beginning (Figure 17) we get the circuit of Figure 18. Then Z_{op}' can be treated as a new operational impedance spectrum. Using the same procedure as that starting from equation [34] one can evaluate R_1 and C_2. If the new operational impedance (now called Z_{op}'') is constant then Z_{op}'' will be equal to R_2. The analytical expression of the operational impedance of the circuit of Figure 19 is written:

$$Z''_{op} = \frac{R_0 + R_1 + R_2 + \{R_1 C_2 R_2 + R_0[C_1 R_1 + C_2 R_2 + C_1 R_2]\}s + R_0 C_1 R_1 C_2 R_2 s^2}{1 + (C_1 R_1 + C_2 R_2 + C_1 R_2)s + R_1 C_1 R_2 C_2 s}, \qquad [36]$$

or using the suitable substitution:

$$Z''_{op} = \frac{X_1 + X_2 s + X_3 s^2}{1 + X_4 s + X_5 s^2}. \qquad [47]$$

Our experience has taught us that starting with 1024 experimental points for both voltage and current signals the iterative procedure described hereabove may be used to satisfactorily analyze a system consisting of up to three resistor-capacitor loops.

In mature plant cells there is a vacuole which occupies 90% of the cellular volume. Therefore, when electrical signals are recorded between the vacuole and the extracellular solution, at least two membranes are in series: the plasmalemma and the tonoplast. Thus, in this case at least two parallel resistor-capacitor loops must be considered in the electrical equivalent circuit (Figure 21). The operational impedance of this circuit may be written:

$$Z_{op} = \frac{R_0 + R_1 + R_2 + (R_1 C_2 R_2 + C_1 R_1 R_2 + R_0 (C_1 R_1 + C_2 R_2))s + R_0 C_1 R_1 C_2 R_2 s^2}{1 + (C_1 R_1 + C_2 R_2)s + C_1 R_1 C_2 R_2 s^2} . \qquad [38]$$

Equations [46] and [48] belong to two different electrical equivalent circuits which have the same operational impedance spectrum. Therefore, in order for these two circuits to have an identical impedance spectrum, each coefficient of the different power of s in the numerator and in the denominator in equation [46] must be equal to those in equation [48] respectively. Using equations [47] and [48] it is easy to find the equations for the transformation of parameters:

$$R_0 = \frac{X_3}{X_5}$$

$$C_1 = \frac{Y_3 - Y_4}{Y_1 - Y_2 Y_4}$$

$$R_1 = \frac{Y_3}{C_1}$$

$$C_2 = \frac{Y_3 - Y_4}{Y_2 Y_3 - Y_1}$$

$$R_2 = \frac{Y_4}{C_2}$$

where

$$Y_1 = X_1 - \frac{X_3}{X_5}$$

$$Y_2 = \frac{X_2 X_5 - X_3 X_4}{X_5}$$

$$Y_3 = \frac{X_4 + \sqrt{X_4^2 - 4X_5}}{2}$$

$$Y_4 = \frac{2X_5}{X_4 + \sqrt{X_4^2 - 4X_5}}$$

5.6.5 Example

When the membrane of Chara corallina is stimulated with a current step of sufficient magnitude the transient voltage response displays an overshoot, which has been attributed to the time- and voltage-dependent conductance of K^+ channels (Hombié and Jenard,

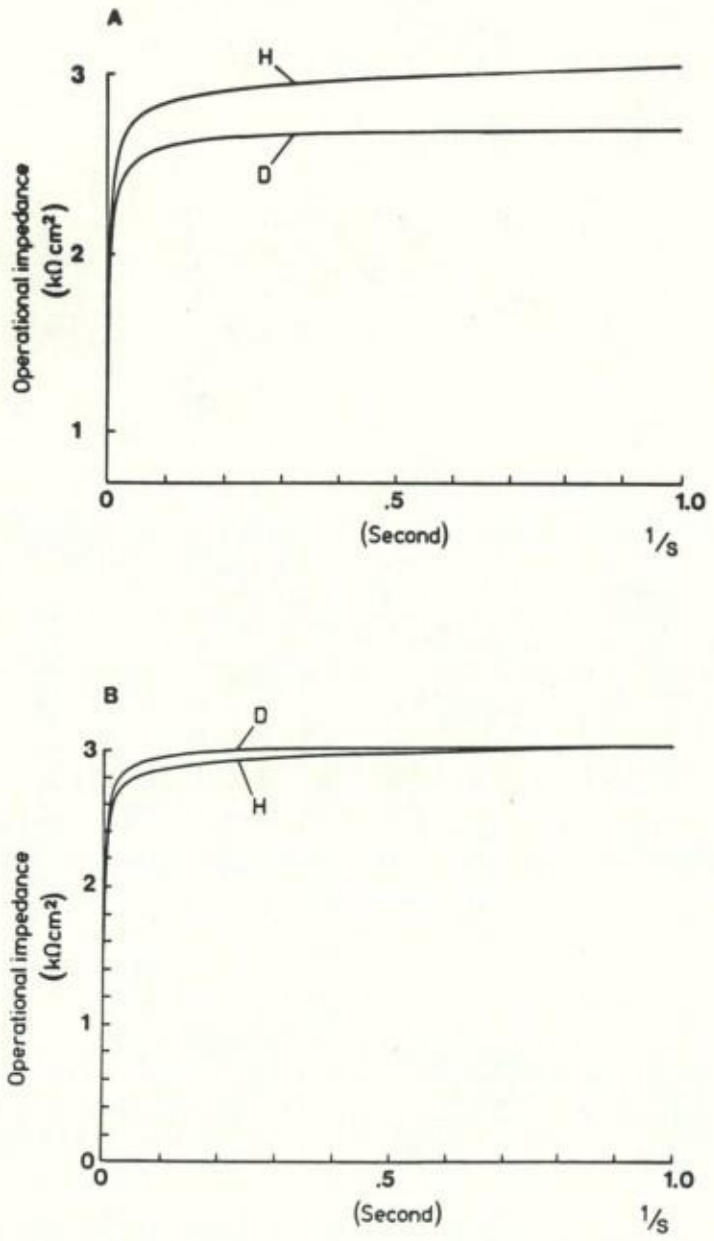

Figure 21: Operational impedance spectra of a Chara cells (Homblé and Jenard 1986).

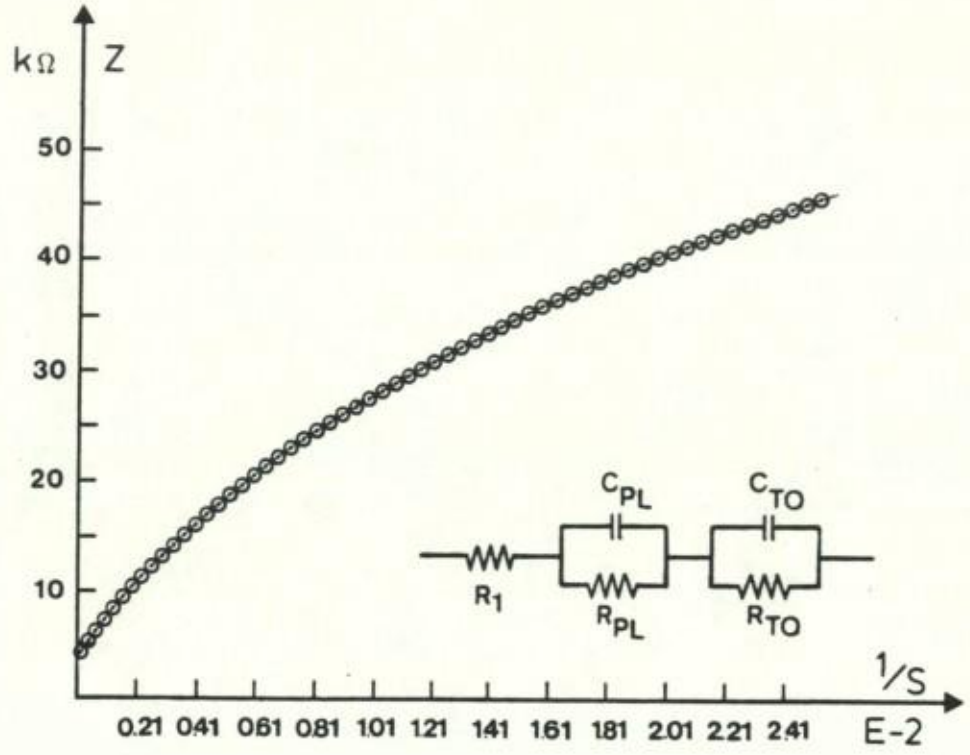

Figure 22: Simulation of operational impedance spectrum of a Chara cell under saturating light at pH 6.0. The calculated values of the components of the elecvtrical equivalent circuit shown in the inlet are: R_1 = 1.0 kΩcm2; R_{pl} = 26.2kΩcm²; C_{pl} = 1.9 μF cm⁻²; Rto = 4.4 kΩcm² and C_{to} = 1.1 μF cm⁻².

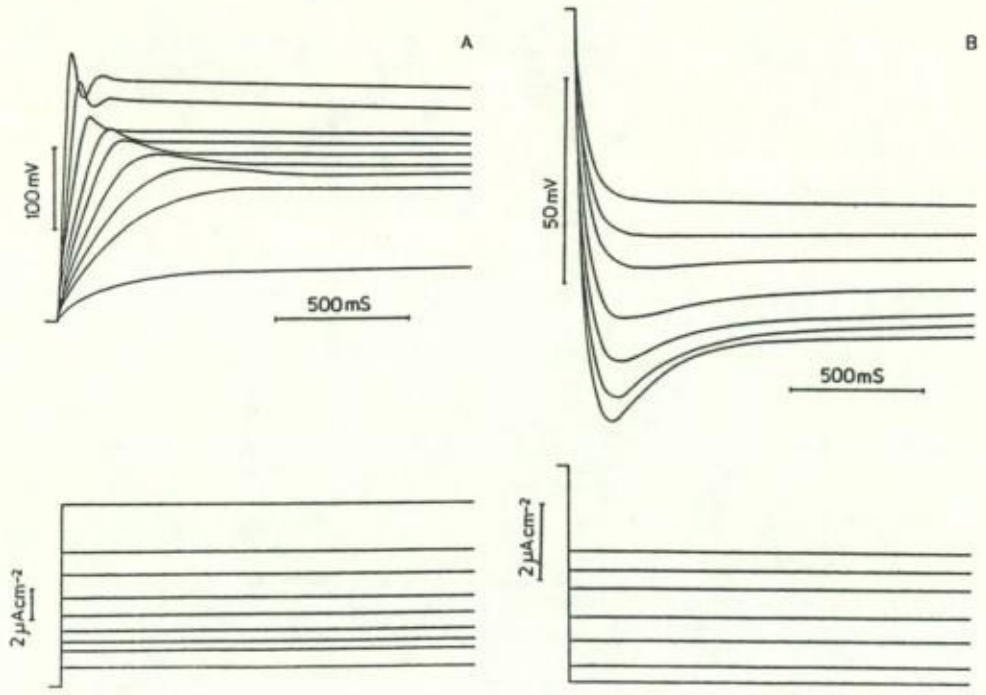

Figure 20: Response of the membrane potential to increasing (A) inward current pulses and (B) outward current pulses (Hombié and Jenard 1984).

1984; Smith, 1984; Homblé, 1985) and could be described as inductive behaviour. The use of a low intensity current stimulus (not causing an overshoot) yields a capacitive like curve (Figure 20). Figure 21 shows the operational impedance of a Chara cell stimulated by a hyperpolarizing and depolarizing current step of 0.5 $\mu A\ cm^{-2}$. Since the steady state behaviour of the membrane is not symmetrical, the depolarizing curve is scaled to the hyperpolarizing curve by multiplying it by a constant factor in order to obtain the upper right point of the operational impedance spectrum in common to both curves (Figure 21B). It then becomes apparent that the spectrum (the change with 1/s) of the membrane operational impedance is also asymmetrical around the resting state. A typical example of the simulation of the membrane impedance spectrum by means of an electrical equivalent circuit is shown in Figure 22.

5.7 The concept of membrane capacitance

Strictly speaking, the capacitive current results in a change in the amount of free charges on each side of the membrane. This current flow does not involve the displacement of charges (ions) through the membrane but a redistribution of the charges on the membrane surface. According to the basic laws of electricity the capacitive current determines the rate at which the voltage across the membrane changes. This is expressed by the equation:

$$i = C\frac{dv}{dt}. \qquad [49]$$

The larger the capacity to be charged, the more current is required to reach a given voltage.

However, there are different kinds of biophysical phenomenon related to ion transport across biological membranes, which can produce an electrical response similar to that of a capacitor. Because these phenomenon are not directly related to the dielectric properties of the membrane, they are usually called pseudo-capacitive effects. It is important to be able to separate these pseudo-capacitance components from the true membrane capacitance, because the later can provide information about the structure and properties of the cell membrane itself.

Passive transport occurs through ion channels at a rate of about 10^7 ions per second. In the membrane each channel opens and closes randomly. The small signal capacitance of a population of voltage dependent ion channels is given by (Ferrier et al., 1985):

$$C(\omega) = -\gamma N_o (V-E)\frac{\left(q'\frac{p}{q}-p'\right)}{\left((q+p)^2+\omega^2\right)}. \qquad [50]$$

where γ is the conductance of a single open channel, N_o is the number of open channels, V is the membrane potential difference, E is the equilibrium potential of the ions crossing the channel, q is the frequency of channels changing from closed to open state, p is the frequency of channels changing from open to closed state and q' and p' are the first

derivatives of q and p with respect to the membrane potential difference. In case the frequency of opening of channels is sufficiently voltage dependent, so that q'p/q is greater than p', a negative membrane capacitance (or pseudo-inductance) will then be measured. Moreover, from equation [50] it may be concluded that an increase in the probability of opening of voltage-dependent ion channels can lead to an apparent (or pseudo-) capacitive effect.

Ion transport and concentration changes occur in the unstirred layers of solution adjacent to each face of the membrane when a current is injected through it. Let us assume that the membrane is surrounded by two solutions made of different concentrations of the same uni-valent binary salt. The current will be carried by negative and positive ions which will, in general, have different transport number (the fraction of current carried by an ion) both in the bathing solutions and in the membrane. As shown by Barry and Hope (1969), the transport number discontinuities at the membrane-solution interfaces will cause solute enhancement or depletion at these interfaces in the unstirred layers width adjacent to the membrane. Electro-osmosis will also cause changes in the solute concentration in the unstirred layers of solution adjacent to the membrane as solute is swept up or away by the electro-osmotic flow which occurs when a current is passed through the membrane. Transport number effects and electro-osmosis effects have opposite consequences on concentration changes at the membrane-solution interfaces. Such effects which change the local concentration at the membrane-solution interface also give rise to an apparent low-frequency (< 0.01 Hz) component of capacitance (Segal 1967; Barry 1977). This is so because the local gradient across the membrane gives rise to a time-dependent diffusion potential, which thus appears as if it were a slowly increasing membrane resistance which mimics a capacitance effect.

Finally, a low-frequency (< 1 Hz) negative capacitance can also result from the proton or hydroxyl diffusion in the unstirred layers adjacent to the membrane (Ferrier et al. 1985; Homblé and Ferrier 1988). This effect is especially significant in plant cells where the membrane conductance is higher for protons (or hydroxyl) than for the other ions. When a steady state ion current crosses the membrane, it is transported away from the membrane in the unstirred layer by means of a concentration gradient-driven diffusion (Ferrier 1981). Because protons (or hydroxyl ions) have a greater diffusion coefficient than the other ions in the unstirred layer, the diffusion-driven component of the current will lag behind the total current which will give rise to a pseudo-inductive effect.

5.8 Conclusion

The impedance spectroscopy estimated by Laplace transform analysis permits one to obtain information quickly about the impedance of plant cells because only a single experimental run is sufficient to obtain the frequency dependence of the membrane impedance. One of the most attractive aspects of impedance spectroscopy as a tool for investigating the electrical properties of plant membranes is the direct connection that often exists between the behaviour of the membrane and that of an idealized model circuit representative of the physical process taking place in the membrane. There are, however, dangers in the indiscriminate use of electrical analogies to describe plant systems. The first point to be made is that electrical equivalent circuits are seldom unique and in many cases other experimental data are often necessary to choose the relevant circuit unambiguously. A further limitation is the frequency-dependent electrical properties of interface layers (for instance, the unstirred layer

adjacent to the membrane surface), which mimic the electrical response of plant membranes. Finally, an important requirement for a valid impedance spectroscopy analysis is that the system must be linear.

6 ION CHANNELS

6.1 Introduction

It is now well documented that there are two differnet kinds of ion transport in the membranes of plant cells: active transport and passive transport (Dainty 1962, Spanswick 1981). Passive transport can be classified into two types: carriers and channels. A carrier is a macromolecule which binds specifically a solute on one side of the membrane to form a complex. This complex can move to the other side of the membrane where the solute is released and the carrier recycled. A channel is generally thought of as a selective aqueous pathway extending from one side to the other side of the membrane. Channel can be characterized by the fact that their rate of ionic transport is much faster than any other known mechanism of ion transport in biological membranes. For instance, the rate of ion transport of the Na^+-K^+ pump is $5\ 10^2\ Na^+/s$ (Jorgensen 1975), that of the carrier valinomycin is $3\ 10^4\ Rb^+/s$ (Benz and Laüger 1976), whereas that of the K^+ channel of Chara corallina protoplasmic drops is $1.5\ 10^7\ K^+/s$ at -75 mV (Homblé et al. 1987).

Ion transport through a channel has been approached in two different but complementary ways: the deterministic approach and the stochastic approach.

In the deterministic approach ion transport is viewed as a continuous function of the physico-chemical parameters and every state of the transport system at a given time can be exactly calculated from a knowledge of its initial state. This method has been well developed in the experimental and theoretical description of ionic current flowing through th nerve axon membrane during an action potential (Hodgkin et al. 1952, Hodgkin and Huxley 1952a, b,c,d). It gives information about the mean behaviour of the whole population of channels present in the membrane.

The stochastic approach arose from the idea that ionic transport through each channel occurs in a way that is discrete and randomized. In this case each state of the transport system at a giventime can only be known with some probability. The experimental application of the stochastic approach to biological cells began with the study of fluctuations of voltage across the axon membrane (Verveen and Derksen 1965, Derksen and Verveen 1966, Verveen et al. 1967). This approach is still being expanded today, particularly with the growing interest in the recently developed tight seal patch-clamp, which permits the study of the stochastic activity of a single channel in a biological membrane (Hamill et al. 1981). The aim of this approach is to obtain information about the molecular mechanisms of a single channel.

This chapter will mainly focus attention on evidence for the presence of ion channels in Characeae's membranes. The results obtained by means of the deterministic approach and those collected by the stochastic approach will be described separately.

6.2 The deterministic approach

6.2.1 Background

Consider the case of a membrane separating two aqueous solutions and assume that the electrical properties of this membrane are maily determined by passive traznsport through ion channels. The net current (I_i) carried by the ion species i can be expressed

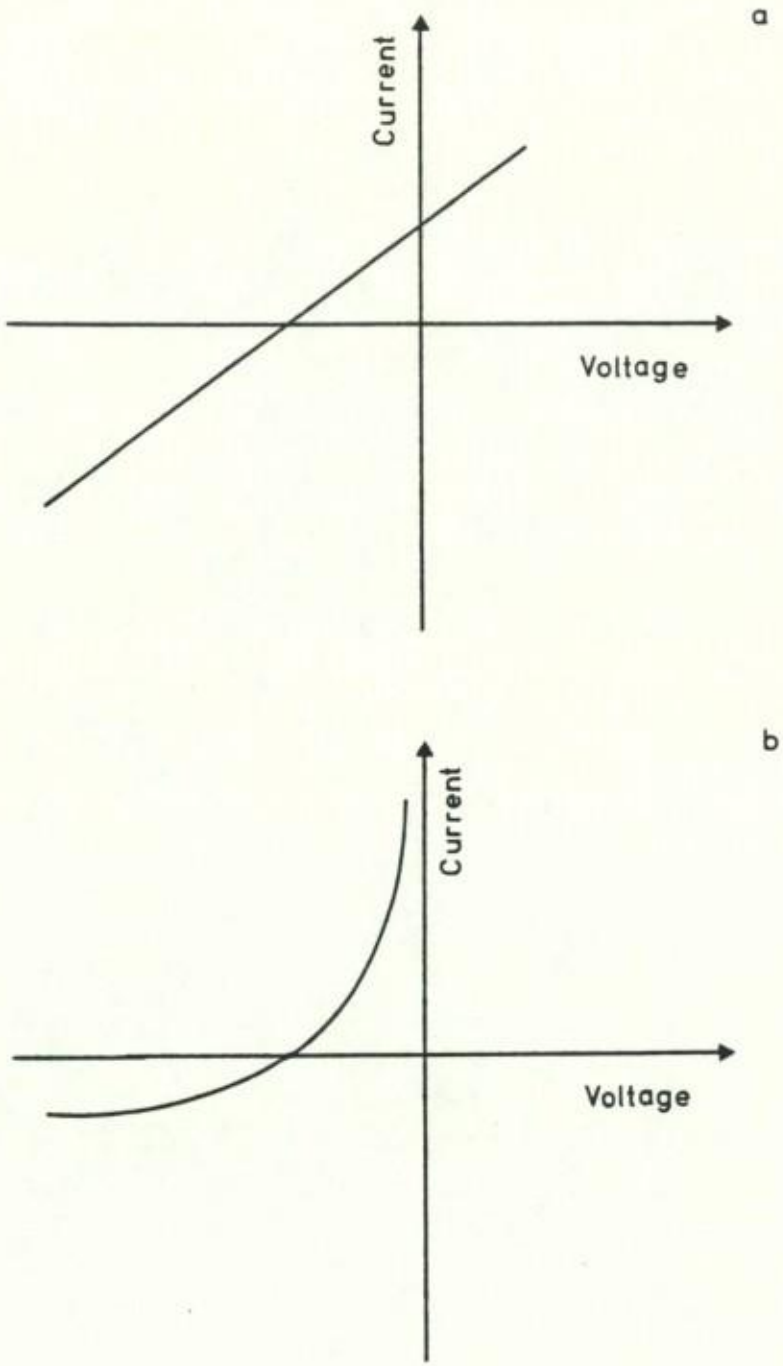

Figure 23: a) Linear and b) non-linear and asymmetric current-voltage curve.

as the product of the membrane conductance for that species (g_i) and the toal driving force acting on that ion species, which is equal to the difference between the membrane potential difference (V) and the equilibrium potential difference for that species (E_i):

$$I_i = g_i(V - E_i). \qquad [51]$$

In a general way g_i is not necessarily a constant. It can be a function of time (t) and of the membrane potential difference. To emphasize this point equation [51] can be rewritten as:

$$I_i(V,t) = g_i(V,t)(V - E_i) \qquad [52]$$

.

From equation [52] it can be seen that when the membrane potential difference is more positive than the equilibrium potential difference the ionic current flowing through the membrane will be positive, i.e., outwards. The membrane potential difference at which no net current flows through the membrane is called the reversal potential. When only one ionic species can cross the membrane the reversal potential is an indication of the equilibrium potential difference for that species. For a membrane permeable to more than one species it is a measure of a "mixed" equilibrium potential difference. In this case its value depends on the different permeant ionic species.

A membrane is depolarized when the potential difference is clamped at a more positive value than the resting potential difference and it is hyperpolarized when the potential difference is clamped at a more negative value than the resting potential difference. For a voltage- and time-dependent ionic conductance the increase and decrease of conductance with time at a fixed potential is called activation and inactivation respectively.

Information about channels can be obtained from analysis of the current-voltage curve of the membrane. For plant cells it can be linear or non-linear and asymmetric (Figure 23). When the current-voltage characteristic is asymmetric the membrane is said to have rectifying properties. A linear current-voltage curve indicates that the ionic conductance is voltage-independent. Non-linearity of the current-voltage curve can arise from a voltage-dependent ionic conductance but also from an asymmetry of the ionic concentrations across the membrane (Hope and Walker 1975).

The membrane selectivity is never absolutely perfect. Even when the membrane conductance seems to be dominated by the presence of only one kind of ion species othe ions can usually flow through the same pathway (Eisenman and Horn 1983).

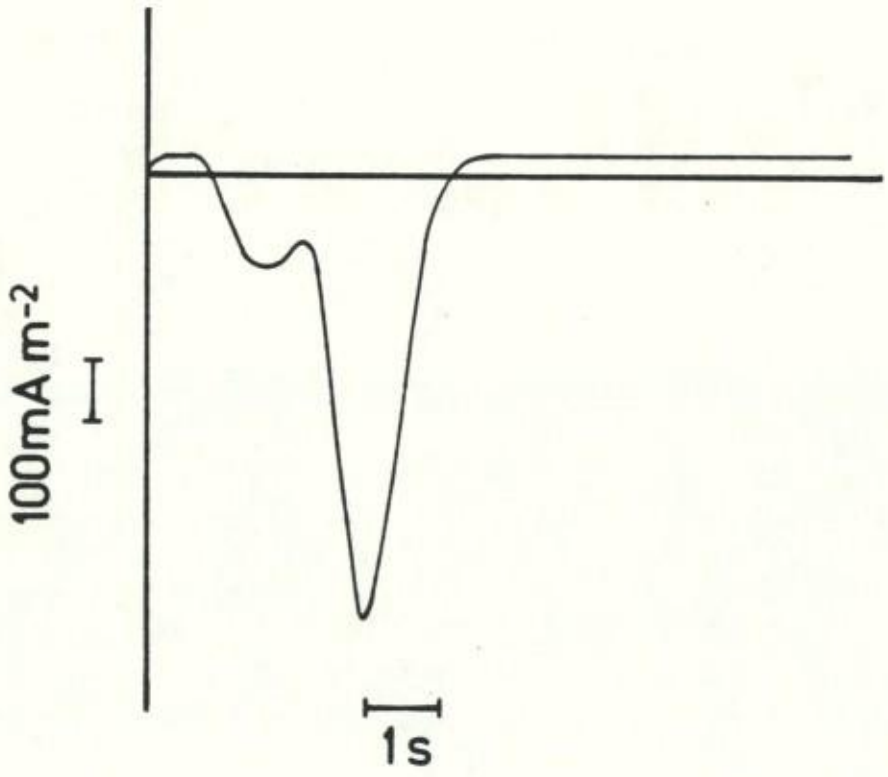

Figure 24: Time course of the ionic current flowing through the membrane of a Characean cell clamped at the threshold potential.

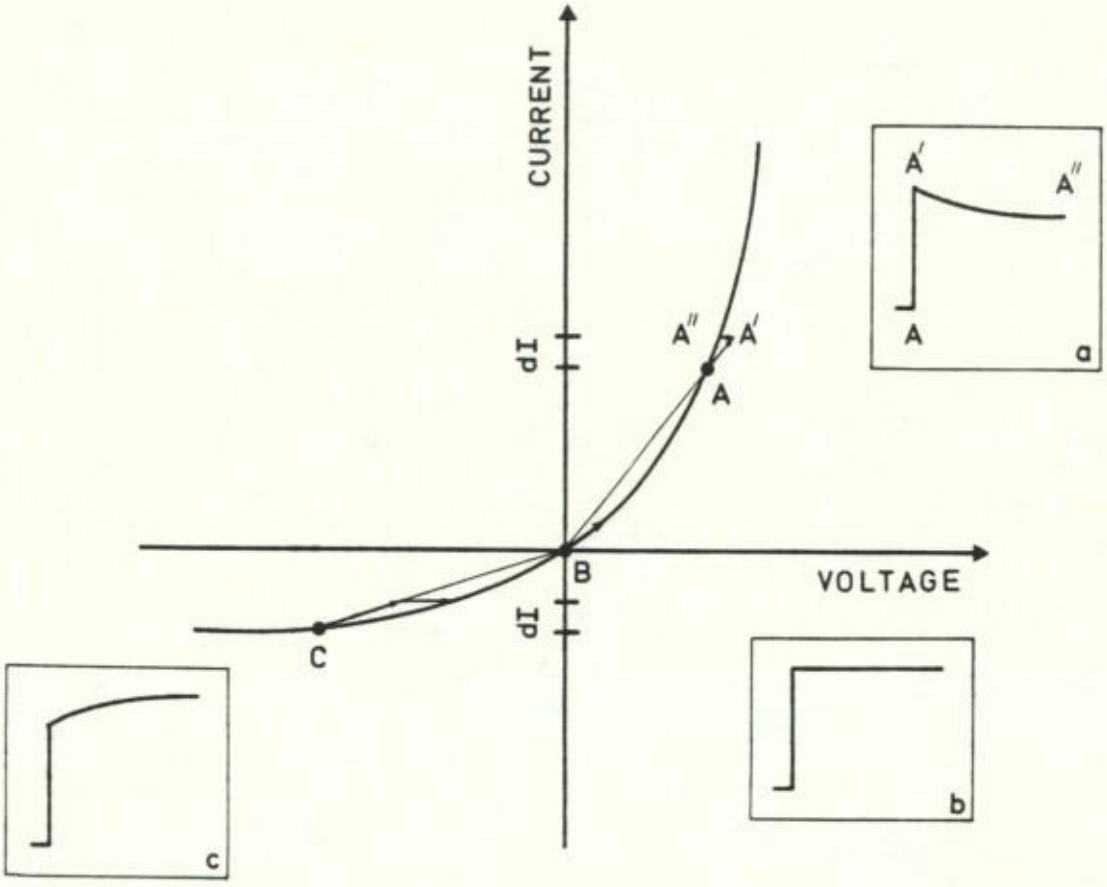

Figure 25: Qualitative plot of the current-voltage curve for potassium channels to explain the pseudoinductive response. The time course of the voltage response to a small current step is shown respectively in inlets a, b and c for a resting potential more negative (A), equal (B) and more positive (C) than the reversal potential for potassium ions. Vertical axis is arbitrarily chosen at the reversal potential.

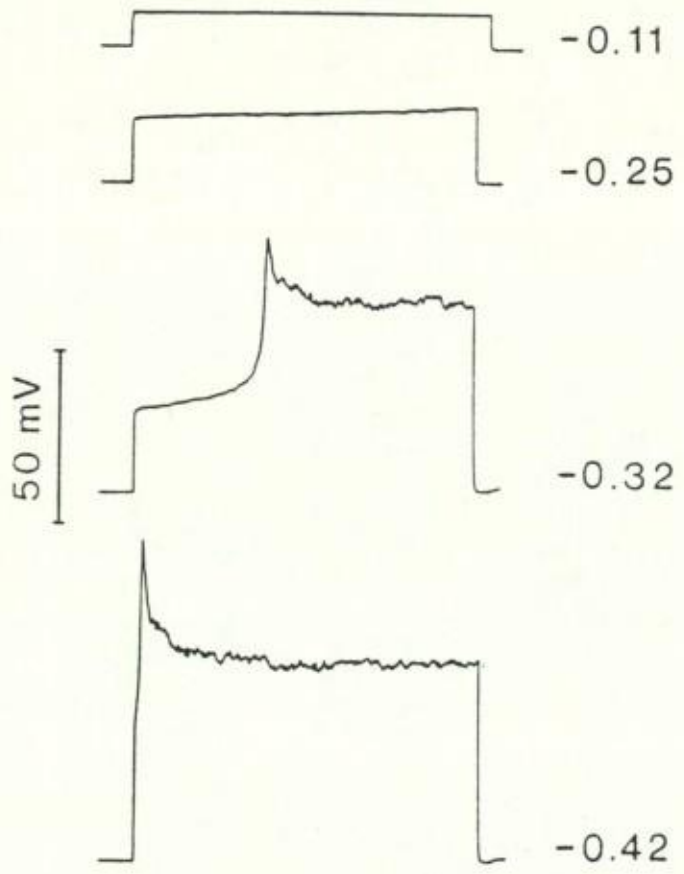

Figure 26: Hyperpolarizing response of a protoplasmic droplet of Chara corallina.

Most of our ideas about membrane channel come from the study of electrical responses of large Characean cells. Among these, for instance, is the action potential, which is a transient depolarizing wave which can be triggered by a suprathreshold stimulus depolarizing the membrane (see Hope and Walker 1975, Findlay and Hope 1976, for general reviews). An action potential can occur at both plasmalemma and tonoplast (Findlay and Hope 1964a, b). When the plasmalemma is voltage-clamped at a slightly more positive value than the threshold two negative transient currents occur followed by one positive current (Volkov et al 1974a, Beilby and Coster 1979a) (in some Nitella species only one of the negative transient currents occurs (Hirono and Mitsui 1981)). The time course of these ionic currents is shown qualitatively in Figure 24. The two negative currents involve the outward movement of K^+.

There are conditions in which the K^+ channels are not blocked and in which a pseudoinductive voltage response is observed when a small constant current is injected through the membrane (Findlay and Coleman 1983, Homblé and Jenard 1984). This kind of response arises because the K^+ current flowing through the membrane is controlled by a time-variant conductance. To understand the meaning of this oscillatory response it is appropriated to consider the steady state current-voltage curve of Figure 25. When the membrane is polarized at point A more positive than the equilibrium potential difference, a small positive current step (dI) will shift the membrane potential difference toward more positive value. If the ionic conductance does not change instantaneously, the respose will follow an excursion along the path A-A' given by the chord conductance of the locus. If the conductance changes with time after the instantaneous response, the membrane potential difference will shift towards a new steady state value (A'-A"). The corresponding qualitative time course of the voltage response drawn in Figure 25a shows that this response gives rise to a pseudoinductive effect. When the same procedure is repeated from point B or C it can be shown that a purely resistive (Figure 25b) or a pseudocapacitive (Figure 25c) response will be observed. Thus the pseudoinductive response indicates the presence of a time-variant ionic conductance which has a non-linear currenbt-voltage characteristic. Moreover, it tells us that the ion flowing through the time-variant conductance is not at equilibrium across the membrane.

When Characean cells are treated in high K^+ concentration (>1 mM) solutions their plasmalemma behaves like a potassium selective electrode and the membrane is said to be in the passive K^+-state. In this condition, hyperpolarization with a constant current step will give rise to a spontaneous increase in the voltage response (Figure 26) indicating a decrease in membrane conductance. This phenomenon is called the hyperpolarizing response (Kishimoto 1966, Shimmen et al. 1976, Homblé 1987).

6.2.2 Chloride channels

Chloride channels are involved in three different phenomena: the action potential, punchthrough and in the hyperpolarizing response. Direct evidence that the membrane permeability to Cl^- ions increases during these phenomena has been obtained by radioactive tracer experiments and chloride concentration measurements with ion specific electrodes (Gaffey and Mullins 1958, Mullins

1962, Hope and Findlay 1964, Haapanen and Skoglund 1967, Coster and Hope 1968, Gradman et al. 1973, Oda 1976, Kikuyama et al. 1984, Tyerman et al. 1986a).

Activation of a chloride conductance at the plasmalemma level during the action potential has been confirmed by experiments using the voltage clamp technique. The negative transient Cl^- current disappears when the membrane potential difference is clamped at the equilibrium potential difference of Cl^- ions. Moreover, the reversal potential shift in the direction predicted theoretically when the external Cl^- concentration is changed (Findlay and Hope 1964b, Kishimoto 1964, Beilby and Coster 1979a, Beilby 1981, Lunevsky et al. 1983).

The Cl^- current of the action potential con be blocked by ethacrynic acid, furesemide (a diuretic), Mn^{2+}, or La^{3+} (Lunevsky et al. 1983, Zherelova et al., 1984, Tsutsui et al. 1986). Ethacrynic acid seems to be a non lethal and relatively specific inhibitor of Cl^- channels in plant cells. La^{3+} is an unspecific inhibitor; it blocks the whole excitation process (Beilby 1984b).

By clamping the membrane of Nitellopsis obtusa at potential differences at which the membrane is permeable to Ca^{2+} ions, Lunevsky et al. (1983) were able to activate the Cl^- channels by increasing the external Ca^{2+} concentration. Also, activation of the Cl^- channels always appears after the activation of the Ca^{2+} channels. These results led these authors to conclude that the Cl^- channels of Nitellopsis obtusa are activated by Ca^{2+}. This conclusion is consistent with the early finding that, in Chara corallina and Nitellopsis obtusa, the Cl^- current of the action potential decreases when the external Ca^{2+} concentration is decreased (Findlay 1961, 1962). Further evidence for the existence of Ca^{2+}-activated Cl^- channels has been obtained using perfused tonoplast free cells of Nitellopsis obtusa in which it was possible to activate the Cl^- channels by an increase in the cytoplasmic concentration of Ca^{2+} ions (Kataev et al. 1984, Shiina and Tazawa 1988). The dependence of the peak value of the Cl^- current on the cytoplasmic Ca^{2+} concentration saturates above 10^{-4} M Ca^{2+}. Prolonged exposure to Ca^{2+} in the cytoplasm leads to irreversible inactivation of the Cl^- channels. Thus, in vivo, the increase in cytoplamic Ca^{2+} concentration arising from an action potential must be sequestred in order to permit the Cl^- channels to remain operating. Sr^{2+} ions but not Ba^{2+} or Mg^{2+} ions can also activate the Cl^- channels but are less effective than Ca^{2+} ions.

There is some evidence that Cl^- channels can be voltage-activated. In Chara corallina and in Nitella flexilis the Cl^- current appears before the Ca^{2+} current when the membrane potential difference is clamped at a value slightly more positive than the threshold value (Volkov 1977, Beilby and Coster 1979a). A change in the external concentration does not affect the magnitude of the voltage-dependent Cl^- current in Nitella axillaris (Kishimoto 1964).

In Chara corallina and Nitella axilliformis the delay of activation of the Cl^- current is also voltage-dependent (Beilby and Coster 1979a, Hirono and Mitsui 1981). It is shorter when the membrane potential difference is clamped at more posisitive values.

In the excited state, the Cl^- channels of Chara australis do not distinguish between Cl^-, Br^- and NO_3^- since the amplitude of the clamp current does not change when the amplitude of the clamp current does not change when these anions are substituted for Cl^- in the external medium (Findlay and Hope 1964b). The selectivity sequence $Cl^- > CH_3SO_4 > K^+ > SO_4^-$ has been found with perfused cells of Nitellopsis obtusa (Kataev et al. 1984). Using perfused cells of Chara australis, Shimmen and Tazawa (1980a) have shown that excitability always occurs if the cytoplasmic Cl^- ions are replaced by methane sulfonate, orthphosphate or PIPES but does not occur if they are replaced by SO_4^{2-}, CH_3COO^-, NO_3^-, F^- and propionate anions. These results suggest that the Cl^- channels of the action potential are relatively nonselective anionic channels.

In Nitella flexilis the magnitude of the Cl^- current of the action potential decreases when the pH of the external solution is increased (Volkov et al. 1979). From their results Volkov et al. (1979) have calculated that dissociated ionic groups with a pK in the range of 8.5 to 8.7 must exist at the outer face of the membrane. Thus the increase in Cl^- current at acid pH can be attributed to the protonation of amine groups which probably constitute the selective filter of the anionic channel.

Temperature strongly affects the properties of the Cl^- channels. The amplitude of the Cl^- current of the action potential increases with temperature (Kishimoto 1972). The rate of the activation and a-inactivation increase when temperature rises (Beilby and Coster 1979c). The delay of activation decreases when the temperature increases. From the voltage-dependence of the enthalpy of the delay of activation of the Cl^- channels, Beilby and Coster (1979c) have calculated that 4 charges per "molecule of channel" must be moved perpendicularly to the membrane before a Cl^- channel is activated.

Cl^- channels are also involved in the excitability of the tonoplast. Their identification rests on the dependence of the magnitude of the action potential on the vacuolar Cl^- concentration (Kikuyama and Tazawa 1976, Shimmen and Nishikawa 1988). and on the fact that the reversal potential of the current is between -50 and -70 mV which is of the same order of magnitude a the equilibrium potential difference of Cl^- ions across the tonoplast (Lunevsky et al. 1983). In Nitellopsis obtusa, the tonoplast Cl^- current is activated after an early transient current tentatively identified as a Ca^{2+} current, and its amplitude can be controlled by the external Ca^{2+} concentration (Berestovsky et al. 1976, Lunevsky et al. 1983). On this basis, Lunevsky et al. (1983) have proposed that the tonoplast Cl^- channels are also Ca^{2+}-activated.

6.2.3 Proton channels

In the light and when the external pH is above 9, the membrane potential difference of Chara corallina is close to the equilibrium potential diffeence for the protons and the membrane hyperpolarizes with a slope of 59 mV/pH unit when the external solution is alkalinized (Bisson and Walker 1980). This indicates that at a pH above 9 the membrane permeability to H^+ id much higher than that for other ions. The membrane is then said to be in the passive H^+-state. In these conditions the membrane conductance is large (up to 4 Sm^{-2}) and is voltage-independent.

At the same membrane potential difference as those recorded in alkaline solution but at more acid pH, when the membrane potential difference is controlled by the electrogenic pump, the H^+ channels are not open suggesting that the H^+ channels are chemically activated.

The fact that DCCD reduces the passive conductance at pH's above 9 supports the idea that the channels a high pH are selective to protons (Bisson and Walker 1980, 1981). DCCD is thought to block the F_o proton channel activity of the H^+-translocating ATPase of chloroplast, mitochondria, bacteria and plants. As electrogenicity in plant cell membranes is attributed to a H^+-translocating ATPase, it is legitimate to wonder whether the H^+ channels observed in Chara corallina at alkaline pH arise from the H^+ pump which would have lost its catalytic activity.

The passive proton permeability which dominates at alkaline pH is suppressed in the dark or in the presence of DCMU, an inhibitor of the electron transport chain in the chloroplast (Bisson 1986). This modulation of the H^+ channels by light is not understood at the present time.

The activation of H^+ channels at alkaline pH can have ipmportant effects on the cell physiology in natural environmental conditons. For instance, in Chara corallina which has alternating acid and alkaline bands (Lucas 1983), the membrane conductance is larger in the alkaline bands than in the acid bands. According to Smith and Walker (1983), the alkaline band specific conductance is at least 5 times greater than the average specific conductance of the whole cell. Furthermore, according to Lucas et al. (1977), the ion transport zone of the alkaline band is at least one-sixth of the total cell surface area. This means that the conductance of the alkaline band would account for at least 80% of the cell total conductance (Homblé and Ferrier 1988). Thus, these experimental results do not agree with the currently accepted hypothesis which assume that in natural conditions the conductance of the membrane (and thus the membrane potential is largely dominated by the proton pump.

6.2.4 Calcium channels

The role of Ca^{2+} in the plant action potential and its relation to cytoplasmic streaming have been reviewed by Beilby (1984b). Therefore, attention will be focused on the identification and the biophysical properties of the Ca^{2+} channels.

Evidence for the presence of Ca^{2+} channels in the membranes of plant cells comes from the study of the ionic currents that flow through the membrane of Characeae during an action potential. When the plamsalemma potential difference of various Characean cells is clamped at a value slightly more positive than the threshold of excitation, a transient negative current similar to the transient Cl^- current occurs and has been attributed to an inward movement of Ca^{2+} ions. In Chara corallina and Nitella flexilis the Ca^{2+} channels are activated after the activation of the Cl^- channels whereas in Nitellopsis obtusa they are activated before the activation of the Cl^- channels (Volkov 1977, Beilby and Coster 1979a, Lunevsky et al. 1983).

The characterization of Ca^{2+} channels is not easy. The reversal potential (about −50 mV) corresponds neither to the equilibrium potential difference for Ca^{2+} ions across the plasmalemma nor to that of any other ion involved in the physiolgy of Characean cells.

In intact cells of Chara corallina only a very small influx of Ca^{2+} is predicted to flow across the plasmalemma during an action potential (Beilby and Coster 1979b), and this explains why no significant change in a Ca^{2+} radiactive tracer can be detected after a number of action potentials has been triggered (Hope and Findlay 1964). However, in perfused cells of Chara corallina the Ca^{2+} influx increases by a factor of 50 to 200 when action potentials are triggered (Hayama et al. 1979). Using the light emitting calcium probe aequorin, an increase in cytoplasmic Ca^{2+} concentration has been measured in both intact and perfused cells when an action potential is triggered (Williamson and Ashley 1982, Kikuyama and Tazawa 1983). The Ca^{2+} action current was not altered significantly by changes in pH, Na^+, or K^+ concentration in the external solution but was sensitive to a change in Ca^{2+} concentration (Beilby and Coster 1979); it is possible to block the Ca^{2+} current but not the Cl^- current in Nitellopsis obtusa cells perfused without ATP (Zherelova et al. 1984).

In order to explain that the reversal potential for Ca^{2+} is much more negative than the expected equilibrium potential difference for Ca^{2+} ions, one must argued either that the Ca^{2+} channels is be nonselective or that there is a high (of the order of 25 mM) local cytoplasmic Ca^{2+} concentration during the course of an action potential.

The effect of various monovalent and bivalent cations on the reversal potential of the Ca^{2+} current has been investigated on Nitella flexilis (Volkov et al. 1982). The following selectivity series was found for the Ca^{2+} channels:

$Ba^{2+} > Sr^{2+} > Ca^{2+} > Mg^{2+} > Cs^+ > K^+ > Na^+ > Li^+$.

The investigation of the selectivity of the Ca^{2+} channels in Nitellopsis obtusa gave the similar sequence (Lunevsky et al. 1980, Lunevsky et al. 1983):

$Ba^{2+} > Sr^{2+} > Ca^{2+} > Mg^{2+}$ for the bivalent cations and,
$Rb^+ > K^+ > Cs^+ > Na^+ > Li^+$ for the monovalent cations.

The monovalent ions affect mainly the amplitude of the ionic current but not the reversal potential whereas bivalent cations shift both of them. The ratio of the selectivity of Ca^{2+} channels for bivalent cations to that for monovalent cations decreases with increase of external concentration. When the external solution contains as many bivalent as monovalent cations (as is the case in the natural environment), the current through the channels is mainly carried by the bivalent cations. As Ca^{2+} ios are usually the main bivalent present in the external solution, it is thus justified to call the channels Ca^{2+} channels.

In Nitella flexilis, the magnitude of the Ca^{2+} current decreases when the external solution is acidified (Volkov et al. 1979) but in Chara corallina a significant effect on the kinetics of activation and inactivation was found only at acid pH (Beilby 1982). Volkov et al. (1979) have calculated that weakly acid groups with a pK in the range of 4.4 to 4.9 must exist at the outer face of the Ca^{2+} channels. The effect of acid pH on the magnitude of the Ca^{2+} current can thus be explained by a protonation of the channels.

An increase in temperature increases the rate of both activation and inactivation process and decreases the delay in activation of the Ca^{2+} channels in Chara corallina (Beilby and Coster 1979c). The activation enthalpies of the activation and inactivation of the Ca^{2+} channels are of the same order of magnitude as those of the Cl^- channels. From their study of the effect of the temperature on the delay of activation of the Ca^{2+} currents, Beilby and Coster (1979c) have calculated that 10 charges per molecule of Ca^{2+} channel must be moved perpendicularly to the membrane before the Ca^{2+} channels are activated.

The presence of Ca^{2+} channels in the tonoplast has been postulated for Nitellopsis obtusa (Berestovsky et al 1976, Lunevsky et al. 1983). The tonoplast Ca^{2+} channels were tentatively identified on the following bases. A) The two transient currents arising during an action potential have similar qualitative characteristics at the tonoplast and at the plasmalemma. At the tonoplast, the second transient current was identified as a Cl^- current (see above). Thus by analogy with the plasmalemma it is postulated that the first transient current is a Ca^{2+} current. B) The reversal potential of the tonoplast Ca^{2+} current lies in the range of value predicted by experiments on reconstituted Ca^{2+} channels in an artificial membrane which was surrounded by a solution similar in composition to that of the vacuole.

6.2.5 Potassium channels

K^+ channels have been identified in various plant cells and are involved in the action potential, the leak conductance, the light-induced potential change, the pseudoinductive response and the hyperpolarizing response.

An increase in the K^+ efflux during the action potential has been measured by radiactive tracers (Gaffey and Mullins 1958, Hope and Findlay 1964a, Oda 1975, Kikuyama et al. 1984), flame photometry (Haapanen and Skoglund 1967, Oda 1976), and atomic absorption spectrometry (Kikuyama et al. 1984). This increase in K^+ efflux was correlated with the positive current which hyperpolarizes the membrane towards its resting value during an action potential (Findlay and Hope 1964b, Kishimoto 1964, Beilby and Coster 1979a, Hirono and Mitsui 1981). The K^+ current of the action potential has its reversal potential close to the equilibrium potential difference for K^+ ions. Further evidence of the involvement of K^+ ions in the action potential has been obtained in perfused tonoplast-free cells of Chara australis in which the length of the time cours of the action potential decreased when the cytoplasmic K^+ concentration increased (Shimmen and Tazawa 1980).

The quaternary ammonium cation tetraethylammonium (TEA) has been used to identify K^+ channels in plant cells. Its action as a blocker of K^+ channels has been well demonstrated in animal cells (Armstrong 1975). In Nitella flexilis, Nitella axilliformis and Nitella mucronata TEA, added in the external solution, prolongs the hyperpolarizing phase of the action potential (Belton and Van Netten 1971, Koppenhöfer 1972, Shimmen and Tazawa 1983). TEA also prolongs the action potential if added to the cytoplasmic solution of perfused tonoplast-free cells of Nitella axilliformis. In these cells the hyperpolarization response which occurs at the end of the action potential time course is only inhibited by TEA if it is added to the external medium (Shimmen and Tazawa 1983). However, in Chara corallina, TEA affects neither the amplitude of the ionic currents flowing during an action potential nor the shape of the action potential (Beilby and Coster 1979a, Shimmen and Tazawa 1983). In Eremosphaera veridis, the shape of the current-voltage curve and the action-potential-like response induced by dark are affected by TEA (Kölher et al. 1983,, Kölher et al. 1986). 10 mM TEA blocks the hyperpolarizing response in Chara inflata (Coleman and Findlay 1983) and the pseudoinductive response of Hydrodictyon africanum (Findlay and Coleman 1983) and of Chara corallina (Homblé 1985). TEA also affects the general shape of the current-voltage curve for the plasmalemma of Chara corallina (Beilby 1985, 1986) and of Nitella flexilis (Sokolik and Yurin 1981, 1986). When tonoplast-free cells of Chara australis were perfused with neutral red a fast light-induced potential change was observed (Kawamura and Tazawa 1980). This response is voltage-dependent (Shimmen and Tazawa 1981) and blocked by TEA when it is added to the external or cytoplasmic solution (Tazawa and Shimmen 1980). The K^+ influx in high-salt corn roots is also afected by TEA (Kochian et al. 1985).

TEA is not the only known K^+ channel blocker. In both animal and plant cells the TEA derivative nonyltriethylammonium (C_9) also blocks K^+ channels and more efficiently (Armstrong 1975, Tazawa and Shimmen 1980, Findlay and Coleman 1983). In Chara corallina, 2,4,6-triaminopyridimidine (TAP) can substitute for TEA for the inhibition of K^+ channels (Keifer and Lucas 1982).

Some inorganic ions also block K^+ channels. Cs^+ decreases the K^+ conductace in Nitella flexilis (Sokolik and Yurin 1986) whereas the duration of the action potential is increased by Cu^{2+} in Nitella mucronata (Koppenhöfer 1972) and by Ba^{2+} in Nitella flexilis (Belton and Van Netten 1971). Many autors have reported that Ca^{2+} decreases but K^+ increases the K^+ conductance of plant cell membranes (Hope and Walker 1961, Spanswick et al. 1967, Smith and Walker 1981, Keifer and Lucas 1982, Bisson 1984, Smith 1984, Homblé 1985). The K^+ conductance decreases at both acid and highly alkaline pH (Bisson and Walker 1981, Sokolik and Yurin 1986, Beilby 1986). But at pH 11 it is possible to shift the membrane from the passive H^+-state by depolarizing the membrane. This transition is reversible but the mechanism by which this transition occurs is not understood at present (Beilby 1986).

The modes of action of organic cations are probably different. C_9 is made up of a hydrophilic head and a more hydrophobic tail. Armstrong (1975) has proposed that the tail could bind to a hydrophobic group in the neighbourhood of the K^+ channel mouth whereas the head would occupy the entrance of the channel. The inorganic ions probably compete for an ionic site either at the ion selective filter or at the gate of the channel.

The initial decrease in conductance during the hyperpolarzing response arises from an inactivation of the K^+ channels (Coleman and Findlay 1985, Homblé 1987). The small increase in conductance which follows has been attributed to an activation of Cl^- channels (Coleman and Findlay 1985). However, with protoplasmic droplets of Chara corallina it has been shown that this slight increase in conductance results from a delayed activation of the K^+ channels which can be blocked by TEA (Homblé 1987).

Most of the electrophysiological investigations of the properties of the K^+ conductance of aquatic plant cells show that the K^+ conductance is time- and voltage-dependent. However a voltage-independent K+ conductance has been reported which accounts for the leak conductance observed when all other ion transports are blocked (Beilby 1985).

In Nitella flexilis, the selectivity series estimated from the shift of the reversal potential of the K^+ current during an action potential is (Sokolik and Yurin 1986):

$K^+ > Rb^+ > NH^{4+} > Na^+ > Li^+ > Cs^+ > TEA$

Sulphydryl reagents like N-ethylmaleimide modify the properties of the K^+ conductance in Chara corallina (Lichtner et al. 1981, Homblé and Jenard 1984); this suggests that SH-groups are needed to maintain the conformation of the K^+ channels.

In Chara corallina, the effect of temperature on the K^+ channels has been studied in the action potential, the pseudoinductive response, and the membrane conductance of cells in the passive K^+-state. From these experiments a value for the activation enthalpy of the K^+ transport ranging from 36 to 44 $KJmol^{-1}$ at 20 °C has been calculated (Beilby and Coster 1976, Homblé and Jenard 1984, Homblé 1985). At the same temperature but in Nitella flexilis an activation enthalpy of about 6 $kJmol^{-1}$ was calculated from the hyperpolarizing phase of the action potential which is thought to be due to a K^+-transport (Blatt 1974). In both Nitella flexilis and Chara corallina the enthalpy of activation increases below 15 °C (Blatt 1974, Homblé 1985). This is consistent with the results of Hope and Aschberger (1970) who have shown, using radiotracers, that the membrane K^+ permeability decreases at low temperature.

6.3 The stochastic approach

Two methods have been developed to obtain information about the molecular mechanism of ion transport: fluctuation analysis (also called noise analysis) and single channel analysis.

6.3.1 Fluctuations analysis

Membrane channels operate stochastically. In a membrane the number of open channels is not constant but fluctuates randomly around an average value. This inherently probabilistic nature of channels leads to fluctuation of the membrane conductance and therefore of the membrane current and of the membrane potential difference. Fluctuation theory has been applied to analysze electrical fluctuation fluctuations of biological membranes so as to get an insight into the molecular mechanisms of ion channels.

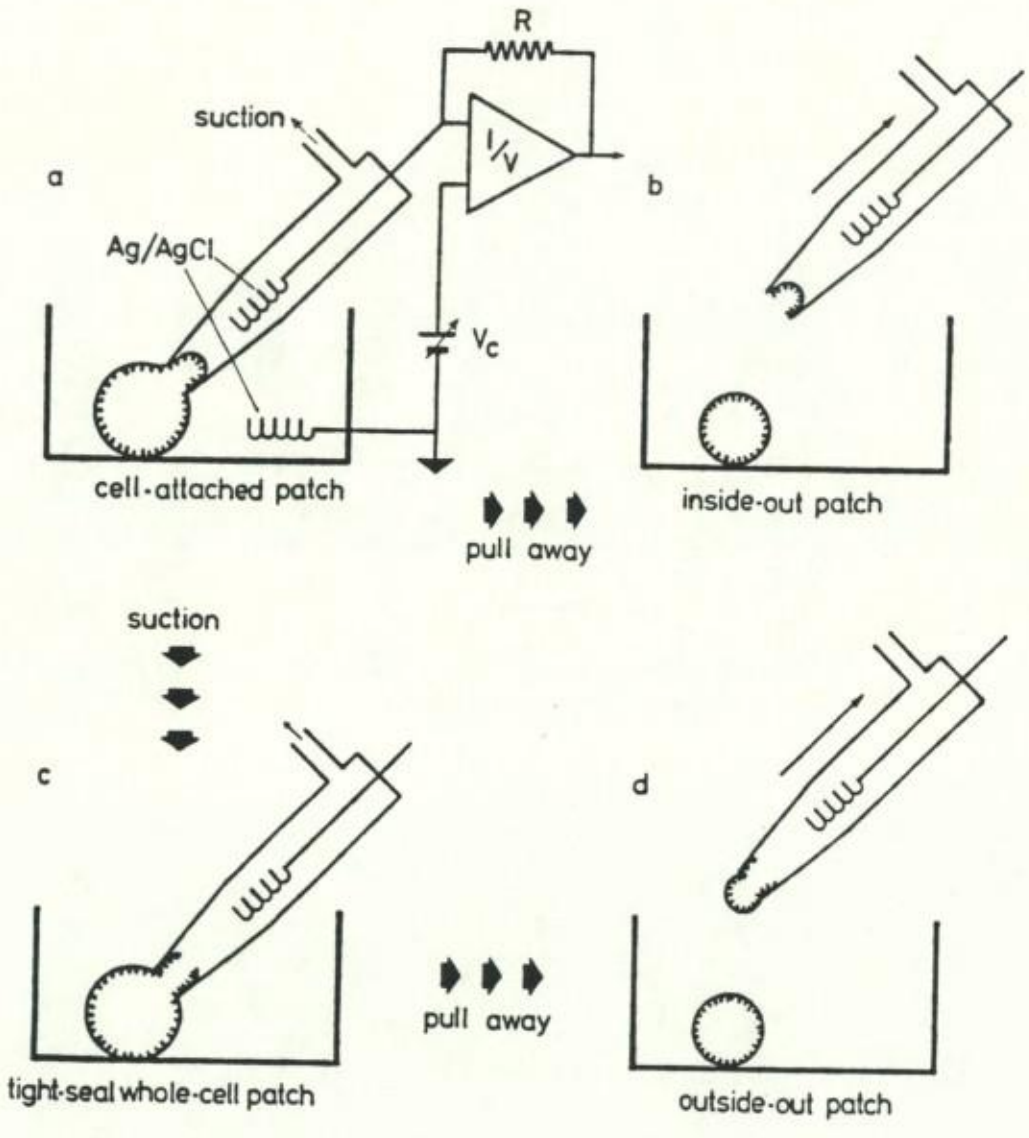

Figure 27: Schematic diagram of the procedure used for patch-clamp techniques. I/V: high gain low input noise current to voltage converter; V_c: voltage command; Ag/AgCl: silver chlorided electrodes.

Channel fluctuations (also called channel noise) are usually characterized by their power spectral density. The power spectral density associated with a set of time series data describes the amplitude and the rapidity of fluctuations in the original record. It is obtained from Fourier analysis of the time series recorded. Fourier analysis of a time series consists in decomposing a function of time into a sum of sine and cosine waves of various frequencies and amplitudes. The power spectral density is obtained from this Fourier decomposition by squaring the sine and cosine amplitude for each frequency, summing them together and dividing by two (averaging). To use noise analysis one must first postulate a model for the channel, from which the probability of finding the channel in its various states can be derived; then use this to calculate the power spectral density. The validity of the model is judged by comparison between the theoretical and the experimental power spectral density.

Most of the analysis of the electrical fluctuations in plant cells has been concerned with the contribution of the electrogenic active transport to the global electrical fluctuations which occur across plant membranes (Roa and Pickard 1976, 1977,Ross and Dainty 1985, 1986, Alexandre et al. 1986).

In Chara corallina the minus two slope of the logarithm of the voltage power spectral density was attributed to the stochastic activity of K^+ channels (Ferrier et al. 1979). The change in electrical fluctuations induced by the presence of gramicidin A (a channel-forming polypeptide) in the membrane of cells of Acer pseudoplatanus was studied by Alexandre et al. (1985). In this case good agreement was observed between the data obtianed on the plant cell membrane and those obtained on a bilayer lipid membrane.

6.3.2 Single channel analysis

Single channels isolated from plant cells were first obtained in bilayer lipid membranes. The recent develpment of the patch-clamp technique has permitted the study of single channel activity in biological membranes (Sakmann and Neher 1984). The method consists of excising a patch of membrane in a clean glass pipette by sucking the membrane into the pipette tip which has a diameter of about 1 μm. The four different types of experimental configuration that can be achieved with the patch clamp technique are described hereafter and in Figure 27.

a) The cell-attached configuration: the initial step consists of pressing a cleaned fine tip glass pipette against the cellular membrane free of connective tissues ar cell wall. Upon application of suction a tight seal of extremely high resistance (about 10 G Ω) forms between the membrane and the inner wall of the glass pipette. This is called the cell-attached patch (Figure 27a). It permits the recording of single channel activity in vivo. This configuration is the easiest to obtain. It disturbs the membrane and its physiological environment to a lesser extend than the other types of experimental configuration.

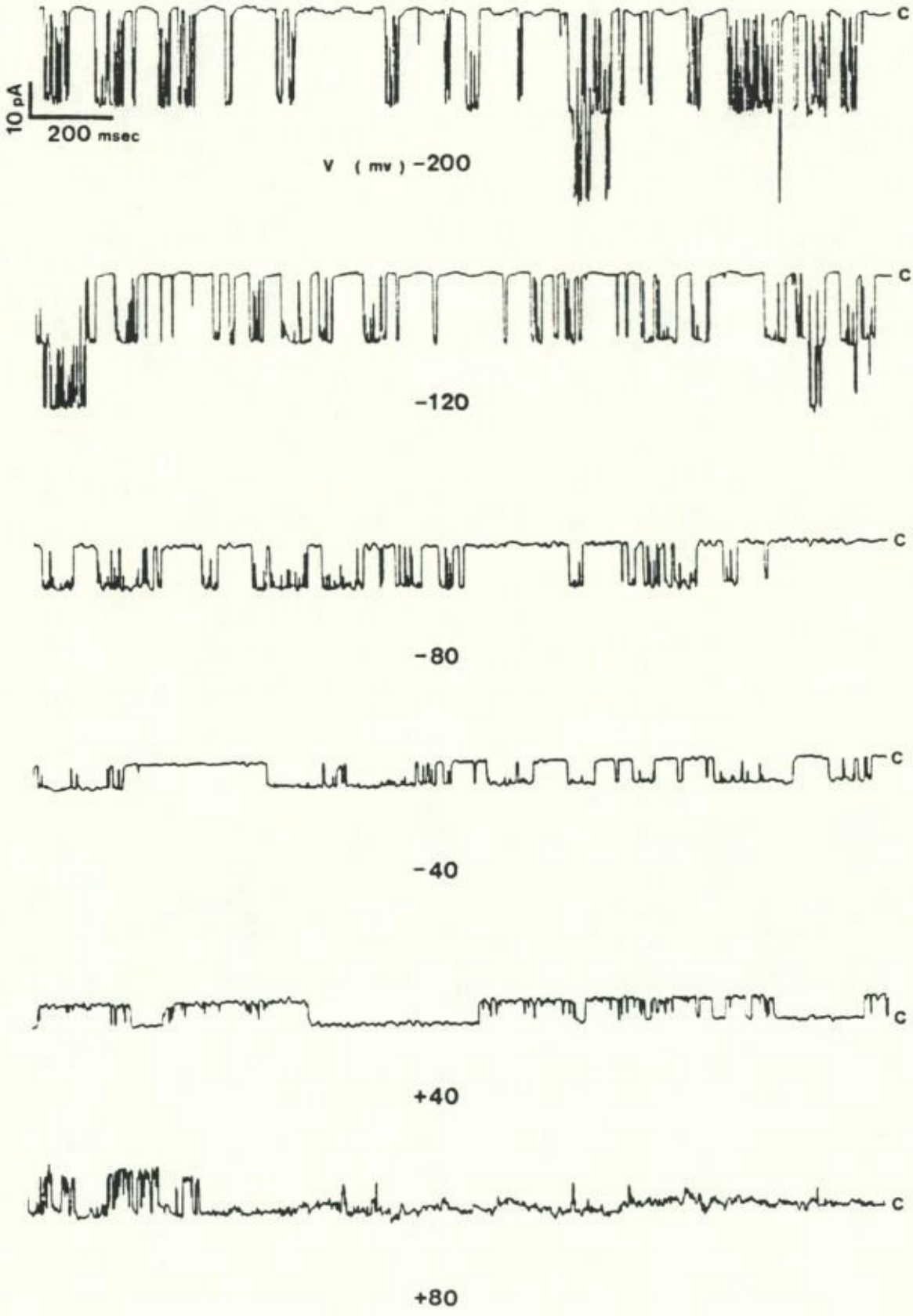

Figure 28: Time course of the current flowing through a single potassium channel

b) The inside-out configuration: because of the high mechanical stability of the glass-membrane seal, further manipulation is possible starting from the cell-attached configuration. When the cell under investigation is attached to its support, a quick withdrawal will break the sealed patch membrane from the remaining cell membrane and form an inside-out configuration (Figure 27b).

c) The tight-seal whole cell configuration: it is created by the rupture of the patch membrane at the stage of cell-attached configuration (Figure 27c). It is obtained by increasing the suction in the pipette until the patch membrane breaks. This configuration allows investigation of small cells under voltage and current clamp techniques and recording of overall current and voltage response of the total number of channels present in the membrane.

d) The outside-out configuration: it differs from the inside-out configuration by presenting the membrane intracellular face towards the pipette solution instead of the outer face. Such configuration can be achieved by forcing the rupture of the sealed membrane from the cell fixed in its tight-seal whole cell configuration (Figure 27d).

The patch-clamp electronic circuit consists of a current to voltage converter provided with a feedback resistor of high value which sets the amplification factor and with a low leakage and low input noise current in order to allow a resolution of a few picoamperes. A high order active filter and a capacitance compensating circuit are usually added in order to improve the noise and time constant performances of the current to voltage converter.

When properly carried out, these preparations contain only one channel and discrete pulses of current originating from and returning to the baseline current level are observed as long as an electrochemical potential difference is applied across the patched membrane (Figure 28). Knowing the channel current (I_s), the membrane potential difference (V) and the reversal potential (E_r) for the ion flowing through the channel, the single channel conductance (γ) can be calculated from:

$$\gamma = \frac{I_s}{(V - E_r)}. \qquad [53]$$

We begin our description of single channels with the Ca^{2+} channel because it was the first channel isolated. It is now ten years since Alexandrov et al. (1976) isolated from the protoplasm of Nitellopsis obtusa a water soluble molecule which had a channel activity when studied in a lipid bilayer membrane. In this pioneer paper the authors reported that the channel seemed to be made up of identical subunits of about 15 pS conductance. Aggregates of 3, 6 or 12 subunits were mostly seen. However, more recently, it has been reported that a single subunit could have a conductance as low as 2.5 pS and that the aggregate most often encoutered consisted of 80 subunits which gave rise to a channel conductance of 200 pS in 100 mM KCl (Volkova et al. 1980). The channel was denaturated by treatment with proteolytic enzymes such as pronase or trypsin but was insensitive to nucleases. It was thermostable (Volkova et al. 1980). Values of 5 kD and 20 kD have been reported for the molecular weight of the channel (Volkova et al. 1980). The ionic

selectivity of this channel was as that determined for the calcium current of the action potential (Alexandrov et al. 1976, Lunevsky et al. 1980). The channel selectivity was independent of the number of subunits. Only the conductance of the channel was proportional to the number of subunits. Whatever the number of subunits forming the channel only two states were observed: open and closed. These facts led Berestovsky and Alexandrov (1983) to propose that the channel is made up of a cluster of about 80 subunits which open and close simultaneously.

Different channels that mediate ion fluxes have been identified by means of the patch-clamp technique in the fresh water alga Chara. Two different K^+ channels and a Cl^- channel have been identified in the tonoplast surrounding protoplasmic droplets formed from Chara (Lühring 1986, Homblé et al. 1987, Homblé 1987, Laver and Walker 1987, Bertl 1989, Tyerman and Findlay 1989) and a Cl^- channel was found in the plasmalemma of Chara (Coleman 1986). Most of these investigations have been done using the cell-attached recording mode which does not permit to control the ionic composition on both side of the membrane. Using this patch-clamp configuration Laver and Walker (1987) have concluded that the large conductance K^+ channel is voltage-dependent. However, because the composition on the inner side of the membrane was not controlled in their experiments it is still possible that the channel was not directly voltage-activated. It could be ligand-activated. In this case, if the concentration of ligand in the vicinity of the channel is voltage-dependent then the channel will appear to be voltage-dependent in the cell-attached recording mode. For instance, Ca^{2+} is known to regulate the properties of some cationic channels in both animal and plant cells (Hedrich and Neher 1987, Schroeder and Hagiwara 1989, Stoeckel and Takeda 1989). The current-voltage characteristic of the large conductance K^+ channel is nonlinear and shows saturation at extreme voltages (Lühring, 1986; Laver and Walker, 1987; Bertl, 1989). Bertl (1989) has shown that a 6-states model is required to account for these properties.

According to Sakano and Tazawa (1986) and Lühring (1986), the membrane surrounding cytoplasmic droplets formed from Chara is mostly tonoplast. This has been confirmed by Bertl (1989) who has suggested that the droplets were enclosed by tonoplast in the right-side-out orientation (cytoplasmic side facing the bath solution).

The voltage-dependent chloride channel found in the plasmalemma of Chara corallina has a unitary conductance of 7 pS (Coleman 1986). The magnitude and the shift of the reversal potential when the extracellular chloride concentration was changed were consistent with thepermeant ion being Cl^-. The channel was activated when the patched membrane was hyperpolarized which led Coleman (1986) to suggest that this channel is implicated in the punchthrough phenomenon.

Using the inside-out configuration, three different channels were found in the vacuolar membrane surrounding protoplasmic droplet of Chara (Homblé et al. 1989). Two of them are selective to K^+ and have a different unitary conductance: 89 and 132 pS in symmetric 150 mM KCl. Two K^+ channels with similar current-voltage characteristic was also observed using the cell-attached configuration (Lühring 1986, Homblé et al. 1987, Laver and Walker 1987, Tyerman and Findlay 1989). In those previous works the composition of the solution on the inner face of the patched

membrane was not controlled which made comparisons uneasy. These two K^+ channels probably account for the time- and voltage-dependent inward current observed on whole droplets (Homblé 1987).

Our statistical analysis of single channel measurements, using the inside-out configuration, shows that the duration of the mean open and closed times of the 132 pS does not depend on the applied voltage. Thus, we can conclude that the channel itself is not voltage-dependent. However, the statistical properties of this channel seems to be voltage-dependent when the channel activity is measured in the cell-attached configuration (Laver and Walker 1987). This suggests that the channel could be regulated by a chemical factor located inside the droplet. The fact that at least two exponential terms were required to fit the closed-time distributions indicates that there are at least two distinct closed states involved in the ion gating reaction. The frequency histograms of the open lifetimes indicate that one open state is involved in the gating mechanism of this channel. The minimum kinetic scheme consistent with these results is:

$$\text{open} = \text{closed}_1 = \text{closed}_2.$$

A K^+ channel with a slow rate of activation was found in the vacuole of various higher plants and termed slow-vacuolar (SV) channel (Hedrich et al. 1986, Coyaud et al. 1987, Colombo et al. 1988). It has a unitary conductance of about 180 pS in symmetrical 200 mM KCl. SV channels are permeable to both cations and anions and are rather unselective. However, the SV-type K^+ channel of barley vacuoles is exclusively permeable to cations (Kolb et al. 1987). The selectivity sequence of the 132 pS K^+ channel of the vacuole of Chara (a lower plant), derived from permeability ratio estimates under biionic conditions, was found to be $K > Cs > Rb > Na$. It has a stronger selectivity for potassium than the SV channel of higher plants. However, our results are consistent with those got on the marine alga Acetabularia which also have a vacuolar channel highly selective to K^+ (Bertl and Gradmann 1987, Bertl et al. 1988).

It has been previously shown that TEA strongly decreases the K^+ conductance of whole droplets (Homblé 1987), but no information has been available about the type of K^+ channel involved and it has not been possible from previous studies to reach conclusions about the mode of action. The effect of TEA was tested on both side of the membrane. The striking differences in the characteristics of the TEA blockade from external and internal sides suggest the existence of two different binding sites for TEA in the channel. In both cases TEA blockade is observed as an apparent reduction in the open channel current, indicating that block and unblock events are too fast to be detected. When TEA is added to the inner side of the membrane the block increases for positive potentials and is relieved at negative potential, indicating that the blocking site senses the electric field. The blocking site on the external side of the membrane is not voltage-dependent at the two TEA concentrations tested.

Outward plasma-membrane K^+ currents activated by membrane depolarization have been reported in other plants, for example Asclepias tuberosa protoplasts (Schauf and Wilson 1987a), trap lobe protoplasts of Dionaea muscipula (Iijima and Hagiwara 1987), motor cells of Samanea saman (Moran et al. 1988) and in stomatal guard cell protoplasts (Hosoi et al 1988, Schroeder 1989).

Nonselective strectch-activated channels have been found in the plasma membrane of cultured tobacco cells protoplasts (Falke et al. 1988) and could function as turgo sensors or mechanosensors.

A 4 nS voltage-dependent anion-nonselective channel has been identified in outer mitochondrial membrane fractions of corn mitochondria included in planar phospholipid bilayer membranes (Smack and Colombini 1985). Evidence for Cl^- channels was found in Asclepias tuberosa protoplasts (Schauf and Wilson 1987b). They were characterized by a large unitary conductance (100 pS) and a strong voltage-dependence. Outwardly conducting K^+ channels have been suggested to represent a predominant pathway for K^+ release from guard cells of Vicia faba (Schroeder et al. 1984, Schroeder et al. 1987) whereas inwardly conducting K^+ channels which are time- and voltage-dependent would represent the pathway for net K^+ uptake during stomatal opening (Schroeder et al. 1987).

A voltage-dependent chloride-selective channel with an unitary conductance of 65 pS in 30 mM KCl was found on isolated membrane patches from osmotically inflated thylakoids of Peperomia metallica (Schonknecht et al. 1988). The prime function of thylakoid membrane is to provide the cell with adenosine triphosphate. ATP synthesis is driven by the by the proton motive force, which is generated and maintained across the inner chloroplast membrane (ICM) by the photosynthesis. According to the chemiosmotic theory ion channel like those found in both plasmalemma and tonoplast would not be expected in the ICM because the high rates of ion transport characteristic of ion transport characteristic of open channels would be expected to dissipate the proton motive force. The presence of ion channels in the ICM might explain the low values of membrane potential difference (+20 mV) recorded using microelectrodes (Vredenberg and Tonk 1975) because they would partially shortcircuit the electrochemical gradient build during the photosynthetic H^+ transport.

7 CONCLUSION

Major progress in understanding of mineral nutrition is being made at the molecular level. In view of the great strength of the new biophysical methods giving access to mechanisms, kinetic analyses on tissue level appear increasingly impotent, as they only allow speculations on the nature of the mechanism of ion transport. The measurement of ion transport through a single ion pump will require new electronic components. However, the very low densities of channels estimate by Homblé et al. (1987) must not discourage biochemists who want to isolate and characterize the proteins which make the channels. Improvement of their methods would permit to understand the structure-function relationship of ion channels.

8 REFERENCES

Abramowitz M, Stegum IA (1970) Handbook of mathematical functions. Dover Publications, New York

Aleksandrov AA, Berestovsky GN, Volkova SP, Vostrikov IYa, herelova OM, Kravchik S, Lunevsky VZ (1976) Reconstitution of single calcium-sodium channels of the cells in lipid bilayers. Doklady Academy Nauk SSSR, 27: 723-726

Alexandre J, Lassales J-P, Thellier M (1985) Voltage noise in Acer pseudoplatanus cells. Basic cellular noise and gramicidin A induced noise. Plant Physiol 79: 546-551

Alexandre J, Lassales J-P, Thellier M (1986) Electrical noise measurements on red beet vacuoles: another way to detect the ATPase activity. Plant Physiol 81: 1147-1150

Armstrong CM (1975) Potassium pores of nerve and muscle membranes. In: "Membranes" vol.3, Eisenman G Ed., Marcel Dekker, New York, pp.325-358

Barry PH, Hope AB (1969) Electroosmosis in membranes: effects of unstirred layers and transport numbers. I Theory. Biophys J 9: 700-728

Barry PH (1977) Transport number effects in the transverse tubular system and their implications for low frequency impedance measurement of capacitance of skeletal muscle fibers. J Membrane Biol 34: 243-292

Beilby MJ (1981) Excitation-revealed changes in cytoplasmic Cl^- concentration in "Cl-starved" Chara cells. J Membrane Biol 62: 207-218

Beilby MJ (1982) Cl^- channels in Chara. Phil Trans R Soc Lond B299: 435-445

Beilby MJ (1984) Calcium and plant action potential. Plant Cell Environ 7: 415-421

Beilby MJ (1985) Potassium channels at Chara plasmalemma. J Exp Bot 36: 228-239

Beilby MJ (1986) Potassium channels and different states of Chara plasmalemma. J Membrane Biol 81: 241-249

Beilby MJ, Coster HGL (1976) The action potential in Chara corallina: effect of temperature. Aust J Plant Physiol 3: 275-289

Beilby MJ, Coster HGL (1979a) The action potential in Chara corallina. II. two activation-inactivation transients in voltage clamps of the plasmalemma. Aust J Plant Physiol 6: 323-335

Beilby MJ, Coster HGL (1979b) The action potential in Chara corallina. III. The Hodgkin-Huxley parameters for the plasmalemma. Aust J Plant Physiol 6: 337-353

Beilby MJ, Coster HGL (1979c) The action potential in Chara corallina. VI. activation enthalpies of the Hodgkin-Huxley gates. Aust J Plant Physiol 6: 354-365

Belton P, Van Netten C (1971) The effects of pharmacological agents on the electrical response of cells of Nitella flexilis. Can J Physiol Pharmacol 49: 824-832

Benz R, Laüger (1976) Kinetic analysis of carrier-mediated ion transport by the charge-pulse technique. J Membrane Biol 27: 171-191

Berestovsky GN, Vostrikov IYa, Lunevsky VZ (1976) Ionic channels of the tonoplast of the Characeae algal cells. The role of calcium ions in excitation. Biofiz 21: 829-833

Berestovsky GN, Aleksandrov AA (1983) The cluster structure and gating mechanism of the reconstructed calcium channel of Characean algal cells. Biofis 28: 816-820

Bertl A, Gradmann D (1987) Current-voltage relationships of potassium channels in the plasmalemma of Acetabularia. J Membrane Biol 99: 41-49

Bertl A, Klieber HG, Gradmann D (1988) Slow kinetics of a potassium channel in Acetabularia. J Membrane Biol 102: 141-152

Bertl A (1989) Current-voltage relationships of a sodium-sensitive potassium channel in the tonoplast of Chara corallina. J Membrane Biol 109: 9-19

Bisson MA, Walker NA (1980) The Chara plasmalemma at high pH. Electrical measurements show rapid specific passive uniport of H^+ or OH^-. J Membrane Biol 56: 1-7

Bisson MA, Walker NA (1981) The hyperpolarization of the Chara membrane at high pH: effects of external potassium, internal pH, and DCCD. J Exp Bot 32: 951-971

Bisson MA, Walker NA (1982) Control of passive permeability in the uChara plasmalemma. J Exp Bot 33: 520-532
Bisson MA (1986) The effect of darkness on active and passive transport in Chara corallina. J Exp Bot 37: 8-21

Blatt FJ (1974) Temperature dependence of the action potential in Nitella flexilis. Biochim Biophys Acta 339: 382-389

Boas ML (1966) Mathematical methods in the physical sciences. John Wiley, New York

Bowman EJ, Siebers A, Altendorf K (1988) Bafilomycins: a class of inhibitors of membrane ATPases from microorganisms, animal cells, and plant cells. Proc Natl Acad Sci USA 85: 7972-7976

Bush DS, Hedrich R, Schroeder JI, Jones RI (1988) Channel-mediated K^+ flux in barley aleurone protoplasts. Planta 76: 368-377

Chanson A, Fischmann J, Spear D, Taiz L (1985) Pyrophosphate-driven proton transport by microsomal membranes of corn coleoptiles. Plant Physiol 79: 159-164

Clint GM, MacRobbie EAC (1987) Sodium efflux from perfused algal cells. Planta 171: 247-253

Coleman HA (1986) Chloride currents in Chara. A patch-clamp study. J Memb Biol 93: 55-61

Coleman HA, Findlay GP (1985) Ion channels in the membrane of Chara inflata. J Membrane Biol 83: 109-118

Colombo R, Cerana R, Lado P, Peres A (1988) Voltage-dependent channels permeable to K^+ and Na^+ in the membrane of Acer pseudoplatanus vacuoles. J Membrane Biol 103: 227-236

Coster HGL, Hope AB (1968) Ionic relations of cells of Chara australis. Aust J Biolo Sci 21: 243-254

Coster HGL, Smith JR (1977) Low frequency impedance of Chara corallina: simultaneous measurements of separate plasmalemma and tonoplast capacitance and conductance. Aust J Plant Physiol 4: 667-674

Coyaud L, Kurkdjian A, Kado R, Hedrich R (1987) Ion channels and ATP-driven pumps involved in ion transport across the tonoplast of sugarbeet vacuoles. Biochim Biophys Acta 902: 263-268

Dainty J, Hope AB (1959) Ionic relations of cells of Chara australis. I. Ion exchange in the cell wall. Aust J Biol Sci 12: 395-411

Dainty J, Hope AB, Denby C (1960) Ionic relations of cells of Chara australis. II. The indiffusible anions of the cell wall. Aust J Biol Sci 13: 267-276

Dainty J, Hope AB (1961) The electric double layer and the donnan equilibrium in relation to plant cell walls. Aust J Biol Sci 14: 541-551

Dainty J (1962) Ion transport and electrical potentials in plant cells. Ann Rev Plant Physiol 13: 379-402

Derksen HE, Verveen AA (1966) Fluctuations of resting membrane potential. Science 151: 1388-1389

Demarty M, Morvan C, Thellier M (1978) Exchange properties of isolated cell walls of Lemna minor L. Plant Physiol 62: 477-481.

Demarty M, Morvan C, Thellier M (1984) Calcium and the cell wall. Plant Cell Environment 7: 441-448

Eisenman G, Horn R (1983) Ionic selectivity: the role of kinetic and equilibrium processes in ion permeation through channels. J Membrane Biol 76: 197-225

Etherton B, Rubinstein B (1978) Evidence for amino acid-H^+ co-transport in oat coleoptiles. Plant Physiol 61: 933-937

Falke LC, Edwards KL, Pickard BG, Misler S (1988) A stretch-activated anion channel in tobacco protoplasts. FEBS Letters 237: 141-144

Ferrier JM, Morvan C, Lucas WJ, Dainty J (1979) Plasmalemma voltage noise in Chara corallina. Plant Physiol 63: 709- 714

Ferrier JM (1980a) Apparent bicarbonate uptake and possible plasmalemma proton efflux in Chara corallina. Plant Physiol 66: 1198-1199

Ferrier JM (1980b) Extracellular ion transport. J Theor Biol 85: 739-743

Ferrier JM (1981) Time-dependent extracellular ion transport. J Theor Biol 92: 363-368

Ferrier JM, Dainty J, Ross SM (1985) Theory of negative capacitance in membrane impedance measurements. J Membrane Biol 85: 245-249

Findlay GP (1961) Voltage-clamp experiments with Nitella. Nature 191: 812-814

Findlay GP (1962) Calcium ions and the action potential in Nitella. Aust J Biol Sci 15: 69-82

Findlay GP, Hope AB (1964a) Ionic relations of cells of Chara australis. VII. The separate electrical characteristics of the plasmalemma and tonoplast. Aust J Biol Sci 17: 62-77

Findlay GP, Hope AB (1964b) Ionic relations of cells of Chara australis. IX. Analysis of transient membrane currents. Aust J Biol Sci 17: 400-411

Findlay GP, Hope AB (1976) Electrical properties of plant cells: methods and findings. In Encyclopedia of Plant Physiology, New series, vol 2A, U Lüttge, MG Pitman eds, 53-92, Springer-Verlag, Berlin

Findlay GP, Coleman HA (1983) Potassium channels in the membrane of Hydrodictyon africanum. J Membrane Biol 75: 241-151

Fujii S, Shimmen T, Tazawa M (1979) Effect of intracellular pH on the light-induced potential change and electrogenic activity in tonoplast-free cells of Chara australis. Plant Cell Physiol 20: 1315-1328

Gaffey CT, Mullins LJ (1958) Ion fluxes during the action potential in Chara. J Physiol 144: 505-524

Gillet C, Lefebvre J (1978) Ionic diffusion through the Nitella cell wall in the presence of calcium. J Exp Bot 112: 1155-1159

Gillet C, Lefebvre J (1981) Estimation of the anion-exchange capacity of the cell wall of Nitella flexilis. J Exp Bot 32: 37-41

Gradmann D, Wagner G, Gläsel RM (1973) Chloride efflux during light-triggered action potentials in Acetabularia mediterranea. Biochim Biophys Acta 323: 151-155

Graeme JG, Tobey GE, Huelsman LP (1971) Operational amplifier. Mc Graw Hill, New York

Grant GT, Morris ER, Rees DA, Smith PJC, Thom D (1973) Biological interactions between polyssacharides and divalent cations: the egg-box model. FEBS Letters 32: 195-198

Gutknecht J (1988) Proton conductance caused by long-chain fatty acids in phospholipid bilayer membranes. J Membrane Biol 106: 83-93

Haapanen L, Skoglund CR (1967) Recording of ionic efflux during single action potentials in Nitellopsis obtusa by means of high-frequency reflectrometry. Acta Physiol Scand 69: 51-68

Hamill OP, Marty A, Neher E, Sakmann B, Sigworth FJ (1981) Improved patch-clamp techniques for high resolution current recording from cells and cell-free membrane patches. Pfluegers Arch 391: 85-100

Harper JF, Surowy TK, Sussman MR (1989) Molecular cloning and sequence of cDNA encoding the plasma membrane proton pump (H^+-ATPase) of Arabidopsis thaliana. Proc Natl Acad Sci USA 86: 1234-238

Hayama T, Shimmen T, Tazawa M (1979) Participation of Ca^{2+} in cessation of cytoplasmic streaming induced by membrane excitation in Characea internodal cells. Protoplasma 99: 305-321

Haynes RJ (1980) Ion exchange properties of roots and ionic interactions within the root apoplast: their role in ion accumulation by plants. Bot Rev 46: 75-99

Hedrich R, Flügge UI, Fernandez JM (1986) Patch-clamp studies of ion transport in isolated plant vacuoles. FEBS Letters 204: 228-232

Hedrich R, Neher E (1987) Cytoplasmic calcium regulates voltage-dependent ion channels in plant vacuoles. Nature 329: 833-836

Hedrih R, Schroeder JI (1989) The physiology of ion channels and electrogenic pumps in higher plants. Ann Rev Plant Physiol 40: 539-569

Hirono C, Mitsui T (1981) Time course of activation in plasmalemma if Nitella axilliformis. In Biochemistry and Function of Channel Proteins, G Matsumoto, M Kotani eds, 135-149, University of Tokyo Press, Tokyo

Hodgkin AL, Huxley AF (1952a) Current carried by sodium and potassium ions through the membrane of the giant axon of Loligo. J Physiol 116: 449-472

Hodgkin AL, Huxley AF (1952b) The components of membrane conductance in the giant axon of Loligo. J Physiol 116: 473-496

Hodgkin AL, Huxley AF (1952c) The dual effect of membrane potential on sodium conductance in the giant axon of Loligo. J Physiol 116: 497-506

Hodgkin AL, Huxley AF (1952d) A quantitative description of membrane current and its implication to conduction and excitation in nerve. J Physiol 117: 500-544

Hodgkin AL, Huxley AF, Katz B (1952) Measurements of the current-coltage relations in the membrane of the giant axon of Loligo. J Physiol 116: 424-448

Homblé F (1984) De l'origine et de la modulation des propriétés électriques membranaires des cellules internodales de Chara corallina. PhD Thesis. Université Libre de Bruxelles. Belgium

Homblé F, Jenard A (1984) Pseudo-inductive behaviour of the membrane potential of Chara corallina under galvanostatic conditions: a time-variant property of potassium channels. J Exp Bot 35: 1309-1322

Homblé F (1985) Effect of sodium, potassium, calcium, magnesium and tetraethylammonium on the transient voltage response to a galvanostatic step and of the temperature on the steady state membrane conductance of Chara corallina. J Exp Bot 36: 1603-1611

Homblé F (1987a) Effect of dinitrophenol on membrane potential, membrane resistance and chlorophyll fluorescence of Chara corallina internodal cells at various pH values. Bioelectrochem Bioenerg 17: 165-174

Homblé F (1987b) A tight-seal whole cell study of the voltage-dependent gating mechanism of K^+ channels of protoplasmic droplets of Chara corallina. Plant Physiol 84: 433-437

Homblé F, Jenard A (1987a) Membrane impedance of internodal cells of Chara corallina obtained by analysis of low level transients. Bioelectrochem Bioenerg 17: 131-139

Homblé F, Jenard A (1987b) Membrane operational impedance spectra in Chara corallina estimated by Laplace transforms analysis. Plant Physiol 81: 919-921

Homblé F, Ferrier J, Dainty J (1987) Voltage-dependent K^+-channel in protoplasmic droplets of Chara corallina. A single channel patch clamp study. Plant Physiol 83: 53-57

Homblé F (1988) A fast and high-current voltage clamp device for biophysical investigations. J Phys E: Sci Instrum 21: 1100-1102

Homblé F (1988) Contribution à l'étude des mécanismes des échanges ioniwues dans la cellule végétale. Concours Annuels de la Classe des Sciences de L'Académie Royale de Belgique

Homblé F, Ferrier JM (1988) Analysis of the diffusion theory of negative capacitance: the role of K^+ and the unstirred layer thickness. J Theor Biol 131: 183-197

Homblé F, Jenard A, Hurwitz HD (1988) Some techniques for investigation of electrochemical and ion transport properties of biological cell membranes: the case of Chara corallina. In Redox Chemistry And Interfacial Behaviour Of Biological Molecules, G Gryhurst and K Niki Eds., Plenum, New York, pp. 583-612

Homblé F, Richter C, Dainty J (1989) Leakage of pectins from the cell wall of Chara corallina in the absence of divalent cations. Plant Physiol Biochem 27: 465-468

Homblé F, Malornikoff A, Lannoye R (1990) Correlation between the banding pattern and the cell wall composition in Chara corallina: a Fourier transform infra-red study. J Plant Physiol (in press)

Hope AB, Aschberger PA (1970) Effect of temperature on membrane permeabilty to ions. Aust J Biol Sci 23: 1047-1060

Hope AB, Findlay GP (1964) The action potential in Chara. Plant Cell Physiol 5: 377-379

Hope AB, Walker NA (1961) Ionic relations of cells of Chara australis R. BR. IV. Membrane potential differences and resistances. Aust J Biol Sci 14: 26-44

Hope AB, Walker NA (1975) The Physiology of giant algal cells. Cambridge University Press, London

Hosoi S, Iino M, Shimazaki K (1988) Outward-rectifying K^+ channels in stomatal guard cell protoplasts. Plant Cell Physiol 29: 907-911

Iijima T, Hagiwara S (1987) Voltage-dependent K channel in protoplasts of trap-lobe cells of Dionaea muscipula. J Membrane Biol 100: 73-81

Jenard A, Hurwitz HD, Homblé F (1986) A simple theoretical model of steady-state electrogenic transfert of reactive species across membranes. Biophys Chem 25: 287-296

Jorgensen PL (1975) Isolation and characterization of the components of the sodium pump. Quart Rev Biophys 7: 239-274

Kataev AA, Zherelova OM, Berestovsky GN (1984) Ca^{2+}-induced activation and reversible inactivation of chloride channels in the perfused plasmalemma of Nitellopsis obtusa. Gen Physiol Biophys 3: 447-462

Kawamura G, Tazawa M (1980) Rapid light induced potential change in Chara cells stained with neutral red in the absence of internal Mg-ATP. Plant Cell Physiol 21: 547-559

Kawamura G, Shimmen T, Tazawa M (1980) Dependence of the membrane potential of Chara cells on external pH in the presence or absence of internal adenosinetriphosphate. Planta 149: 213-218

Keifer DW, Lucas WJ (1982) Potassium channels in Chara corallina. Plant Physiol 69: 781-788

Keifer DW, Spanswick RM (1978) Activity of the electrogenic pump in Chara corallina as inferred from measurements of the membrane potential, conductance, and potassium permeability. Plant Physiol 62: 653-661

Kikuyama M, Tazawa M (1976) Tonoplast action potential i Nitella in relation to vacuolar chloride concentration. J Membrane Biol 29: 95-110

Kikuyama M, Tazawa M (1983) Transient increase of intracellular Ca^{2+} during excitation of tonoplast-free cells. Protoplasma 117: 62-67

Kikuyama M, Oda K, Shimmen T, Hayama T, Tazawa M (1984) Potassium and chloride effluxes during excitation of Characeae cells. Plant Cell Physiol 25: 965-974

Kimpel DL, Togasaki RK, Miyachi S (1983) Carbonic anhydrase in Chlamydomonas reinhardtii. I. Localiation. Plant Cell Physiol 24: 255-259

Kishimoto U (1961) Current voltage relations in Nitella. Biol Bull 121: 370-371

Kishimoto T (1964) Current voltage relations in Nitella. Jap J Physiol 14: 515-527

Kishimoto U (1966) Hyperpolarizing response in Nitella internodes. Plant Cell Physiol 7: 429-439

Kishimoto U (1972) Characteristics of the excitable Chara membrane. Adv Biophys 3:199-226

Kishimoto U (1974) Transmembrane impedance of the Chara cell. Jpn J Physiol 24: 403-417

Kitasato H (1968) The influence of H^+ on membrane potential and ion fluxes of Nitella. J Gen Physiol 52: 60-

Kochian LV, Xin-zhi J, Lucas WJ (1985) Potassium transport in corn roots. Plant Physiol 79: 771-776

Kohn R (1975) Ion binding on polyuronates -- alginate and pectin. Pure Appl Chem 42: 371-397

Kolb H-A, Köhler K, Martinoia E (1987) Single potassium channels in membranes of isolated mesophyll barley vacuoles. J Membrane Biol 95: 163-169

Köhler K, Geisweid H-J, Simonis W, Urbach W (1983) Changes in membrane potential and resistance caused by transient increase of potassium conductance in the unicellular green alga Eremosphaera viridis. Planta 159: 165-171

Köhler K, Steigner W, Kolbowski J, Hansen U-P, Simonis W, Urbach W (1986) Potassium channels in Eremosphaera viridis. Planta 167: 66-75

Koppenhöfer E (1972) Die wirkung von kupfer, TTX, cocain und TEA auf das ruhe- und aktionspotential on Nitella. Pflüger Arch 336: 299-309

Laver DR, Walker NA (1987) Steady-state voltage-dependent gating and conduction kinetics of single K^+ channels in the membrane of cytoplasmic drops of Chara australis. J Membrane Biol 100: 31-42

Laver DR, Fairley KA, Walker NA (1989) Ion permeation in a K^+ channel in Chara australis: direct evidene for diffusion limitation of ion flow in a maxi-K channel. J Membrane Biol 108: 153-164

Lichtner FT, Lucas WJ, Spanswick RM (1981) Effect of sulfhydryl reagents on the biophysical properties of the plasmalemma of Chara corallina. Plant Physiol 68: 899-904

Lucas WJ, Smith FA (1973) The formation of alkaline and acid regions at the surface of Chara corallina cells. J Exp Bot 24: 1-14

Lucas WJ (1975) Photosynthetic fixation of ^{14}Carbon by internodal cells of Chara corallina. J Exp Bot 26: 331-346

Lucas WJ (1976) Plasmalemma transport of HCO_3^- and OH^- in Chara corallina: non-antiporter systems. J Exp Bot 27: 19-31

Lucas WJ (1977) Circulating electric currents between acid and alkaline zones associated with HCO_3^- assimilation in Chara. J Exp Bot 28: 1190-1206

Lucas WJ, Ferrier JM, Dainty J (1977) Plasmalemma transport of OH^- in Chara corallina. Dynamics of activation and deactivation. J Membrane Biol 32: 49-73

Lucas WJ (1982) Mechanism of acquisition of exogenous bicarbonate by internodal cells of Chara corallina. Planta 156: 181-192

Lucas WJ (1983) Photosynthetic assimilations of exogenous HCO3- by aquatic plants. Ann Rev Plant Physiol 34: 71-104

Lühring H (1986) Recording of single K^+ channels in the membrane of cytoplasmic drop of Chara australis. Protoplasma 133: 19-28

Lunevsky VZ, Zherelova OM, Alexandrov AA, Vinokurov MG, Berestovsky GN (1980) Model of selective calcium channel of Characean alga cells. Biofiz 25: 685-691

Lunevsky VZ, Zherelova OM, Vostrikov IY, Berestovsky GN (1983) Excitation of Characeae cell membranes as a result of activation of calcium and chloride channels. J Membrane Biol 72: 43-58

Marmarelis PZ, Marmarelis VZ (1978) Analysis of physiological system: the white-noise approach. Plenum Press, New York

Moran N, Ehrenstein G, Iwasa K, Mischke C, Bare C, Satter RL (1988) Potassium channels in motor cells of Samanea saman: a patch clamp study. Plant Physiol 88: 643-648

Morvan C, Demarty M, Thellier M (1979) Titration of isolated cell walls of Lemna minor L. Plant Physiol 63: 1117-1122

Mullins LJ (1962) Efflux of chloride ion during the action potential of Nitella. Nature 196:986-987

Oda K (1975) Recording of the potassium efflux during a single action potential in Chara corallina. Plant Cell Physiol 16:525-528

Oda K (1976) Simultaneous recording of potassium and chloride effluxes during an action potential in Chara corallina. Plant Cell Physiol 17: 1085-1088

Ogata K (1983) The water-film electrode: a new device for measuring the Characean electro-potential and -conductance distributions along the length of the internode. Plant Cell Physiol 24: 695-703

Ogata K, Chilcott TC, Coster HGL (1983) Spatial variation of the electrical properties of Chara australis. I. Electrical potentials and membrane conductance. Aust J Plant Physiol 10: 339-351

Ogata K, Toko K, Fujiyoshi T, Yamafuji K (1987) Electric inhomogeneity in membranes of Characean internode influenced by light/dark transition, O_2, N_2, CO_2-free air and extracellular pH. Biophys Chem 26: 71-81

Pedersen PL, Carafoli E (1987) Ion motive ATPases. I. Ubiquity, properties, and significance to cell function. TIBS 12: 146-150

Poole RJ (1978) Energy coupling for membrane transport. Ann Rev Plant Physiol 29: 437-460

Price GD, Badger MR, Bassett ME, Whitecross MI (1985) Involvement of plasmalemmasomes and carbonic anhydrase in photosynthetic utilization of bicarbonate in Chara corallina. Aust J Plant Physiol 12: 241-256

Rea L, Poole RJ (1985) Proton-translocating inorganic pyrophosphatase in red beet (Beta vulgaris L.) tonoplast vesicles. Plant Physiol 77: 46-52

Reinhold L, Kaplan A (1984) Membrne transport of sugars and amino acids. Ann Rev Plant Physiol 35: 45-83

Richards JL, Hope AB (1974) The role of protons in determining membrane electrical characteristics in Chara corallina. J Membrane Biol 16: 121-144

Richter C (1986) Ion exchange properties of cell walls. M.Sc. Thesis. University of Toronto, Canada

Roa RL, Pickard UF (1976) The use of membrane electrical noise in the study of Characean electrophysiology. J Exp Bot 27: 460-472

Roa RL, Pickard UF (1977) Further experiments on the low frequencey excess noise of the vacuolar resting potential of Chara braunii. J Exp Bot 28: 1-16

Ross S, Dainty J (1985) Membrane electrical noise in Chara corallina. I. A low frequency spectral component. Plant Physiol 79: 1021-1025

Ross S, Dainty J (1986) Membrane electrical noise in Chara corallina. II. Effects of inhibitors on the low frequency spectral component. Plant Physiol 79: 1026-1029

Ross S, Ferrier J, Dainty J (1985) Frequency-dependent membrane impedance in Chara corallina estimated by Fourier analysis. J Membrane Biol 85: 233-243

Sanders D (1980) Control of Cl influx by cytoplasmic Cl^- concentration. J Membrane Biol 52: 51-60

Sanders D (1980b) The mechanism of Cl^- transport at the plasma membrane of Chara corallina: I. Cotransport with H^+. J Membrane Biol 53: 129-141

Sanders D, Hansen U-P (1981) Mechanism of Cl- transport at the plasma membrane of Chara corallina: II. Transinhibition and the determination of H^+/Cl^- biding order from a reaction kinetic model. J Membrane Biol 58: 139-153

Sakano K, Tazawa M (1986) Tonoplast origin of the envelope membrane of cytoplasmic droplets prepared from Chara internodal cells. Protoplasma 131: 247-249

Sakmann B, Neher E (1984) Patch clamping techniques for studying ionic channels in excitable membranes. Ann Rev Physiol 46: 455-472

Schauf CL, Wilson KJ (1987a) Effects of abscissic acid on K^+ channels in Vicia faba guard cell protoplasts. Biochim Biophys Res Com 145: 284-290

Schauf CL, Wilson KJ (1987b) Properties of K^+ and Cl^- channels in Asclepias tuberosa protoplasts. Plant Physiol 85: 413-418

Schönknecht G, Hedrich R, Junge W, Raschke K (1988) A voltage-dependent chloride channel in the photosynthetic membrane of a higher plant. Nature 336: 589-592

Schroeder JI, Hedrich R, Fernandez JM (1984) K^+ selective single channels in guard cell protoplasts of Vicia faba. Nature 312: 361-362

Schroeder JI, Raschke K, Neher E (1987) Voltage dependence of K^+ channels in guard-cell protoplasts. Proc Natl Acad Sci USA 84: 4108-4112

Schroeder JI (1989) Quantitative analysis of outward rectifying K^+ channel currents in guard cell protoplasts from Vicia faba. J Membrane Biol 107: 229-235

Schroeder JI, Hagiwara S (1989) Cytosolic calcium regulates ion channels in the plasma membrane of Vicia faba guard cells. Nature 338: 427-430

Schweiger RG (1962) Acetylation of alginic acid. II. Reactions of algin acetates with calcium and other divalent ions. J Org Chem 27: 1789-1791

Schweiger RG (1964) Acetyl pectates and their reactivity with polyvalent metal ions. J Org Chem 29: 2973-2975

Segal JR Electrical capacitance of ion-exchanger membranes. J Theor Biol 14: 11-34

Sentenac H, Grignon C (1981) A model for predicting ionic equilibrium concentrations in cell walls. Plant Physiol 68: 415-419

Shiina T, Tazawa M (1988) Ca^{2+}-dependent Cl^- efflux in tonoplast-free cells of Nitellopsis obtusa. J Membrane Biol 06:135-139

Shimmen T, Kikuyama M, Tazawa M (1976) Demonstration of two stable potential state of plasmalemma of Chara without tonoplast. J Membrane Biol 30, 249-276

Shimmen T, Tazawa M (1980a) Intracellular chloride and potassium ions in relation to excitability of Chara membrane. J Membrane Biol 55: 223-232

Shimmen T, Tazawa M (1980b) Dependency of H^+ efflux on ATP in cells of Chara australis. Plant Cell Physiol 21: 1007-1013

Shimmen T, Tazawa M (1983) Activation of K^+-channel in membrane excitation on Nitella axilliformis. Plant Cell Physiol 24: 1511-1524

Shimmen T, Nishikawa S (1988) Studies on the tonoplast action potential of Nitella flexilis. J Membrane Biol 101: 133-140

Singer SJ, Nicolson GL (1972) The fluid mosaic model of the structure of cell membranes. Science 175: 720-731

Slayman CL, Slayman CW (1974) Depolarization of the plasma membrane of Neurospora during active transport of glucose: evidence for a proton-dependent cotransport system. Proc Natl Acad Sci USA 71: 1935-1939

Smack DP, Colombini M (1985) Voltage-dependent channels found in the membrane fraction of corn mitochondria. Plant Physiol 79: 1094-1097

Smith FA, Raven JA (1979) Intracellular pH and its regulation. Ann Rev Plant Physiol 30: 289-311

Smith FA (1984a) Regulation of the cytoplasmic pH of Chara corallina: response to changes in external pH. J Exp Bot 35: 43-50

Smith FA (1984b) Regulation of the cytoplasmic pH of Chara corallina in the absence of external Ca^{2+}: its significance in relation to the activity and control of the H^+ pump. J Exp Bot 35: 1525-1536

Smith FA (1985) Biological occurence and importance of HCO_3^- utilising systems: macroalgea (Charophytes). In Inorganic carbon uptake by aquatic photosynthetic organism, WJ Lucas and JA Berry Eds, ASPP, Rockville)

Smith FA, Walker NA (1989) Transport of potassium in Chara australis: I. A symport with sodium. J Membrane Biol 108: 125-137

Smith JR, Walker NA (1983) Membrane conductance of Chara measured in the acid and basic zones. J Membrane Biol 73: 193-202

Smith PT, Walker NA (1981) Studies on the perfused plasmalemma of Chara corallina: I. Current-voltage curves: ATP and potassium dependence. J Membrne Biol 60: 223-236

Smith PT (1984) Electrical evidence from perfused and intact cells for voltage-dependent K^+ channels in the plasmalemma of Chara australis. Aust J Plant Physiol 11: 303-318

Sokolik AI, Yurin VM (1981) Transport properties of potassium channels of the plasmalemma in Nitella cells at rest. Sov Plant Physiol 28: 206-212

Sokolik AI, Yurin VM (1986) Potassium channels of plasmalemma of Nitella cells at rest. J Membrane Biol 89: 9-22

Somers GF (1973) The affinity of anion cell walls for calcium ions. Amer J Bot 60: 987-990

Spanswick RM, Stolarek J, Williams EJ (1967) The membrane potential of Nitella translucens. J Exp Bot 18: 1-16

Spanswick RM (1972) Evidence for an electrogenic ion pump in Nitella transluscens. I. The effects o pH, K^+, Na^+, light and temperature on membrane potential and resistance. Biochim Biophys Acta 288: 73-89

Spanswick RM (1974) Evidence for an electrogenic ion pump in Nitella transluscens. II. Control of the light-stimulated component of the membrane potential. Biochim Biophys Acta 33: 387-398

Spanswick RM (1981) Electrogenic ion pumps. Ann Rev Plant Physiol 32: 267-289

Spear DG, Barr JK, Barr CE (1969) Localization of hydrogen ion and chloride fluxes in Nitella. J Gen Physiol 54: 397-414

Steigner W, Köler K, Simonis W, Urbach W (1988) Transient cytoplasmic pH changes in correlation with opening of potassium channels in Eremosphaera. J Exp Bot 39: 23-36

Stoeckel H, Takeda K (1989) Calcium-activated, voltage-dependent, non-selective cation currents in endosperm plasma membrane from higher plants. Proc R Soc Lond B237: 213-231

Takeshige K, Hager A (1988) Ion effects on the H^+-translocating adenosine triphosphatase and pyrophosphatase associated with the tonoplast of Chara corallina Plant Cell Physiol 29: 649-657

Taylor AO, Bonner BA (1967) Isolation of phytochrome from the algae Mesotaenium and the liverwort Sphaerocarpos. Plant Physiol 42: 762-766

Tazawa M, Shimmen T (1980) Demonstration of the K^+ channel in the plasmalemma of tonoplast-free cells of Chara australis. Plant Cell Physiol 21: 1535-1540

Tazawa M, Shimmen T (1982) Control of electrogenesis by ATP, Mg^{2+}, H^+ and light in perfused cells of Chara. In Current topics in membranes and transport vol 16 49-67

Tester M (1988) Pharmacology of K^+ channels in the plasmalemma of the green ala Chara corallina. J Membrane Biol 103: 159-169

Tester M (1988) Blockade of potassium channels in the plasmalemma of Chara corallina by tetraethylammonium, Ba^{2+}, Na^+ and Cs^+. J Membrane Biol 105: 77-85

Tester M (1988) Potassium channels in the plasmalemma of Chara corallina are multi-ion pores: voltage-dependent blockade by Cs^+ and anomalous permeabilties. J Membrane Biol 105: 87-94

Thompson EW, Preston RD (1967) Proteins in the cell walls of some green algea. Nature 213: 684-685

Toko K, Hayashi K, Yoshida T, Fujiyoshi T, Yamafuji K (1988) Oscillations of electric spatial patterns emerging from the homogeneous state in characean cells. Eur Biophys J 16: 11-21

Tsutsui I, Ohkawa T, Nagai R, Kishimoto U (1986) Inhibition of Cl^- channel activation in Chara corallina membrane by lanthanum ion. Plant Cell Physiol 27: 1197-1200

Tyerman SD, Findlay GP, Paterson GJ (1986a) Inward membrane current in Char inflata: I. A voltage- and time-dependent Cl^- component. J Membrane Biol 89: 139-152

Tyerman SD, Findlay GP, Paterson GJ (1986a) Inward membrane current in Char inflata: II. Effects of pH, Cl^--channel blockers and NH_4^+, and significance for the hyperpolarized state. J Membrane Biol 89: 153-161

Tyerman SD, Findlay GP (1989) Current-voltage curves of single Cl^- channels which coexist with two types of K^+ channel in the tonoplast of Chara corallina. J Exp Bot 40: 105-117

Tyree MT (1972) Ion exchange and the transport of water and solutes in Characean cell walls. Ph.D. Thesis. Churchill College, Cambridge, Great Britain

Van Cutsem P, Gillet C (1982) Activity coefficients and selectivity values of Cu^{++}, Zn^{++} and Ca^{++} ions adsorbe in the Nitella flexilis L. wall during triangular ion exchanges. J Exp Bot 33: 847-853

Verveen AA, Derksen HE (1965) Fluctuations in membrane potential of axon and the problem of coding. Kibernetik 2: 152-160

Verveen AA, Derksen HE, Schick K (1967) Voltage fluctuations of neural membranes. Nature 216: 588-589

Volkov GA (1977) Activation and current-voltage characteristics of excitable channels of the early ion flux in the plasmalemma of Nitella flexilis cells. Dokl Akad Nauk SSSR 237: 1533-1535

Volkov GA, Platonova LV, Skobeleva OV (1974) Nonsteady-state voltage-current relations of plasmalemma and tonoplast in Nitella flexilis cells. Dokl Akad Nauk SSSR 214: 959-961

Volkov GA, Platonova LV, Skobeleva OV (1979) Selective centers of excitable channels of the early ionic current of Nitella flexilis cells. Dokl Akad Nauk SSSR 245: 984-987

Volkov GA, Platonova LV, Skobeleva OV (1982) Selective properties of cations channels of the plasmalemma of cell of Nitella flexilis. Biofiz 27: 62-67

Volkova SP, Lunevsky VZ, Spiridonov NA, Vionokurov MG, Berestovsky GN (1980) On chemical composition of calcium channels in characean algla cells. Biofiz 25: 537-542

Vorobiev LN, Musaev NA (1979) Electrical characteristics of the cell wall and plasmalemma of Nitellopsis obtusa. Low frequency impedance. Sov Plant Physiol 26: 570-577

Vredenberg WJ, Tonk WJM (1975) Biochim Biophys Acta 387: 580-587

Walker NA, Smith FA (1977) Circulating electric currents between acid and alkaline zones associated with HCO_3^- assimilation in Chara. J Exp Bot 28: 1190-1206

Walker NA, Beilby MJ, Smith FA (1979) Amine uniport at the plasmalemma of Charophyte cells: I. Current-voltage curves, saturation kinetics, and effects of unstirred layers. J Membrane Biol 49: 21-55

Walker NA, Smith FA, Cathers IR (1980) Bicarbonate assimilation by fresh-water Charophytes and higher pants: I. Membrane transport of bicarbonate ions is not proven. J Membrane Biol 57: 51-58

Wang Y, Leigh RA, Kaestner KH, Sze H (1986) Electrogenic H^+ pumping pyrophosphatase in tonoplast vesicles of oat roots. Plant Physiol 81: 497-502

Williamson RE, Ashley CC (1982) Free Ca^{2+} and cytoplamic streaming in the alga Chara. Nature 96: 647-651